N-GLYCOSYLATION OF IMMUNOGLOBULIN G AND TOTAL PLASMA PROTEINS IN CORONARY ARTERY DISEASE

RADOVANI, BARBARA

Doctoral thesis / Doktorski rad

2023

University of Zagreb

FACULTY OF SCIENCE

DEPARTMENT OF BIOLOGY

Barbara Radovani

N-GLYCOSYLATION OF IMMUNOGLOBULIN G AND TOTAL PLASMA PROTEINS IN CORONARY ARTERY DISEASE

DOCTORAL THESIS

Zagreb, 2023

Sveučilište u Zagrebu

PRIRODOSLOVNO-MATEMATIČKI FAKULTET
BIOLOŠKI ODSJEK

Barbara Radovani

N-GLIKOZILACIJA IMUNOGLOBULINA G I UKUPNIH PROTEINA PLAZME U KORONARNOJ BOLESTI SRCA

DOKTORSKI RAD

Zagreb, 2023

Zahvale

Hvala mom mentoru doc. dr. sc. Ivanu Gudelju na pruženoj prilici i na neizmjernoj pomoći pri izradi ovog rada. Ivane, hvala ti na iskazanom povjerenju, prenesenom znanju i svakom savjetu te na ugodnoj i konstruktivnoj radnoj atmosferi.

Velika hvala svima iz Genosova tima, a posebno veseloj i pametnoj ekipi iz sobe 168 na zanimljivoj svakodnevnici, svim razgovorima, pomoći, utjehama, savjetima i zabavnim druženjima.

Hvala mojim roditeljima, sestri i Riu na pruženoj ljubavi i nesebičnoj podršci u svemu što radim. Ništa od ovog ne bi bilo moguće bez vas.

Na kraju, hvala mom Kikiju, na neprocjenjivoj podršci, ljubavi i razumijevanju kroz sve uspone i padove. Bez tebe, moj život ne bi bio isti.

INFORMATION ABOUT THE MENTOR

Assistant Professor Ivan Gudelj, Ph.D. graduated from the Faculty of Pharmacy and Biochemistry, University of Zagreb in 2013. After completing his studies, he joined Genos Ltd as a PhD researcher while simultaneously enrolling in the Postgraduate PhD programme "Biochemistry" at the Faculty of Science, University of Zagreb. In Genos he was involved in the development of new analytical methods and their validation for N-glycosylation analysis and participated in EU projects. As part of his PhD, he spent six months as a short-term scholar at Yale University, School of Medicine, USA, where he worked on molecular cloning, protein expression and purification, and virus-mediated transfection. In addition, he spent four months at the University of Rijeka, Department of Biotechnology, where he worked on a new analytical approach in mass spectrometry (MALDI) for glycosylation analysis. He received his PhD in 2017 and continued to work as a senior researcher at Genos Ltd., where his main focus was discovering the role of different glycosylation patterns in cardiovascular disease. He was also employed at Genos Glycoscience Ltd. where he worked on the development of a biological aging test, preparing the test launch and organizing production and marketing. Since 2020 he is a principal investigator of project "Glycosylation in cardiovascular diseases" funded by the Croatian science foundation. He has been working as an assistant professor at the University of Rijeka, Department of Biotechnology since 2020, where he is the head of the course "Analytical Chemistry" in the Pharmacy program of the Faculty of Medicine, as well as "Drug Toxicology" at the Research and Drug Development program at the Department of Biotechnology. During his academic and professional career, he published more than 40 scientific papers in international journals and several book chapters.

N-GLYCOSYLATION OF IMMUNOGLOBULIN G AND TOTAL PLASMA PROTEINS IN CORONARY ARTERY DISEASE

BARBARA RADOVANI

University of Rijeka, Department of Biotechnology

Radmile Matejčić 2, 51000 Rijeka, Croatia

Coronary artery disease (CAD) is the most common cardiovascular disease (CVD), resulting from chronic inflammation of the coronary arteries due to the formation of atherosclerotic plaques, and its presence is a significant marker of adverse cardiovascular (CV) events. Previous research has linked N-glycosylation, a highly regulated posttranslational modification, to the development of atherosclerotic plaques. Therefore, the aim of this work was to determine whether N-glycosylation of total plasma proteins and, in particular, immunoglobulin G (IgG) is associated with CAD. Sex-stratified analysis of N-glycosylation of total plasma proteins and IgG revealed significant changes associated with CAD, with different patterns observed in men and women. Highly branched sialylated plasma N-glycan structures with terminal fucose were positively associated, whereas biantennary sialylated IgG N-glycan structures were negatively associated with CAD. Overall, protein N-glycosylation emerges as a significant factor in CAD, with glycan-based biomarkers showing promise for predicting cardiovascular health.

(117 pages, 13 figures, 23 tables, 272 references, original in English)

Keywords: glycosylation, immunoglobulin G, plasma proteins, coronary artery disease, inflammation, biomarker

Mentor: Assistant professor Ivan Gudelj, PhD, Department of Biotechnology, Rijeka

Reviewers:

Professor Olga Gornik Kljaić, PhD, Faculty of Pharmacy and Biochemistry, Zagreb

Associate Professor Petra Korać, PhD, Faculty of Science, Zagreb

Assistant Professor Toma Keser, PhD, Faculty of Pharmacy and Biochemistry, Zagreb

Substitute reviewer: Professor Biljana Balen, PhD, Faculty of Science, Zagreb

N-GLIKOZILACIJA IMUNOGLOBULINA G I UKUPNIH PROTEINA PLAZME U KORONARNOJ BOLESTI SRCA

BARBARA RADOVANI

Sveučilište u Rijeci, Odjel za Biotehnologiju

Radmile Matejčić 2, 51000 Rijeka, Hrvatska

Koronarna bolest srca (KBS) najčešća je kardiovaskularna bolest (KVB), koja nastaje kao posljedica kronične upale koronarnih arterija uslijed stvaranja aterosklerotskih plakova, a njezina je prisutnost značajan biljeg štetnih kardiovaskularnih (KV) događaja. Prethodna su istraživanja povezala N-glikozilaciju, visoko reguliranu posttranslacijsku modifikaciju, s razvojem aterosklerotskih plakova. Stoga je cilj ovog doktorskog rada bio utvrditi je li N-glikom ukupnih proteina plazme, a posebice imunoglobulina G (IgG), povezan s KBS-om. Spolno stratificirana analiza N-glikozilacije ukupnih proteina plazme i IgG otkrila je značajne promjene povezane s KBS-om, s različitim obrascima uočenim u muškaraca i žena. Visoko razgranate sijalizirane N-glikanske strukture proteina plazme s terminalnom fukozom bile su pozitivno povezane, dok su biantenarne sijalizirane IgG N-glikanske strukture bile negativno povezane s KBS-om. Sve u svemu, N-glikozilacija proteina pojavljuje se kao značajan čimbenik u KBS-u, te biljezi temeljeni na glikanima predstavljaju potencijal za predviđanje kardiovaskularnog zdravlja.

(117 stranica, 13 slika, 23 tablice, 272 literaturna navoda, jezik izvornika: Engleski)

Ključni riječi: glikozilacija, imunoglobulin G, proteini plazme, koronarna bolest srca, upala, biomarker

Mentor: Doc. dr. sc. Ivan Gudelj, Odjel za biotehnologiju, Rijeka

Ocjenjivači:

Prof. dr. sc. Olga Gornik Kljaić, Farmaceutsko-biokemijski fakultet, Zagreb

Izv. prof. dr. sc. Petra Korać, PMF, Zagreb

Doc. dr. sc. Toma Keser, Farmaceutsko-biokemijski fakultet, Zagreb

Zamjena: Prof. dr. sc. Biljana Balen, PMF, Zagreb

TABLE OF CONTENTS

1. INTRODUCTION

Cardiovascular diseases (CVDs) encompass a group of conditions affecting the heart and blood vessels. CVDs stand as the leading cause of mortality worldwide and impose a substantial burden on public health systems (1). Among CVDs, coronary artery disease (CAD) stands out as the primary cause of death, claiming nine million lives in 2021 (1). Although preventive measures for CAD primarily rely on traditional risk factors such as hyperlipidemia, diabetes mellitus, smoking, and hypertension (2), it has been observed that individuals classified as high-risk may not always develop CAD, while those classified as low or intermediate risk may succumb to the disease (3–7). Consequently, the identification of new risk factors and the potential to influence them hold immense significance.

In this context, posttranslational modifications (PTMs) are emerging as a potential for the development of new disease-specific biomarkers. PTMs play a key role in numerous biological processes by significantly affecting protein structure and dynamics through covalent modifications such as proteolytic cleavage and the addition of modifying groups (e.g., acetyl, phosphoryl, glycosyl, and methyl) to amino acids (8). Glycosylation is a vital and tightly regulated PTM in which complex sugar molecules (glycans) are covalently attached to protein, lipid and RNA backbones (9–11). Protein glycome (complete repertoire of glycans found on the surface of proteins) is involved in various biological processes, such as regulating protein function and stability, mediating intercellular interactions, modulating intracellular signaling, and influencing cellular immunogenicity (12,13). The two major protein glycosylation classes are N- and O-linked glycans (described in detail in the section "Overview of protein glycosylation"), with N-glycans being easier to analyze in the released form than O-glycans, since a universal enzyme is available only for the release of N-glycans (14).

Over the past decade, a number of research studies have identified protein glycosylation as a potential valuable biomarker for early detection and progression of disease (15–24). Research has found alterations in glycosylation associated with numerous inflammatory diseases, including CVD (15,25,26). A growing body of evidence highlights the importance of glycosylation alterations in CVD development, and it shows that glycan signatures hold promise as potential biomarkers for CVD (27,28). For instance, atherosclerosis, a common underlying condition of CVD, involves the formation of atherosclerotic plaques and narrowing of arterial lumens due to inflammation-driven accumulation of leukocytes, lipoproteins, and other cells in the arterial intima. This inflammatory process contributes to changes in glycosylation of endothelial cells and lipoproteins, which prove critical at the early stages of atherosclerotic plaque development (29–33). In addition, systemic inflammation response

leads to an increase in plasma protein concentration accompanied by significant changes in their glycome (34–36).

While N-glycosylation of plasma proteins, comprising IgG, remains relatively stable in healthy individuals (37,38), sensitivity of its glycan make-up to changes that occur in an organism emphasizes its potential for becoming a biological marker. Altered glycosylation of IgG and total plasma proteins has been found to be associated with CVD development, independent of other known risk factors (39–41). Interestingly, recent research has even proposed an IgG N-glycome-based index to assess and predict cardiovascular health (42). On the other side, changes in serum protein glycosylation have been observed in CAD, with elevated levels of the inflammatory biomarker GlycA, an nuclear magnetic resonance (NMR) signal originating from N-acetylglucosamine from highly-branched N-glycan structures, in serum showing an independent association with the presence and severity of CAD (43). Therefore, investigating distinct IgG and total plasma protein glycosylation traits could aid in stratifying risk phenotypes for CAD development.

Given the significant role of glycosylation in the development of cardiovascular disease, monitoring N-glycan patterns may serve as an early indicator of pathogenic cardiovascular processes, potentially providing clinical benefits for the timely diagnosis and prevention of CVD. Therefore, it is of utmost importance for future research to understand which changes in glycosylation act as risk factors for CVD and how they can be influenced.

1.1 Purpose and objectives of the research

The research in this dissertation focuses on the identification of N-glycans of total plasma proteins and IgG associated with CAD to find new markers for early detection, monitoring and prediction of the disease. Glycomic analysis is performed on blood plasma samples collected from participants without prior clinical manifestations of CVDs who underwent coronary computed tomography angiography (CCTA) because of suspected CAD, as part of the CAPIRE study to identify novel mechanisms contributing to or protecting against coronary atherothrombosis (44).

Previous studies have indicated the predictive and diagnostic potential of N-glycans in different conditions related to CVD (39–41,45). However, this study is the first to comprehensively analyse N-glycan alterations in individuals with angiographically diagnosed CAD, with samples collected at the time of enrolment and after 2 years of follow-up, and to examine the association between the presence of specific N-glycan structures and the incidence of adverse cardiovascular events during the 8-year follow-up period. This will allow the detection of N-glycan alterations at a clinically relatively early stage in the diagnosis of CAD and potentially reveal the involvement of N-glycosylation in the mechanism of the development of CAD.

The main objectives of this research are to identify N-glycan structures on both total plasma proteins and IgG that: a) are associated with angiographically diagnosed CAD, b) allow prediction and early detection of individuals at increased risk for developing CAD, and c) are associated with the incidence of adverse cardiovascular events. Considering the severity of CAD and the often-untimely detection resulting in lifelong therapy and/or even the development of life-threatening complications, the search for new potential markers for early detection of the disease is of great importance. Therefore, it is hypothesised that N-glycosylation of IgG and total plasma proteins differs significantly in individuals with angiographically diagnosed CAD compared with individuals with clean coronary arteries and shows an association with the incidence of adverse cardiovascular events.

Glycomic analysis includes enzymatic deglycosylation of IgG and plasma proteins, fluorescent labelling and purification of released N-glycans, and analysis of fluorescently labelled N-glycans by ultra-high performance liquid chromatography based on hydrophilic interactions with fluorescence detection (HILIC-UHPLC-FLR). Statistical analysis includes processing of the results using R programming. Briefly, association analyses between CAD status and baseline glycomic measurements are performed using a regression model, while for two-time

points analysis of CAD samples through their observation period, linear mixed-effects model (LMM) is implemented. Relationship between N-glycans and the occurrence of major adverse cardiac events (MACE) is examined using cox proportional-hazards model.

The scientific contribution of this research is the discovery of new potential markers that could independently distinguish individuals at increased risk for developing coronary atherosclerosis from individuals with clean coronary arteries. Based on the knowledge of the role of these glycan structures in (patho)physiological processes, their role in the mechanism of CVDs will be proposed, which would lead to a better understanding of the disease itself and to the identification of potential therapeutic targets.

2. LITERATURE OVERVIEW

2.1 Overview of protein glycosylation

Glycosylation, a crucial and tightly regulated co- and post-translational modification, involves the enzymatic, site-specific attachment of complex sugar molecules (glycans) to protein, lipid or RNA backbones (9–11). Alongside DNA, proteins, and lipids, glycans constitute one of the major components of cells. Their absence is embryologically lethal, underscoring their indispensable role in multicellular life (46). While many glycans reside on the outer surfaces of cellular and secreted proteins, simpler yet highly dynamic protein-bound glycans are also prevalent in the nucleus and cytoplasm, exerting regulatory effects. Due to their ubiquitous and intricate nature, glycans exhibit an extremely diverse range of biological functions. They range from subtle to those that are critical to the development, function, and/or survival of an organism (12). At the cellular level, glycans participate in nearly all physiological processes, including protein folding and transportation, cell adhesion, signaling, proliferation, differentiation, migration, survival, development, and immunity (9,12).

There are several types of glycosylation, however glycans covalently attached to a polypeptide backbone of glycoproteins are commonly classified into O- and N-glycans (47). An O-glycan is often attached to the polypeptide via N-acetylgalactosamine (GalNAc) to a hydroxyl group of a serine or threonine residue and can be extended to various structural core classes. An N-glycan is an oligosaccharide covalently linked to an asparagine residue which is part of the consensus peptide sequence (Asn-X-Ser/Thr) of a polypeptide chain, where X is any amino acid except proline. Mammal N-glycans share a common core region made of five monosaccharides and can generally be divided into three main classes: the oligomannose (or high-mannose) type, the complex type, and the hybrid type (Figure 1).
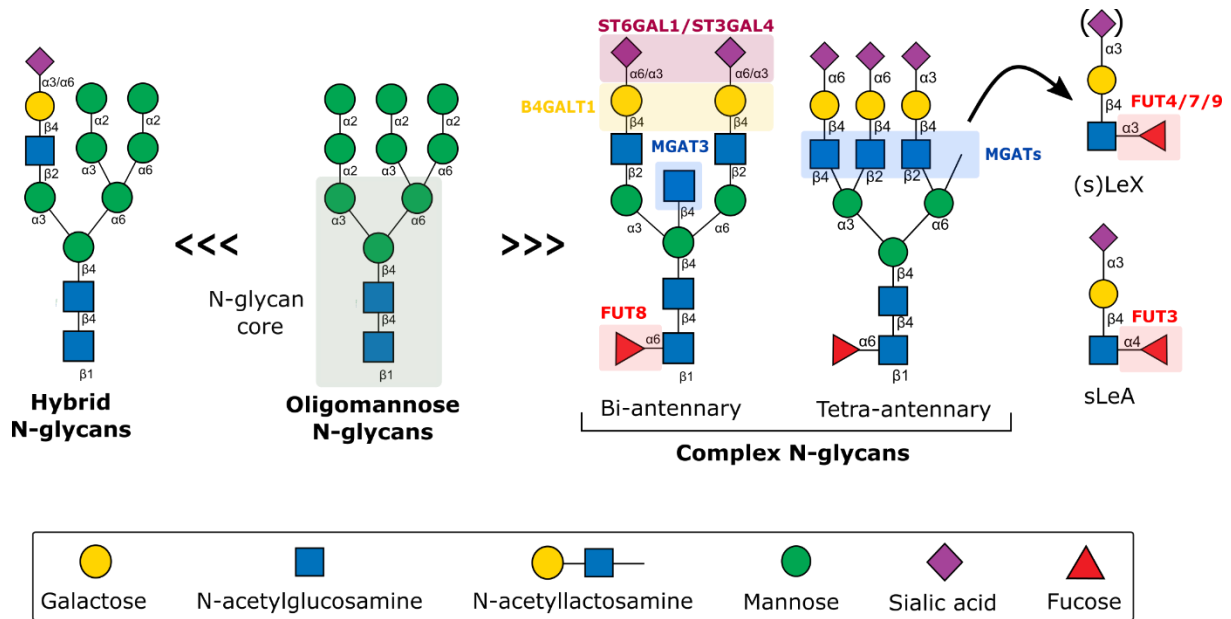
Figure 1. Examples of three N-glycan types: oligomannose (mannose residues attached to the core), complex (two or more antennae attached to core via N-acetylglucosamine) and hybrid glycans (it has one or more oligomannose branches and one branch of complex structure). All N-glycans share a common core (marked with light green rectangle). Relevant glycosyltransferases are shown: B4GALT1, β-1,4-Galactosyltransferase 1; FUT, Fucosyltransferase; MGAT, N-acetylglucosaminyltransferase; ST3GAL4, β-Galactoside α-2,3-Sialyltransferase 4; ST6GAL1, β-Galactoside α-2,6-Sialyltransferase 1.

In eukaryotes, the assembly of glycans bound to cellular and secreted proteins occurs predominantly in the endoplasmic reticulum (ER) and Golgi apparatus (GA), with the initial steps of N-glycosylation occurring in the ER, whereas further enzymatic processing of the N-glycans occur further along the secretory pathway at the luminal side of the ER and GA compartments. In these organelles, glycan biosynthesis consists of a series of steps controlled by expression, activity and trafficking of numerous glycosyltransferases and glycosidases, competition between these enzymes and availability of sugar donors and other substrates (48). Unlike the genome, exome, or proteome, glycome has no direct template but is a consequence of the current state of the organism. Thus, small environmental changes in response to intrinsic and extrinsic signals can cause dramatic changes in the glycan repertoire produced by a particular cell. This goes hand in hand with the phenomenon of microheterogeneity that is characteristic of glycosylation (47). Essentially, a polypeptide encoded by a single gene can exist in numerous glycoforms, each representing a distinct molecular species. Microheterogeneity may be quite limited at a given site, while it may be extensive at other sites. This may be manifested, for example, by an increased number of antennae, the absence or presence of certain monosaccharides (galactose, N-acetylneuraminic (sialic) acid (Neu5Ac), fucose, N-acetylglucosamine (GlcNAc)), and/or a diversification of saccharide linkages leading to different ligand epitopes.

It is this variable and dynamic nature of glycosylation that makes it a powerful means of generating and modulating biological diversity and complexity. The sugar components of glycoproteins not only form important structural features, but also modulate or mediate a variety of their functions in (patho)physiological states (10). Technological advances in research tools have begun to overcome many of the challenges posed by the complexity of glycoconjugates, leading to a better understanding of the physiological and pathological processes regulated by glycans (49,50). Alterations in protein N-glycosylation have already been described for many diseases (15,25,26,51–54), and it has been shown that N-glycans have great potential as diagnostic and prognostic biomarkers for cancer, metabolic disorders, CVDs, and other chronic inflammatory states (18,20,26,27).

2.2 Human plasma protein N-glycosylation

Plasma proteins constitute a significant portion of the human proteome and play essential roles in various physiological processes. These proteins are primarily released into the circulatory system by B cells (immunoglobulins, Igs) or hepatocytes and other liver cell types (16). They serve diverse functions, including coagulation, receptor interactions, immunity, nutrient and gas transportation, among others (55). Glycosylation is observed in the majority of human plasma proteins, with the exception of the most abundant protein - albumin. The N-glycosylation profiles of over 20 different plasma proteins have been characterized thus far (16). In addition to immunoglobulins, several extensively studied plasma glycoproteins include haptoglobin (HPT), α1-acid glycoprotein (AGP-1), fibrinogen, α1-antitrypsin (A1AT), and α1-antichymotrypsin (AACT). Analysis of their individual N-glycosylation profiles has revealed both protein-specific N-glycan structures and shared N-glycans present on multiple plasma proteins (Figure 2). In addition, plasma proteins with multiple N-glycosylation sites often exhibit glycosylation site specificity (16). Glycan structures of plasma glycoproteins are composed of several monosaccharides: fucose, galactose, mannose, GlcNAc and sialic acid (16,56). Fucose can be core- or antennary- bound; Antennary fucose is in most cases attached to GlcNAc bound to one of the two mannoses that mark the beginning of branching of the glycan structure (57). Galactose is bound to the aforementioned GlcNAc, and sialic acid to galactose. In addition to the initial part of each branch (antenna), GlcNAc can also be attached to the central mannose of the common glycan core, and is then called bisecting GlcNAc (16,56). Total plasma N-glycosylation is highly informative but difficult to comprehend because of the complex contributions from relative protein glycoforms and overall glycoprotein abundances.
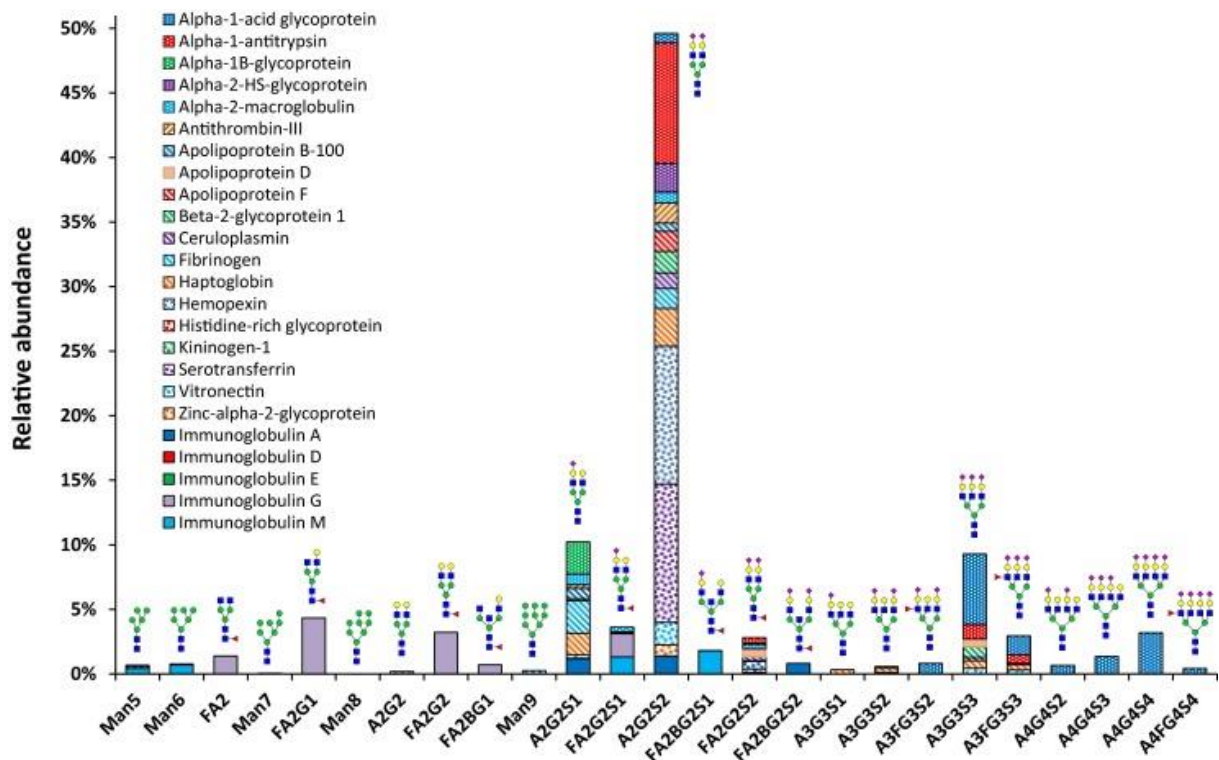
Figure 2. Schematic representation of the relative protein contribution to each specific glycan composition. From: Clerc F, Reiding KR, Jansen BC, Kammeijer GS, Bondt A, Wuhrer M. Human plasma protein N-glycosylation. Glycoconj J. 2016 Jun;33(3):309-43. doi: 10.1007/s10719-015-9626-2.

While the N-glycome of human plasma protein is quite stable within the individual (37,58), it is extremely sensitive to changes in individual's homeostasis, reflecting either the cellular state at the time of protein secretion or dysregulation of circulating glycosyltransferases/glycosidases responsible for extrinsic (de)glycosylation of proteins (10,16,36). Therefore, it is very important to understand the relative contribution of genetic and environmental factors to the plasma protein N-glycome, as well as impact of the (patho)physiological state of a given organism. Large-scale population studies indicated variation in heritability of specific plasma N-glycome traits. Overall, many traits show rather high heritability, contributing significantly to interindividual variation within population, but also to variations between populations (59,60). On the protein level, highest heritability was observed in N-glycans specific for IgG, while N-glycome of plasma proteins that are part of acute phase reactants exhibited lowest heritability (60). The influence of genetic makeup has been demonstrated in genome-wide association studies (GWAS) of single nucleotide polymorphisms (SNPs) with plasma protein N-glycosylation traits, providing insights into the molecular mechanisms regulating glycosylation (61–64). GWAS demonstrated the association of genetic variants for glycosyltransferases with the corresponding glycosylation phenotype and provided insights into the regulation of glycosylation at the transcription factor level. In

addition, associations were found with genes for which a possible functional relationship to glycosylation is still unknown (61).

Along with the strong genetic influence, environmental and pathological effects on plasma protein N-glycome have also been reported. A significant association between plasma/serum total N-glycome and sex, age, body mass index (BMI), smoking, diet, and stress has been demonstrated (65–68). In addition, dysregulation of plasma N-glycosylation has been linked to the development and progression of a variety of diseases, including cancer, metabolic disorders, CVD, and other inflammatory diseases, making N-glycosylation a target for diagnosis and therapeutic intervention (16,25–27,38,54,65,69–71). Alterations in plasma protein N-glycosylation likely reflect chronic inflammation as an underlying condition of aging (inflammaging), obesity, smoking, and unhealthy diet, as well as numerous chronic diseases. Collectively, these changes include an increase in the number of antennae (tri- and tetra-antennary N-glycans), increased antennary fucosylation, and increased α2,6- and α2,3-sialylation on highly branched N-glycans. Antennary fucose and α2,3-linked sialic acid are structural motifs of inflammation-associated sialyl Lewis X (sLeX) and sialyl Lewis A (sLeA) epitopes found on plasma proteins.

In addition to the disease association and biomarker potential of total plasma protein N-glycome, GlycA is another inflammation biomarker derived from plasma protein N-glycome. Whereas plasma N-glycome refers to the measurement of the abundance of various N-glycans bound to plasma proteins, GlycA is a complex heterogeneous NMR signal specifically derived from GlcNAc residues of branched plasma N-glycans bound to acute phase proteins (72), and has been shown to correlate with a broad spectrum of inflammatory diseases (43,73–77). Overall, currently available data indicate that plasma N-glycosylation plays a role in numerous pathological conditions and that N-glycans could be used as biomarkers, prognostic tools, or even as anchor points for targeted treatments.

2.2.1 The role of N-glycosylation in immunological function of plasma proteins

Plasma N-glycosylation affects protein properties such as folding, solubility, stability, and localization and is involved in a variety of biological processes (16,78). Plasma proteins have multiple N-glycosylation sites, and their glycoforms may differ by site occupancy (macroheterogeneity) and occupying glycan structures (microheterogeneity). Diversity of N-glycans is dependent on numerous factors that can influence the biosynthesis process, including genetic regulation, enzyme activity, availability of nucleotide sugars, and accessibility of a

particular glycosylation site (16,64,79,80). As mentioned previously, most profound inflammation mediated alterations of plasma N-glycome include high branching (tri- and tetra-antennary glycans) and elevated levels of the sLeX epitope, which have been detected on plasma proteins such as HPT, AGP-1, A1AT, and AACT (16,81,82). One of the examples of N-glycosylation-mediated modulation include sLeX epitope on the AGP-1; sLeX has been shown to play a role in anti-neutrophil activity of AGP-1 (83) and is crucial for its binding to the adhesion molecules such as E-selectin expressed on the endothelium (84). Proinflammatory cytokines such as interleukin 1β (IL-1β), interleukin 6 (IL-6), and tumor necrosis factor α (TNFα) were suggested to affect plasma protein N-glycan biosynthesis in hepatocytes (85–89). *In vitro* study suggested that the increased branching and abundance of sLeX epitope on AGP-1 may be due to cytokine-mediated upregulation of the enzymes responsible for sLeX epitope formation, β-galactoside α-2,3-sialyltransferase 4 (ST3GAL4) and fucosyltransferase 6 (FUT6) (85,86). TNFα has also been shown to increase sLeX synthesis by stimulating the expression of ST3GAL4 and FUT4 through NF-kB-p65 dependent transcriptional regulation (89,90). Of genetic factors, the regulation of plasma protein sLeX formation has been linked to hepatocyte nuclear factor 1α (HNF1α) and its transcriptional cofactor HNF4α (63). HNF1α/HNF4α interaction induces *de novo* and salvage synthesis of GDP-fucose and regulates the expression of relevant fucosyltransferases ultimately leading to higher biosynthesis of sLeX epitope. Furthermore, increased hexamine biosynthesis pathway (HBP) flux and higher UDP-GlcNAc levels in hepatocytes during chronic inflammation may lead to increases in tri- and tetra-antennary N-glycans on plasma proteins. Glucose and glutamine are donor molecules that play a direct role in controlling HBP flux and levels of UDP-GlcNAc (crucial substrate for N-glycan branching). During prolonged inflammation, there is an increased uptake of glutamine in the liver and an increase in liver glucose production due to TNFα-activated NF-kB transcriptional regulation (91–93). This leads to elevated levels of UDP-GlcNAc and increased branching of plasma protein N-glycans. Additionally, the branching of N-glycans present on liver membrane transporters for glucose and glutamine increases the binding affinity of galectins, protecting them from endocytosis while forming a positive feedback loop that enhances substrate uptake (94).
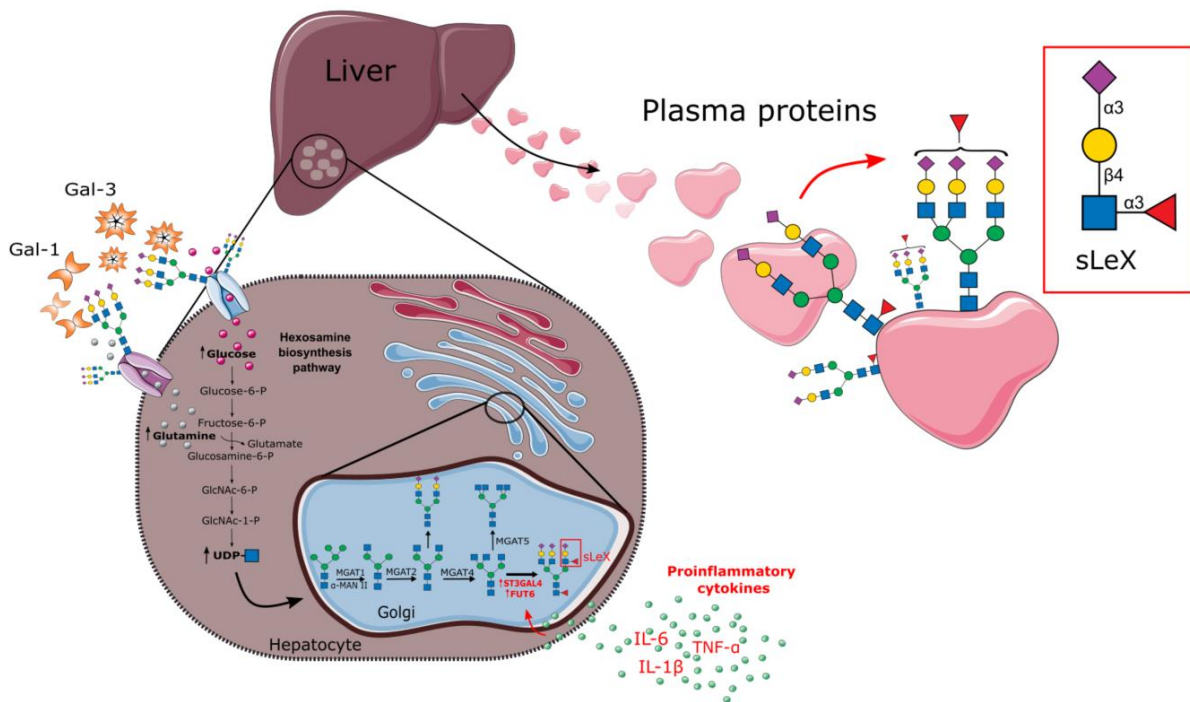
Figure 3. Overview of altered N-glycosylation pathways regarding plasma proteins under the influence of inflammation. In inflammation, increased flux of the hexamine biosynthetic pathway (HBP) and consequently increased UDP-GlcNAc levels in hepatocytes can lead to increased branching of N-glycans, whereas proinflammatory cytokines induce higher expression of the enzymes ST3GAL4 and FUT6, which are responsible for the synthesis of the inflammatory epitopes sLeX and sLeA. Together, these changes contribute to the propagation of the inflammatory state.

In addition, liver-produced acute phase protein β-galactoside α-2,6-sialyltransferase 1 (ST6GAL1) is also upregulated and released into circulation during inflammation, although its exact role remains unclear. However, research has shown that a loss of hepatic ST6GAL1 can cause problems with liver metabolism and changes in the N-glycan profile of circulating glycoproteins (95). This can result in spontaneous liver inflammation and disease. Chronic alcohol exposure has been shown to downregulate hepatic ST6GAL1 expression, leading to metabolic dysfunctions and altered glycosylation (96). This highlights the role of lifestyle in the regulation of hepatic ST6GAL1, which may contribute to the development of inflammation and disease. In summary, inflammation triggers changes in N-glycosylation of plasma proteins, while at the same time altered N-glycosylation contributes to proinflammatory transformation of secreted plasma proteins, thus providing a positive feedback mechanism that maintains the inflammatory state.

2.3 Immunoglobulin G N-glycosylation

The most prevalent class of immunoglobulins in human plasma is immunoglobulin G (IgG), accounting for 75% of all antibodies and 10-20% of total plasma protein (16,97). It plays a

critical role in the human adaptive immune system and bridges the gap between innate and adaptive immunity due to its versatility (98). With variable fragment antigen-binding (Fab), IgG recognizes and binds antigens with high affinity and is able to directly neutralize pathogens and toxins (99). At the same time, IgG can interact with type I and type II Fcγ receptors on the surface of immune cells such as B lymphocytes, macrophages, and natural killer cells (NK cells) via its crystallizable fragment (Fc) part and trigger opsonization and phagocytosis of microorganisms by antibody dependent cellular phagocytosis (ADCP), mediate antibody dependent cellular cytotoxicity (ADCC), and inhibit or activate other immune cells (99). In addition, the interaction of the Fc domain with other components of the immune system, such as complement component C1q, mannose binding lectin (MBL), and mannose receptor, activates the complement system and causes lysis of microorganisms or damaged autologous cells through complement dependent cytotoxicity (CDC) (36).

Glycans make up about 15% of the weight of IgG (100) and their importance is evident from the fact that removal of these glycans results in partial or complete loss of IgG function (100–102). Each IgG molecule contains a conserved N-glycosylation site at Asn-297 in the constant region of heavy chain 2 on Fc domain (35). Glycans are not only a structural component of the IgG molecule, but also play a crucial functional role by altering the binding affinity of IgG to its corresponding ligands (Figure 4). This affects many biological processes in which IgG is involved, such as its half-life, clearance, transport across the placenta, activation of immune effector cells, and complement activation (100,103–108). The Fab region of IgG can also have additional N-glycosylation sites introduced through somatic hypermutation during the affinity maturation process in germinal centers. Approximately 15-20% of IgG molecules from healthy individuals have been observed to have glycans in their variable region of the heavy chain (109,110). Fab glycans can affect the stability, half-life and antigen-binding of IgG, and are suggested to be involved in the modulation of immune response (110–114).

All IgG N-glycans have a common conserved pentasaccharide core sequence consisting of two GlcNAc and three mannose residues branching into two antennae (56). This core is most frequently extended by a GlcNAc added to each of the mannoses, followed by further addition of bisecting GlcNac and/or core fucose, whereas the antennae can be further extended by the addition of galactose, followed by sialic acid (100). In addition, some oligomannose glycans with five to nine mannose residues have been observed at the N-glycosylation sites of IgG (100). To date, over 30 different N-glycan structures have been identified in the Fab and Fc portions of polyclonal serum IgG (115).
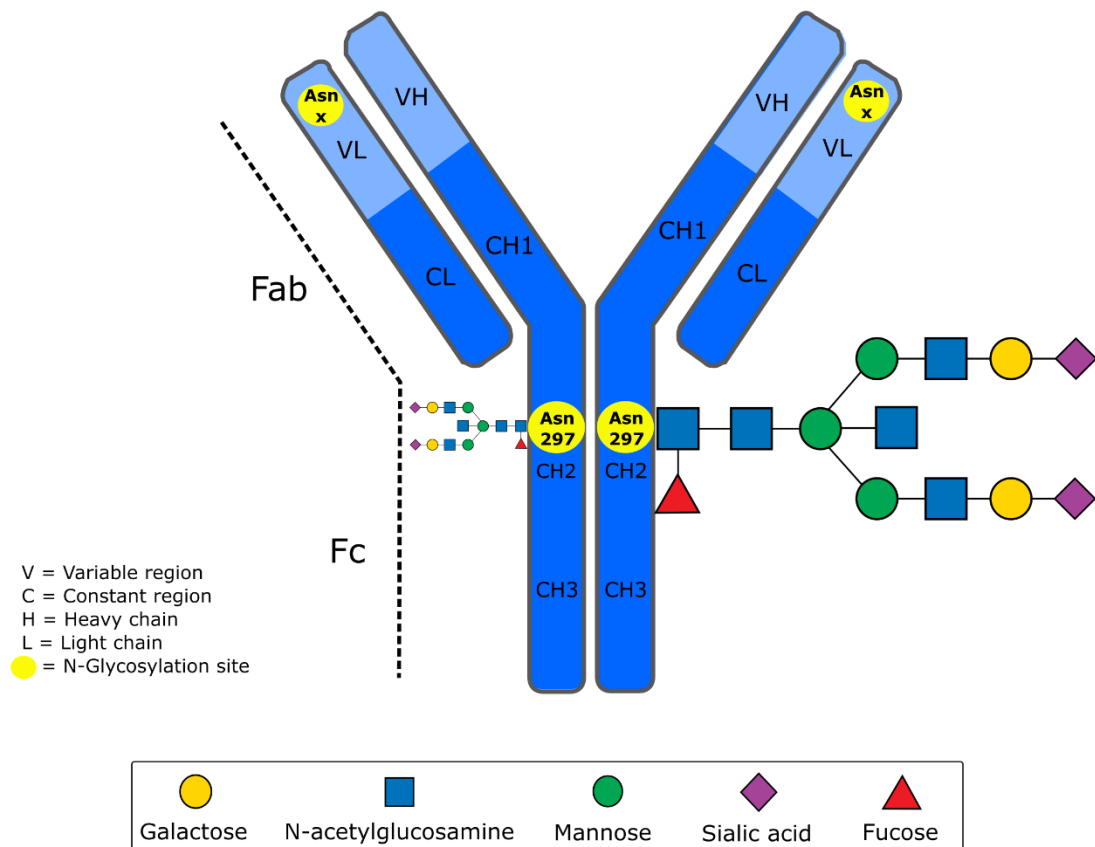
Figure 4. Schematic representation of immunoglobulin G (IgG). IgG protein is composed of two heavy and two light chains. IgG protein can also be divided into two functional fragments: antigen-binding fragment (Fab) which binds antigen and crystallizable fragment (Fc) which is important for effector functions such as ADCC or complement activation. Each heavy chain of Fc fragment contains a covalently attached N-glycan to highly conserved N-glycosylation site located at position asparagine (Asn) 297. In addition, some IgG molecules can contain N-glycans in the Fab fragment (~20% of IgG molecules).

Because of their structural complexity and the lack of sophisticated analytical techniques, IgG glycans have only recently become a subject of scientific attention, especially over the past decade in parallel with the development of high-throughput methods for IgG glycome analysis (50). Studies have shown that IgG glycosylation patterns, characterized by a lower abundance of galactosylated and sialylated structures and sometimes a higher abundance of structures with bisecting GlcNAc, are associated with many inflammatory diseases and are also often associated with disease severity (15,116,117). Of note, this pattern is also associated with increasing age (inflammaging) (15,118). IgG glycome composition has been shown to be significantly influenced by genes (60,119–121), but also by environmental factors and lifestyle (hormonal status, age, BMI, smoking, dietary supplements, and exercise) (22,122–130). IgG glycans serve as a link between an individual's genetic information and the influence of their environment. The makeup of an individual's IgG glycome can be altered by various health conditions, both physiological and pathological, making it a valuable indicator of a person's

overall health. It can also enhance existing disease biomarkers and provide insights into disease development, progression, prognosis, and response to treatment.

2.3.1 The role of N-glycosylation in immunological function of IgG

The composition of N-glycans bound to the Fc region of IgG modulates its functional properties and activity and is critical for interactions with various receptors and ligands (131–134), as shown on Figure 5. Alterations in the N-glycosylation profile of IgG can disrupt these interactions and lead to a variety of diseases and pathological conditions (15,116,117). The association of multiple glycan features with a variety of diseases suggests that there may be multiple pathways, rather than just one, associated with IgG glycosylation that play a role in disease development and progression. However, the most studied are variations in the IgG glycoprofile associated with changes in the expression or activity levels of the major glycosyltransferases and glycosidases due to specific genetic polymorphisms and/or under the influence of proinflammatory cytokines (36).

2.3.1.1 Galactosylation

In healthy adults, on average 15% of IgG Fc glycoforms have both arms terminating in galactose, 35% have a terminal galactose residue missing from one or the other arm, and another 35% IgG Fc glycoforms are agalactosylated (100,135,136). Galactosylation influences the inflammatory potential of IgG by modulating binding affinities to downstream effector molecules, namely complement components and FcγRs. IgG Fc glycans lacking galactose at their terminal ends are thought to activate the complement through the alternative pathway and through lectin pathway by binding MBL, thereby promoting inflammation (103,137). While agalactosylated IgG is considered to promote inflammation due to its association with many diseases (15), the role of terminal galactosylation in this regard is still a matter of debate. On one hand, IgG glycans decorated with galactoses are thought to have anti-inflammatory effects by binding to the inhibitory FcγRIIb receptor and suppressing the proinflammatory activity of the complement component C5a (138). On the other hand, Fc galactosylation has been shown to increase the affinity of IgG for activating FcγRs, leading to ADCC (132,139). Even though the recent study states that Fc galactosylation activates the classical complement pathway by promoting hexamerization of IgG, enhancing C1q avidity, and increasing CDC activity (104), the overall conclusion on the effect of terminal galactosylation on C1q binding and/or CDC activity is still unclear, as up-regulatory, unchanged, and even down-regulatory effects have been previously reported (134). While the biological functions of (a)galactosylated IgG are

being deciphered, the regulation of its biosynthetic process is even more unclear. Decreased IgG galactosylation has been observed in peripheral B cells from rheumatoid arthritis (RA) patients and has been associated with decreased β-1,4-galactosyltransferase 1 (B4GALT1) activity, although no differences in B4GALT1 expression were observed between RA patients and healthy controls. It has been suggested that this may be due to stress-related disturbances in the Golgi, which may affect the proper targeting and function of B4GALT1 (140). Moreover, proinflammatory cytokines are known to modulate IgG glycosylation (36), and a recent GWAS study showed a correlation between IL-6 signaling (SNPs in the IL6ST (gp130) gene) and low serum IgG galactosylation (120). Cytokine mediated T cell-dependent activation of B cells was also suggested to alter N-glycosylation of secreted IgG. In studies with mice, it has been observed that proinflammatory cytokines (interferon γ (IFN-γ), interleukin 17 (IL-17) and IL-6) produced by T helper 1 (Th1), T helper 17 (Th17), and T follicular helper (Tfh) cells indirectly maintain the agalactosylated state of IgG by activating B cells (141,142). However, the opposite was observed in a recent study showing that stimulation of human B cells with IFN-γ leads to increased IgG galactosylation, accompanied by upregulation of B4GALT1 (143). Interestingly, binding of e.g., IFN-γ to its receptor leads to activation of JAK/STAT pathway known to target genes that appear to promote inflammation (144), therefore it is plausible that targeted genes include galactosyltransferases.

2.3.1.2 Sialylation

In a healthy individual, about 10-15% of serum IgG are sialylated, with most of them having monosialylated glycoforms (15). The attachment of sialic acid to the terminal end of IgG N-glycans prolongs the half-life of IgG in serum (145), and is critical for the modulation of the inflammatory immune response (36). Highly sialylated IgG have a low affinity for activating FcγRIIIa, leading to a decrease in ADCC (146,147). At the same time reports on the effect of sialylation on C1q binding and CDC induced by the classical pathway are inconsistent (132,148). In autoimmunity, lack of sialylation is thought to contribute to chronic inflammation. It has been shown that interleukin 23 (IL-23) induces Th17 cells to release cytokines interleukin 21 (IL-21) and interleukin 22 (IL-22), which decrease the expression ST6GAL1, leading to hyposialylation (149). IgG hyposialylation can also be induced by Tfh cells, particularly Tfh17 and Tfh1 cells. Tfh17 cells decrease the expression of ST6GAL1 from autoantibody-producing B cells via the OX40-OX40L (TNF receptor superfamily) interaction. An increased number of Tfh17 cells expressing OX40 were observed in RA patients, and their frequency was negatively correlated with ST6GAL1 expression. Blocking the OX40-OX40L

pathway resulted in a decrease in Tfh17 cells and an increase in IgG sialylation (150). In addition, interleukin 27 (IL-27) stimulates Tfh1 to produce IFN-γ, which decreases ST6GAL1 expression in cultured B cells by binding to the B cell intrinsic IFN-γR and activating the JAK1/2 signaling pathway (142). The effect of T cell cytokines on IgG sialylation is supported by evidence that T cell-independent B cell activation leads to the synthesis of sialylated IgG, which can suppress B cell activation independently of FcγRIIb (141), and may promote an inhibitory feedback mechanism by binding to CD22 on the B cell surface (151). In addition to inflammatory cytokines, sex hormones are shown to modulate IgG glycosylation. Estrogen induces increase in IgG Fc sialylation through increased expression of ST6GAL1 in splenic plasmablasts, which corelates with the decreased IgG sialylation and increased RA risk under conditions of low estrogen levels (e.g., menopause) (152). In recent years, several studies suggested B cell-independent IgG sialylation (153,154), presumably by hepatic ST6GAL1 present in the circulation, although this appears to be an inflammation-dependent rather than a constitutive process (155). Strikingly, Oswald et al. pointed out in their study that IgG sialylation indeed occurs after release from a B cell but is not dependent on ST6GAL1 activity localized in plasma (156). Furthermore, they demonstrated a model in which IgG glycosylation is driven by intracellular trafficking in B cells, explaining why ST6GAL1 expressed in B cells is dispensable for IgG sialylation *in vivo* (157).

2.3.1.3 Core fucosylation

More than 90% of Fc glycans on IgG in healthy humans have fucose bound to their core, which is in contrast to most other plasma proteins that are not core fucosylated (16,122). The absence of core fucose significantly increases the affinity of IgG for FcγRIIIa and FcγRIIIb (132,158,159). This enhances downstream effector functions, particularly NK cell-mediated ADCC, by up to 100-fold. Although modification of N-glycosylation of IgG is known to have a significant effect on FcγRIIIa binding, several studies have emphasized the role of N-glycosylation of FcγRIIIa in IgG binding affinity. The presence of oligomannose N-glycans on FcγRIIIa resulted in a significant increase in binding affinity for afucosylated IgG (160–162). This finding was associated with decreased expression of α-mannosidase in NK cells (163). Afucosylation has been associated with many diseases (164), but the mechanisms of regulation are still being deciphered. Recently, abnormal expression of the FUT8 and IKZF1 genes in B cells producing thyroid peroxidase antibody (TPOAb) was associated with a decrease in IgG core fucosylation observed in autoimmune thyroid disease (165). These genes have previously been linked to afucosylated IgG N-glycans (120). The exact mechanism is still unclear, but the

IKZF1 gene encodes the transcription factor Ikaros, which may indirectly regulate fucosylation in B cells by promoting the addition of bisecting GlcNAc, which in turn inhibits core fucosylation (120). Of note, several SNPs near the IKZF1 gene have been associated with malignancies, infectious diseases, and autoimmune diseases (166). In addition to genetic predisposition, expression of the relevant enzymes is also altered in pathological conditions. Elevated plasma levels of α-L-fucosidase (FUCA-1) have been significantly associated with chronic inflammation and autoimmune disease (167), raising questions about the role of extracellular IgG defucosylation in inflammation. On the contrary, Plomp et al. found that IgG core fucosylation actually increases with higher degrees of inflammation, as observed in some autoimmune patients (168). Huang et al. investigated further and found that there was increased IgG core fucosylation in the serum of RA patients, accompanied by a decrease in α2,6-sialylation. In addition, α2,6-sialylation of IgG was increased in $Fut8^{-/-}$ mice (169). These results suggest that disease-specific, inflammation-related changes in IgG glycome may play a role in different mechanisms of disease pathophysiology.

2.3.1.4 Bisecting GlcNAc

Only about 10% of all IgG Fc glycans contain a bisecting GlcNAc (135). Bisecting GlcNAc has been identified as a proinflammatory feature in various inflammatory diseases (15). It is known that afucosylated IgG plays a critical role in enhancing ADCC, but it has also been reported that the addition of bisecting GlcNAc to IgG Fc glycans results in slight increase of ADCC (159). However, because the presence of bisecting GlcNAc prevents the addition of the core fucose residue (120,170), it may be difficult to determine the individual roles of these two glycosylation features (159). However, it is known that epigenetic changes and proinflammatory triggers during inflammation lead to an increase in bisecting GlcNAc on IgG Fc glycans. Studies have shown that abnormal methylation in the promoter region of the MGAT3 gene (encoding the N-Acetylglucosaminyltransferase 3 (MGAT3) that produces bisecting GlcNAc structures) leads to a higher abundance of bisecting GlcNAc on IgG glycans in Crohn's disease (CD) patients, suggesting a potential role of bisecting GlcNAc in the development of CD (171). In addition, a study by Ho et al. showed that transforming growth factor β1 (TGF-β1) may have contradictory effects on bisected IgG depending on the state of inflammation and presence of tissue fibrosis (172). Although further research is needed to understand the specific mechanisms that influence the formation of bisected IgG, its role in inflammation is widely recognized.

The addition of **α2,6 sialylation** lowers the binding affinity of IgG for activating **FcγRIIIa**, ultimately decresing **ADCC.** The effect of sialylation on C1q binding and activation of CDC is still ambiguous. Generally, **IgG hyposialylation** is considered a **proinflammatory trait** and associated with many inflammatory diseases.

Bisecting GlcNAc has been identified as a **proinflammatory feature** in various inflammatory diseases. The addition of bisecting GlcNAc to IgG Fc glycans is associated with an increase in **ADCC**.

Agalactosylated IgG is thought to activate the **complement** via the **lectin pathway** by binding to **MBL** and/or the **alternative pathway**. **Galactosylated IgG** is presumably binds to the inhibitory **FcγRIIb** receptor and suppresses **C5a**. However, Fc galactosylation has also been shown to increase the affinity of IgG for **activating FcγRs**, leading to **ADCC**. The effect of galactosylation on **C1q binding and/or CDC activity** is still unclear.

The absence of **core fucose** significantly increases the affinity of IgG for **FcγRIIIa** and **FcγRIIIb,** thereby enhancing downstream effector functions, particularly **NK cell-mediated ADCC**, by up to 100-fold.

Figure 5. Schematic representation of the main IgG N-glycan traits and their proposed proinflammatory and anti-inflammatory properties.

2.4 N-glycosylation in cardiovascular diseases

CVDs are a group of diseases affecting the heart and blood vessels. They include, between the others, acute and chronic coronary artery disease (CAD), heart failure and arrhythmia, stroke, and arterial hypertension (173). CVDs are the leading cause of morbidity and mortality worldwide, as reflected by the fact that the number of deaths from CVDs has steadily increased from 12.1 million in 1990 to 20.5 million in 2021 (1,173). Therefore, primary prevention and early detection of cardiovascular events have significant benefits for improving population health and reducing CVD-related mortality (174,175). Currently, prevention efforts focus primarily on the classic cardiovascular disease risk factors, including nonmodifiable factors such as family history, age, race and sex, as well as smoking, hypertension, hypercholesterolemia, hyperlipidemia, and diabetes, which are usually caused by unhealthy diet, physical inactivity, and alcohol abuse (174). It would be beneficial to identify accurate CVD-specific biological markers, as this would help in prevention and early detection. In recent decades, developments in medicine, biochemistry, and molecular biology have contributed significantly to the discovery of novel potential risk factors and therapeutic targets for CVDs. These include inflammatory mediators (176,177), growth factors (178), markers of hemostasis/thrombosis/ferroptosis (179,180), RNAs (181,182), and posttranslational

modifications (PTMs) of proteins (183,184). PTMs are thought to play an important role in the development and pathogenesis of CVD (183,184). PTMs associated with CVDs are broad, ranging from nonenzymatic (e.g., carbamylation and glycation) to enzymatically regulated ones such as phosphorylation and glycosylation (28,183,184). A growing body of research shows that alterations in protein glycosylation are involved in the CVD development through various molecular mechanisms and thus have significant biomarker potential for disease development and progression as well as for therapeutic monitoring (26,28).

2.4.1 Alterations of N-glycosylation in atherosclerosis

While there are few distinct mechanisms responsible for CVD development, atherosclerosis is the most dominant underlying pathology. It is a progressive process involving dyslipidemia, inflammation, accumulation of immunological cells in the arterial intima, and endothelial dysfunction, leading to the formation of atherosclerotic plaques and arterial lumen narrowing (185). Therefore, elucidating novel molecular mechanisms (e.g., glycosylation) associated with the development of atherosclerosis would be beneficial in prevention of CVDs.

2.4.1.1 The role of N-glycosylation in the process of atherogenesis

Leukocyte recruitment is a key step for the successful initiation of atherosclerosis and occurs predominantly in the inflamed endothelium. Indeed, inflammation is the trigger for the early stages of the atherosclerotic process, and an increase in inflammatory cytokines has been associated with a higher risk of developing CVDs (186) and they are implicated to significantly modulate N-glycan processing (36). Therefore, it is no surprise that N-glycosylation alterations, of both endothelial cells and leukocytes, have been associated with the development of atherosclerosis. The initial stage of leukocyte recruitment is dependent on the interaction of selectins and their ligands. Selectins are Ca^{2+}-dependent lectins whose minimal recognition determinant is (6-sulfo) sLeX epitope on N- and/or O-glycans bound to glycoproteins expressed on surface of the endothelium (36). The synthesis of (6-sulfo) sLeX epitope is regulated by several distinct glycosyltransferases, including ST3GAL4, FUT4 and FUT7. Thus, disrupted expression or activity of these enzymes may be involved in excessive leukocyte trafficking, and consequently in the initiation of atherosclerotic lesions (187). In addition, co-regulated expression of transporters for CMP-sialic acid and GDP-fucose, essential for the synthesis of (6-sulfo) sLeX, occurs in inflammation, which is not common in physiological conditions. Therefore, it has been suggested that there must be an inflammation-induced transcriptional regulation for Golgi membrane transporters that support trafficking of substrates

necessary for synthesis of (6-sulfo) sLeX N-glycans (188). Moreover, presence of sLeX has not been only observed at the endothelial surface; an increased abundance of sLeX epitope together with high branching of N-glycans has been observed on several plasma proteins indicating a systematic response of an organism to inflammation (described in detail in section "The role of N-glycosylation in biological function of plasma proteins").

After capture by selectins, firm endothelial adhesion of leukocytes is mediated by intercellular cell adhesion molecule 1 (ICAM-1) and vascular cell adhesion molecule 1 (VCAM-1). One of the most prominent changes observed on the surface of ICAM-1 and VCAM-1 is increased expression of oligomannose N-glycan structures (29). Increased abundance of oligomannose structures has been implicated to be a consequence of proinflammatory stimulation, possibly by inhibition of early mannose-trimming enzymes (α-mannosidase). Conversely, enzymatic removal of high-mannose N-glycans, or masking mannose residues with lectins, strongly decreased monocyte adhesion under the flow (30). Not surprisingly, increased presence of high-mannose ICAM-1 (HM-ICAM-1) results in high-affinity leukocyte binding (189). In particular, this phenomenon is seen in CD16+ proinflammatory monocytes, which have a higher affinity for HM-ICAM-1 molecules in atherosclerotic lesions compared with complex α-2,6-sialylated ICAM-1 (190,191). Moreover, sialylation of endothelial adhesion molecule β-catenin seems to prevent both atherosclerosis development and monocyte transendothelial migration, however expression of ST6GAL1 was shown to be significantly decreased in the vascular endothelium during atherogenesis, consequently decreasing sialylation (192). In addition, ST6GAL1 downregulation could also result from cleavage by Beta-Site APP-Cleaving Enzyme 1 (BACE1), which is dramatically upregulated during macrophage differentiation (193). Consequential hyposialylation leads to the activation of α4β1 integrins on monocytes, resulting in increased adhesion to the endothelium through VCAM-1.

Furthermore, dysfunction of lipid metabolism is the major risk factor for atherosclerosis. Lipoproteins are known to play a crucial role in atherosclerosis, with low-density lipoprotein (LDL) and very-low-density lipoprotein (VLDL) promoting proatherogenic activities, while high-density lipoprotein (HDL) exhibits multiple anti-atherogenic activities by facilitating the efflux of intracellular cholesterol through reverse cholesterol transport (194). Both HDL and LDL carry highly sialylated N-glycans, which modulate their function (33,195–197). Desialylation of HDL particles reduce their ability of cholesteryl esterification, impairs reverse cholesterol transport, and affects their association with lipases, ultimately impacting plasma triglyceride levels and increasing the risk of CAD. Additionally, under pathological conditions,

aberrations in HDL N-glycosylation, particularly in sialylation, can alter its immunomodulatory capacity (26). HDL glycosylation can also be used as a biomarker; HDL glycome distinguished between individuals who had CAD from those who did not within a group of individuals equally at risk for heart disease (32). In addition, desialylation of LDL N-glycans leads to cellular cholesteryl ester accumulation, contributing to the development of coronary atherosclerosis. The uptake of desialylated LDL by macrophages can be mediated via scavenger and galactose-specific lectin receptors. In contrast, this effect was not observed with fully sialylated LDL particles (26). Mutations in the gene encoding asialoglycoprotein receptor-1 (ASGR-1), a hepatic receptor that removes glycans from the circulation, have been associated with reduced cholesterol levels and a lower risk of CAD (198). Moreover, a recent study indicated that deletion of ASGR-1 has atheroprotective effects in macrophages and *Apoe$^{-/-}$* mice and alters plaque glycome, suggesting ASGR-1 as a therapeutic target and biomarker of atherosclerosis as well as a regulator of plaque glycome (199). Similarly, N-glycosylation of lectin-like oxidized low density lipoprotein receptor 1 (ox-LDL receptor 1) has also been implicated to contribute to the pathogenesis of atherosclerosis (200,201). Furthermore, a study by Betteridge et al. reported visualization of changes in the vascular endothelium after exposure to neuraminidase (202). The enzyme cleaved the sialic acid residues, which reduced the depth of the endothelial glycocalyx and increased vascular permeability. Interestingly, trans sialidase, enzyme which transfers sialic acids from protein donors to other acceptors, has been isolated from human atherogenic serum and suggested to be responsible for desialylation of LDL (203). Therefore, the discovery of this enzyme and the results of subsequent studies led to conclusions about the possible effect of trans sialidase on the initiation and development of atherosclerosis (204). Moreover, sialylation has been demonstrated to be protective against IgG-VLDL interplay in arterial lesion formation in rabbits (205). This was further supported in humans, as it was observed that IgG core-fucosylated digalactosylated monosialylated glycan, FA2G2S1, is strongly negatively correlated with VLDL levels which itself has been associated with hypertriglyceridemia and dyslipidemia in general (39). Worth mentioning are also apolipoproteins, the protein component of lipoproteins, which play an important role in lipid transport, lipoprotein assembly, and receptor recognition. Although glycan repertoire of several apolipoproteins remains undefined, glycan moieties play an integral role in apolipoprotein function. So far determined alterations in apolipoprotein glycosylation revolve mostly around (de)sialylation and correlate with several diseases manifesting in dyslipidemias (206).

2.4.1.2 The role of N-glycosylation in systemic response to atherosclerosis

In addition to significant alterations in the N-glycosylation of endothelial cells and lipoproteins, a similar trend has been observed on several plasma proteins indicating a systematic response of an organism to inflammation (207). A recently published study investigated the association of plasma proteins with coronary atherosclerosis and found that patients with stable plaques had higher levels of acute phase proteins (AGP-1, A1AT, ceruloplasmin and ACT), hemopexin, and HPT compared to patients with unstable plaques. It was suggested that this could be due to the fact that inflammatory processes are more pronounced and persistent in patients with stable fibrous plaques (208). This finding is consistent with previous research indicating that the vascular expression of AACT is associated with human vascular diseases, atherosclerosis of the carotid arteries, and abdominal aortic aneurysm, and that AACT contributes to the stability of plaques (209). Earlier research on sexual dimorphism in carotid atherosclerotic plaques found that the content of acute phase proteins AGP-1 and AACT was significantly increased in lesions in women compared to men (210). Additionally, studies have shown a direct link between elevated ceruloplasmin levels and the frequency of CAD, as well as an association with a higher risk of myocardial infarction (211). Taking into the account the importance of plasma proteins in development of atherosclerotic plaques and importance of glycosylation in protein function, glycome alterations of plasma proteins could lead to significant protein dysfunction that could contribute to atherogenesis. As mentioned previously, most profound changes of plasma proteins include presence of sLeX epitope and increased branching (36). Terminal fucosylation and α2,3 sialylation are critical for sLeX epitope synthesis, and cytokine-mediated upregulation of the hepatic enzymes ST3GAL4 and FUT6 (86), crucial for sLeX biosynthesis, may be responsible for the observed increase in abundance of sLeX epitope. In addition, GlycA, a complex heterogeneous NMR signal originating from a subset of branched N-glycan residues on plasma proteins (72), has been shown to be a strong predictor of CVDs and adverse CV events (21,73,75,212–214). Plasma N-glycans were also shown to be associated with hypercholesterolemia, which is a major risk factor for the development of atherosclerosis. Specifically, high-mannose and complex N-glycans correlated with plasma cholesterol levels (215). Recent study by Wittenbecher et al. showed predictive values of several plasma N-glycans, including complex N-glycans such as FA2G2S1 and A2G2S2, for calculating risk of type 2 diabetes and CVD events (41).

Among myriad of plasma proteins, IgG is crucial for modulating the immune-inflammatory response that plays a key role in the pathogenesis of atherosclerosis (216,217). Atherosclerosis

involves IgG against LDL, oxidized LDL (ox-LDL), and apolipoprotein B (ApoB) (218). While it was found that IgG isolated from atherosclerotic mice greatly promote atherosclerosis (219), high levels of anti-ApoB IgG decrease a risk of coronary events (220). Moreover, as mentioned earlier, *in vitro* experiments have shown that IgG-VLDL interaction contribute to the formation of arterial lesions (205). Therefore, it is not surprising that IgG N-glycosylation is suggested to play an important role in the development of atherosclerosis (among other CVDs) and N-glycosylation alterations have been shown as a risk factor for atherosclerosis, independent of other established risk factors (39,40). To that note, sialylation has been demonstrated to be protective against IgG-VLDL interplay (205), which was further supported in humans, as it was observed that IgG monosialylated glycan structure (FA2G2S1) is strongly inversely correlated with VLDL (39). Also, it was observed that the increased presence of bisecting GlcNAc in IgG glycome was positively associated with atherosclerotic plaques in carotid and femoral arteries. In contrast, sialylated glycans without bisected GlcNAc were negatively associated (39). These alterations (decreased sialylation and increased bisecting GlcNAc) were also indicated to contribute to the development of vascular cognitive impairment in individuals with atherosclerosis (221). Decrease in sialylation of IgG is associated with increased complement activation, which is associated with atherosclerosis and CVD (222,223).

Decreased IgG galactosylation and sialylation are also associated with hypertension (224,225), an established risk factor for CVD, including coronary atherosclerosis (226). Similar trend was observed in a mouse study investigating the link between obesity and hypertension (125). IgG from mice with induced obesity by a high-fat diet (HFD) showed hyposialylation compared to control mice. When transferred to IgG-deficient mice, the hyposialylated IgG caused an increase in blood pressure, demonstrating the functional role of IgG in hypertension development. Notably, in HFD-fed mice supplemented with a sialic acid precursor, N-acetyl-D-mannosamine (ManNAc), IgG sialylation was restored, protecting the mice from obesity-induced hypertension development (125). Lastly, it was found that type 2 diabetes was associated with a decrease in IgG galactosylation and sialylation and an increase in the level of bisected IgG glycoforms (227). The fact that all above mentioned conditions are associated with similar IgG N-glycome traits further validates the "common soil" hypothesis underlying the pathogenesis of cardiometabolic disorder (228).

Interestingly, there is bidirectional causality between IgG N-glycosylation and metabolic traits (BMI, fasting plasma glucose, blood pressure, and lipids, with the corresponding abnormal

conditions being obesity, diabetes, hypertension, and dyslipidemia) through independent biological pathways - further suggesting that reciprocal regulation and coexistence between IgG N-glycans and metabolic traits might accelerate the progression of CVDs (229).

Besides all mentioned conditions presenting higher risk of developing atherosclerosis, aging is a known nonmodifiable risk factor for coronary atherosclerosis, and a link between increased abundance of mannosylated glycans on cardiomyocytes and GDP-mannose pyrophosphorylase B (GMPPB), an enzyme responsible for the synthesis of GDP-mannose, has been demonstrated in the aging heart (230). Interestingly, high plasma mannose concentrations have recently been shown to be associated with CAD independently of traditional CVD risk factors and to be an independent predictor of adverse CVD events (231). Lastly, the total plasma sialic acid (TSA) level, which includes bound and free Neu5Ac, was identified as a key metabolite that increased in the plasma of patients with CAD. Sialic acid and its regulatory enzyme neuraminidase 1 (NEU-1) seem to play a key role in triggering myocardial ischemic injury. Targeting Neu5Ac and NEU-1 may serve as a new avenue for therapeutic intervention of myocardial ischemia injury (232,233).

2.4.2 N-glycosylation in other cardiovascular diseases

Besides the already discussed impact of N-glycosylation changes in development of atherosclerosis, N-glycans also have an immense impact on distinct glycoproteins that are essential for normal cardiovascular function. In aortic valve stenosis (AS), lumican found in the thickened and calcified areas of the aortic valves has been shown to be hypoglycosylated. Specifically, there is a reduced amount of lumican N-glycans carrying keratin sulfate structure compared to the non-thickened and non-calcified areas. This hypoglycosylated lumican has been found to promote the adhesion of macrophages to the aortic valve tissue, leading to chronic inflammation and calcification of AS valves (234). It was also shown that human aortic valve structure is spatially defined by N-glycomic signaling, and any dysregulation can contribute to the AS development (235). In addition, decreased core fucosylation of N-glycans presented on the TGF-β1 receptor (236) and epidermal growth factor receptor (EGFR) (237) has been identified as a pivotal factor in deregulating the signaling pathways involved in cardiac tissue remodeling, thus contributing to cardiac hypertrophy and heart failure (238–240). Ion channels are a crucial protein group for normal cardiovascular function, and their N-glycosylation has been shown to be crucial for their activity. Aberrant N-glycans, especially sialylated structures, on potassium and sodium channels, may impair their gating function,

leading to arrhythmic activities (28). Furthermore, N-glycosylation is spatially and temporally regulated in the myocardium, and different spatio-temporally regulated glycosylation of ion channels, such as sialylation of sodium channels, can significantly impact cardiac electrical signaling (241). Strikingly, it was just recently reported that glycan profiles differ in each region of the cardiac tissue and change with aging (242). Plasma proteins are also becoming a target of interest in CVD, and in addition to their association with atherosclerosis, a recent study has shown that atrial fibrillation (AF) has a unique N-glycan signature in which a decrease in bisecting structures and an increase in FA2G1 show a departure from the changes observed in atherosclerotic CVDs and diabetes (45).

2.5 Glycosylation alterations as potential biomarker for CVDs

Glycosylation changes have the potential to serve as biomarkers for CVD prevention, early detection, and progress monitoring. Researchers have worked to discover glycan biomarkers from easily obtained samples such as plasma, a particular protein isolated from it, or the amount of a particular monosaccharide. GlycA, for example, has been linked to a wide range of CVDs (243). It has been associated with increased risk of various subtypes of heart failure (244), prevalent carotid plaque, peripheral artery disease (213), coronary artery calcium in individuals at low cardiovascular risk (245), subclinical coronary disease (214) and with risk of future cardiovascular events and differential response to treatment (246). In addition, elevated GlycA levels have also been associated with subclinical coronary atherosclerosis in patients with rheumatoid arthritis, psoriasis, and lupus (73,76,247). In addition, GlycA is relatively easy to measure and interpret, and as NMR technology becomes increasingly available in the clinic, relatively rapid adoption of this method in routine clinical laboratories is possible, especially since the cost of analysis is negligible once NMR equipment is acquired. However, the method has its limitations; GlycA is also associated with other diseases related to general inflammation, since its signal comes mainly from acute phase proteins (72).

On the other hand, analysis of total plasma protein N-glycome provides information on the N-glycan composition of proteins included in GlycA signal as well as other proteins such as IgG, α2-macroglobulin, ceruloplasmin and fibrinogen, further extending the information on N-glycosylation. Plasma protein N-glycome has been linked to CVDs and associated complications (41,248), and could potentially serve as a valuable complementary test to current diagnostic biomarkers. It provides more specific information about changes in the abundance of certain N-glycan structures, which allows the development of different models for each CVD

and thus improves the GlycA specificity problem. However, it is more complex and expensive and would likely take longer to be introduced into routine laboratories.

The problem of specificity can be overcome by analyzing glycosylation of specific protein, such as IgG. Findings of a recently published study suggested that IgG N-glycan profiles might be potential biomarker of suboptimal health status (SHS) and shed light on future studies investigating the pathogenesis of progression from SHS to non-communicable diseases (NCDs) such as CVD (23). As mentioned previously, higher abundance of bisecting GlcNAc in IgG N-glycome was positively associated with the presence of femoral and carotid atherosclerotic plaques, whereas sialylated glycans lacking bisecting GlcNAc were negatively associated (39). Moreover, specific IgG N-glycans were associated with CVD risk beyond classical risk factors and clinical parameters, in sex-specific matter. In women, IgG glycoform FA2G1 was inversely associated with CVD risk, whereas in men, a weighted score based on IgG glycoforms FA2BG2S1 and FA2G2S2 was associated with higher CVD risk (40). IgG N-glycosylation is also extensively associated with CHA_2DS_2-VASc score for the stroke risk in patients with AF. In particular, strongest association were found for bisected IgG glycan structure FA2B (45). Recently, a study by Wu et al. developed IgG N-glycosylation cardiovascular age (GlyCage) index for assessing and predicting CV health based on glycomic analysis. The strongest contributors to GlyCage index were fucosylated N-glycans with bisecting GlcNAc (FA2B) and digalactosylated N-glycans with bisecting GlcNAc (A2BG2) (42).

Lastly, the measurement of a specific monosaccharide level in CVD has also shown biomarker potential. High plasma mannose levels were associated with coronary atherosclerosis and myocardial infarction independently of traditional CVD risk factors (231,249), while core fucose level has been associated with cardiac remodeling, hypertrophy, and heart failure (240). The degree of core fucosylation related to cardiac remodeling can be easily detected by core fucose-specific lectins; therefore, core fucosylation can be considered as a candidate biomarker of cardiac pathology (240). In addition to mannose and core fucose, elevated sialic acid concentration in plasma and serum has been positively correlated with the presence of CVD (250), especially with atherosclerosis and CAD, independently of other risk factors (233). Targeting Neu5Ac metabolism seems to be a promising approach for the development of new therapeutic strategies for CVDs. Of all proteins involved in Neu5Ac metabolism, NEU-1 is the most likely therapeutic target, and its inhibition has been proposed as a potential therapeutic approach for atherosclerosis (251–254) and cardiomyopathy (255,256). NEU-1 was identified

as a critical driver of cardiac hypertrophy (257) and its abnormal activation has been linked to CAD and, in particular, to acute myocardial infarction, whereas silencing NEU-1 reduced TSA, improved myocardial ischemic injury, reduced inflammatory cell accumulation, and improved cardiac function (232). Interestingly, some neuraminidase inhibitors such as oseltamivir and zanamivir are recognized as influenza agents, raising the possibility of expanding their medical use to protect cardiomyocytes and the heart from myocardial injury in some cases (232). In this regard, a clinical trial in which patients with chronic heart failure receive either oseltamivir or placebo (in addition to standard heart failure therapy) is currently underway to determine the effect of oseltamivir on serum Neu5Ac levels and to evaluate clinical outcomes in patients with heart failure using oseltamivir (ClinicalTrials.gov Identifier: NCT05008679).

3. MATERIALS AND METHODS

3.1 Participants of the study

3.1.1 CAPIRE study

Blood plasma samples from 472 participants in the CAPIRE study were used for this study. CAPIRE (ClinicalTrials.gov Identifier: NCT02157662) is a multicenter, prospective, observational study designed to identify novel mechanisms to promote or protect against coronary atherothrombosis (44). The study enrolled male and female subjects aged 45 to 75 years who underwent 64-slice computed tomography angiography (CCTA) for suspected coronary atherothrombosis without prior clinical manifestations of CAD, including acute myocardial infarction, unstable angina, chronic stable angina, prior percutaneous or surgical coronary revascularization, and heart failure. On the basis of CCTA, participants were divided into CAD− (clean coronary arteries, n=316) and CAD+ (coronary atherosclerosis extended to > 5 of the 16 segments according to the AHA classification (258), n=156). Samples were collected at two time points – at enrollment in the study and after a 2-year follow-up period. Samples from each participant enrolled in the study were collected in a single dedicated biological bank (SATURNE-1; Mario Negri Institute of Pharmacological Research, Milan, Italy).

The exclusion criteria for CAPIRE participants were as follows: (a) previous cardiovascular events (acute myocardial infarction, unstable angina, chronic stable angina, previous percutaneous or surgical coronary revascularization, heart failure), (b) previous heart disorders such as dilated cardiomyopathy (regardless of aetiology), obstructive hypertrophic cardiomyopathy, atrial fibrillation, and myocarditis, and (c) active inflammatory or neoplastic disease.

Participants were followed up for a total of eight years, with detailed data on health status and the occurrence of major adverse cardiac events (MACE) being recorded.

The CAPIRE study was conducted in accordance with the guidelines of the Declaration of Helsinki on Medical Research Involving Human Subjects and was approved by the Research Ethics Committee at each sampling site, while the research conducted within this dissertation was approved by Ethics Committee of the Faculty of Medicine, University of Zagreb.

3.3 Analysis of N-glycans

Before analysis, all plasma samples were randomly distributed to 96-well sample collection plates, taking into account sex and age of the participants and the study group to which they were assigned. Five standard samples were added to each plate to eliminate experimental error and a one water sample was added as a blank. For the determination of N-glycans of total plasma proteins, 10 µL of plasma was used, whereas IgG was isolated from 100 µL of plasma using a 96-well protein G monolithic plate (BIA Separations, Ajdovščina, Slovenia). N-glycans were enzymatically released from proteins with N-glycosidase F, fluorescently labeled with 2-aminobenzamide (2-AB) and purified. The fluorescently labeled N-glycans were analyzed by HILIC-UHPLC-FLR.

3.3.1 Isolation of IgG

Isolation of IgG from plasma samples followed a protocol based on immunoaffinity chromatography (115). IgG was isolated from 100 µL of plasma using a 96-well protein G monolithic plate. The plasma was first diluted 7-fold with phosphate buffer (1x PBS) and then transferred to a wwPTFE Acroprep 0.45 µm filter plate with polypropylene membrane. Plasma was purified by vacuum filtration using a filter plate manifold stand coupled with the vacuum pump. The filtered plasma (flow-through) was collected in the 96-well 2 mL collection plate and transferred to a preconditioned 96-well protein G monolithic plate.

The protein G monolithic plate was preconditioned before transferring the filtered plasma. Preconditioning was done in the following order: first, the storage buffer was filtered through, then the plate was washed with 2 mL of ultra-pure water, 2 mL of 1x PBS, and 1 mL of 0.1 M formic acid (HCOOH) per well. The plate was then neutralized with 2 mL of 10x PBS per well and equilibration was performed with 2 washes with 2 mL of 1x PBS per well.

After binding of IgG from plasma to protein G within the plate, the protein G monolithic plate was washed three times with 2 mL of 1x PBS per well to remove any unbound proteins. IgG was eluted with addition of 1 mL of 0.1M HCOOH per well of the protein G monolithic plate and collected in a 1 mL collection plate. The collection plate containing the eluted IgG was removed from the manifold stand and 170 µL of neutralization buffer (1M ammonium bicarbonate, NH_4HCO_3) was added to the wells. 300 µL of the IgG eluates was transferred to a new 1 mL collection plate and dried overnight in a concentration centrifuge while the remaining volume of IgG eluate was stored in the freezer at -20 °C.

After IgG isolation, it is necessary to regenerate and properly store the protein G monolithic plate. The protein G monolithic plate was placed on the manifold stand, and a waste collection basin placed under it. First, 2 mL of 0.1M HCOOH was added to each well of the protein G plate, then 2 mL of 10x PBS and lastly 4 mL of 1x PBS. All solutions filtered through the protein G plate. In the end, storage buffer was added on the protein G plate, and the plate was stored at 4 °C.

3.3.2 Deglycosylation, labeling of N-glycans and purification

Dried IgG samples were denatured by resuspension in 30 μL of 1.33% sodium dodecyl sulfate (SDS) followed by incubation at 65°C for 10 minutes. Plasma samples (10 μl) were denatured with the addition of 20 μl of 2% SDS and by incubation at 65 °C for 10 minutes. After denaturation, the protocol for deglycosylation, labeling and purifying of N-glycans was identical for IgG and plasma samples. 10 μL of 4% Igepal was added to neutralize the excess SDS, and samples were put on shaker for 15 minutes. Subsequently, N-glycans were released by adding 1.2 U PNGase F in 10 μL of 5x PBS per sample, followed by overnight incubation at 37 °C.

The released N-glycans were labeled with fluorescent dye 2-AB. 25 μL of the prepared labeling solution was added to each sample, after which the samples were incubated at 65 °C for two hours. Residual dye and other reagents were removed from the sample by solid phase extraction (SPE) using a wwPTFE Acroprep 0.20 μm polypropylene membrane filter plate. After incubation for two hours, 700 μL of acetonitrile (CH_3CN) was added to the samples. The filter plate was preconditioned with 200 μL of 70% ethanol (CH_3CH_2OH), 200 μL ultra-pure water, and then 200 μL 96% CH_3CN per well. The samples were transferred to a filter plate and vacuum was applied to remove solvent from the samples, while the glycans were being bound to the hydrophilic-enriched membranes in the wells of the filter plate. The samples were then washed five times with 200 μL of 96% CH_3CN per well, after which the glycans were eluted from the plate with 180 μL of ultra-pure water.

3.3.3 HILIC-UHPLC-FLR analysis of 2-AB labelled N-glycans

Fluorescently labelled N-glycans were analyzed by HILIC-UHPLC-FLR on an Acquity UPLC H-Class instrument (Waters, USA) consisting of a quaternary solvent manager, a sample manager, and a fluorescence detector set with excitation and emission wavelengths of 250 and 428 nm, respectively. The instrument was controlled by Empower 3 software, build 3471 (Waters, Milford, USA). Samples were kept at 10 °C before injection, and the separation

temperature was 60 °C for IgG and 25 °C for plasma N-glycans. Glycans were separated with Waters chromatographic glycan BEH columns, using a 150 mm column to separate plasma protein glycans and a 100 mm column for the separation of IgG glycans. Solvent A, the hydrophilic fraction of the mobile phase, was 0.1M ammonium formate (NH_4HCO_2), pH 4.4. Solvent B, the hydrophobic fraction of the mobile phase, was 100% CH_3CN (LC-MS grade purity). Plasma protein glycans were separated using a linear gradient of 70-53% solvent B at a flow rate of 0.56 ml/min in a 25-minute analytical run (Table 1). Separation of IgG glycans was performed with a linear gradient of 75-62% solvent B at a flow rate of 0.4 ml/min in a 29-minute analytical run (Table 2).

Table 1. Solvent gradient used during N-glycosylation analysis of total plasma proteins

Time (min)	Flow (mL/min)	Solvent A (%)	Solvent B (%)
0.00	0.561	30	70
1.47	0.561	30	70
24.81	0.561	47	53
25.50	0.250	100	0
28.00	0.250	100	0
29.00	0.250	30	70
32.50	0.561	30	70
45.00	0.400	0	100
55.00	0.000	0	100

Table 2. Solvent gradient used during N-glycosylation analysis of IgG

Time (min)	Flow (mL/min)	Solvent A (%)	Solvent B (%)
0.00	0.400	25	75
29.00	0.400	38	62
30.00	0.400	100	0
32.00	0.400	100	0
33.00	0.400	25	75
38.00	0.400	25	75
39.00	0.400	0	100
47.00	0.000	0	100

Samples for analysis were prepared by mixing with 100% CH_3CN (LC-MS purity level) in a ratio of 25:75 (v:v) for IgG N-glycans, and 30:70 (v:v) for plasma proteins N-glycans. The method was calibrated using an external standard of hydrolyzed and 2-AB labeled glucose oligomers (dextran), by means of which the retention times of individual glycans were

converted into glucose units (GU). After the system has been equilibrated to starting conditions and the FLR detector has been stabilized, an analysis was run. In each UHPLC analysis, samples were run along with blanks and internal UHPLC standards prepared in-house following internal standardized operational protocol (2-AB labeled N-glycans from pooled IgG). Data processing was performed using an automatic processing method with a traditional integration algorithm, after which each chromatogram was manually corrected to maintain the same intervals of integration for all the samples. Before manual integration, quality control (QC) of all chromatograms was performed. This included sufficient intensity of the signal for the integration and acceptable shape (without tailing, fronting, and peak splitting) of all peaks, absence of baseline drift, absence of significant shift of chromatogram peaks (≤ 0.05 glucose units) and dextran ladder (≤ 0.06 min), and absence of any unexpected peaks within the chromatogram. Chromatogram of total plasma proteins was separated into 39 glycan (chromatographic) peaks (GP1 – GP39), and the chromatogram of IgG into 24 glycan (chromatographic) peaks (GP1 – GP24) (Figures 6 and 7, Table 3) within which the glycan structures were previously determined and known (53,108). The relative amount of glycans within each peak is expressed as a percentage of the total area of all integrated peaks, calculated according to the following formula:

$$GP1 = \frac{GP1}{GP_{total}} \times 100$$

where GP_{total} represents the total integrated area, i.e., the sum of all individual GPs (GP1 + GP2 + ... + GP39, for plasma protein glycans, and GP1 + GP2 + ... + GP24 for IgG glycans). The amount of glycans for the remaining glycan GPs of plasma proteins or IgG is calculated in the same way. This procedure is referred to as normalization of GPs to the total area of the chromatogram.

In addition to the directly measured glycan traits, derived glycan traits were also calculated based on similar structural features of the analyzed glycans (e.g., number of glycan branches, presence of core fucose, oligomannose glycans, etc.). A total of 9 derived traits were calculated for the N-glycome of IgG and 16 for the N-glycome of total plasma proteins. Table 4 shows the calculation of the derived glycan traits.
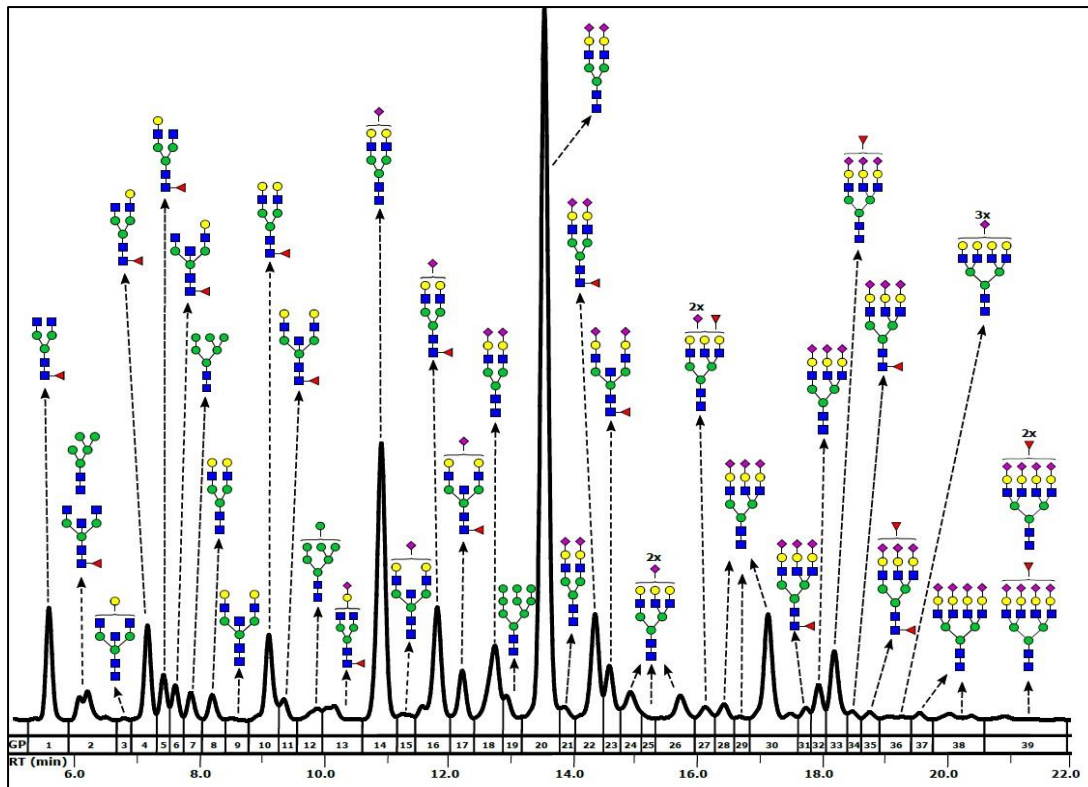
Figure 6. Representative chromatogram of N-glycans released from total plasma proteins. Blue squares, green circles, yellow circles, purple diamonds, and red triangles represent N-acetylglucosamine (GlcNAc), mannose, galactose, N-acetylneuraminic acid (sialic acid), and fucose. GP – glycan peak.
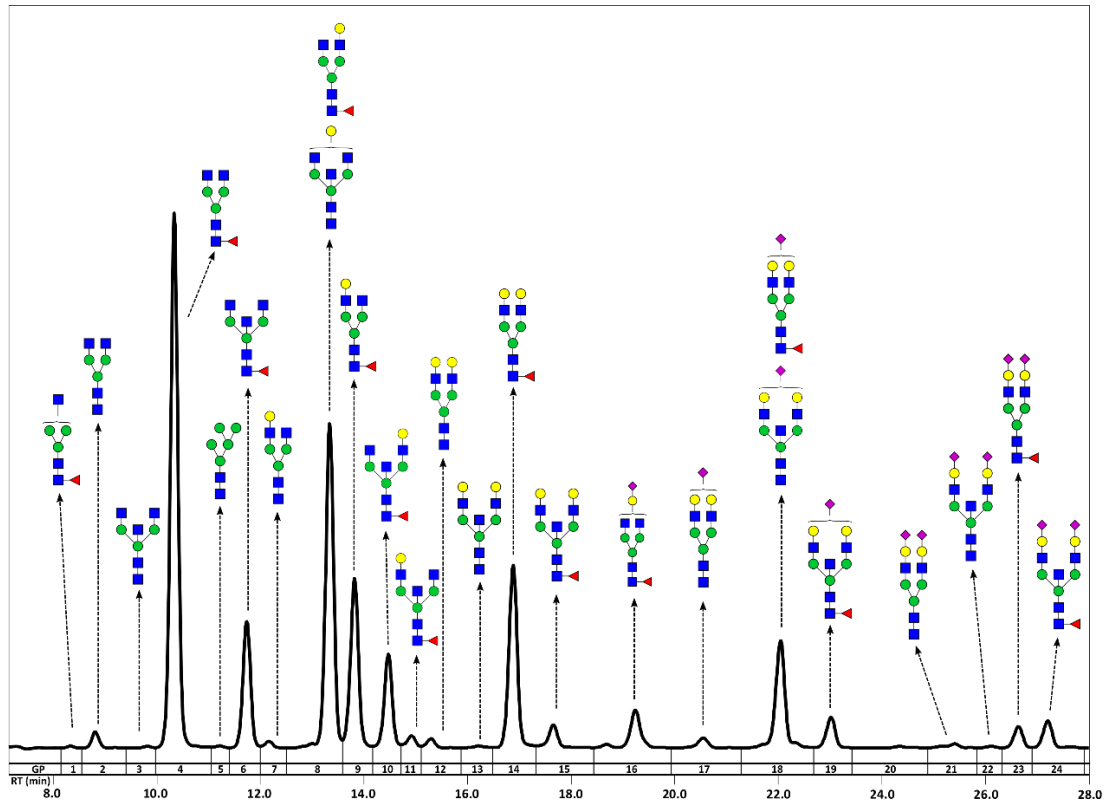
Figure 7. Representative chromatogram of N-glycans released from IgG. Blue squares, green circles, yellow circles, purple diamonds, and red triangles represent N-acetylglucosamine (GlcNAc), mannose, galactose, N-acetylneuraminic acid (sialic acid), and fucose. GP – glycan peak.

Table 3. Detailed description of major glycan structures corresponding to every plasma protein and IgG individual glycan peak (GP)*

Origin	Glycan peak	Glycan structure	Description
plasma	GP1	FA2	core fucosylated, biantennary
plasma	GP2	FA2B; M5	core fucosylated, biantennary with bisecting GlcNAc; high mannose
plasma	GP3	A2BG1	monogalactosylated, biantennary with bisecting GlcNAc
plasma	GP4	FA2[6]G1	core fucosylated and monogalactosylated, biantennary
plasma	GP5	FA2[3]G1	core fucosylated and monogalactosylated, biantennary
plasma	GP6	FA2[6]BG1	core fucosylated and monogalactosylated, biantennary with bisecting GlcNAc
plasma	GP7	M6	high mannose
plasma	GP8	A2G2	digalactosylated, biantennary
plasma	GP9	A2BG2	digalactosylated, biantennary with bisecting GlcNAc
plasma	GP10	FA2G2	core fucosylated, digalactosylated, biantennary
plasma	GP11	FA2BG2	core fucosylated, digalactosylated, biantennary with bisecting GlcNAc
plasma	GP12	M7	high mannose
plasma	GP13	FA2G1S1	core fucosylated, monogalactosylated and monosialylated biantennary
plasma	GP14	A2G2S1	digalactosylated and monosialylated biantennary
plasma	GP15	A2BG2S1	digalactosylated and monosialylated biantennary with bisecting GlcNAc
plasma	GP16	FA2G2S1	core fucosylated, digalactosylated and monosialylated biantennary
plasma	GP17	FA2BG2S1	core fucosylated, digalactosylated and monosialylated biantennary with bisecting GlcNAc
plasma	GP18	A2G2S2	digalactosylated and disialylated biantennary
plasma	GP19	M9	high mannose
plasma	GP20	A2G2S2	digalactosylated and disialylated biantennary
plasma	GP21	A2G2S2	digalactosylated and disialylated biantennary
plasma	GP22	FA2G2S2	core fucosylated, digalactosylated and disialylated biantennary
plasma	GP23	FA2BG2S2	core fucosylated, digalactosylated and disialylated biantennary with bisecting GlcNAc
plasma	GP24	A3G3S2	trigalactosylated and disialylated triantennary
plasma	GP25	A3G3S2	trigalactosylated and disialylated triantennary

Table 3 - continued

Origin	Glycan peak	Glycan structure	Description
plasma	GP26	A3G3S2	trigalactosylated and disialylated triantennary
plasma	GP27	A3F1G3S2	antennary fucosylated, trigalactosylated and disialylated triantennary
plasma	GP28	A3G3S3	trigalactosylated and trisialylated triantennary
plasma	GP29	A3G3S3	trigalactosylated and trisialylated triantennary
plasma	GP30	A3G3S3	trigalactosylated and trisialylated triantennary
plasma	GP31	FA3G3S3	core fucosylated, trigalactosylated and trisialylated triantennary
plasma	GP32	A3G3S3	trigalactosylated and trisialylated triantennary
plasma	GP33	A3F1G3S3	antennary fucosylated, trigalactosylated and trisialylated triantennary
plasma	GP34	FA3G3S3	core fucosylated, trigalactosylated and trisialylated triantennary
plasma	GP35	FA3F1G3S3	core fucosylated, antennary fucosylated, trigalactosylated and trisialylated triantennary
plasma	GP36	A4G4S3	tetragalactosylated and trisialylated tetraantennary
plasma	GP37	A4G4S4	tetragalactosylated and tetrasialylated tetraantennary
plasma	GP38	A4G4S4	tetragalactosylated and tetrasialylated tetraantennary
plasma	GP39	A4F1G4S4; A4F2G4S4	antennary fucosylated, tetragalactosylated and tetrasialylated tetraantennary; antennary difucosylated, tetragalactosylated and tetrasialylated tetraantennary;
Origin	**Glycan peak**	**Glycan structure**	**Description**
IgG	GP1	FA1	core fucosylated, monoantennary
IgG	GP2	A2	agalactosylated, biantennary
IgG	GP3	A2B	biantennary with bisecting GlcNAc
IgG	GP4	FA2	core fucosylated, biantennary
IgG	GP5	M5	high mannose
IgG	GP6	FA2B	core fucosylated, biantennary with bisecting GlcNAc
IgG	GP7	A2[3]G1	monogalactosylated, biantennary
IgG	GP8	A2BG1; FA2[6]G1	monogalactosylated, biantennary with bisecting GlcNAc; core fucosylated and monogalactosylated, biantennary
IgG	GP9	FA2[3]G1	core fucosylated and monogalactosylated, biantennary
IgG	GP10	FA2[6]BG1	core fucosylated and monogalactosylated, biantennary with bisecting GlcNAc
IgG	GP11	FA2[3]BG1	core fucosylated and monogalactosylated, biantennary with bisecting GlcNAc
IgG	GP12	A2G2	digalactosylated, biantennary

Table 3 - continued

IgG	GP13	A2BG2	digalactosylated, biantennary with bisecting GlcNAc
IgG	GP14	FA2G2	core fucosylated, digalactosylated, biantennary
IgG	GP15	FA2BG2	core fucosylated, digalactosylated, biantennary with bisecting GlcNAc
IgG	GP16	A2BG1S1	monogalactosylated and monosialylated biantennary with bisecting GlcNAc
IgG	GP17	A2G2S1	digalactosylated and monosialylated biantennary
IgG	GP18	A2BG2S1; FA2G2S1	digalactosylated and monosialylated biantennary with bisecting GlcNAc; core fucosylated, digalactosylated and monosialylated biantennary
IgG	GP19	FA2BG2S1	core fucosylated, digalactosylated and monosialylated biantennary with bisecting GlcNAc
IgG	GP20	structure not determined	
IgG	GP21	A2G2S2	digalactosylated and disialylated biantennary
IgG	GP22	A2BG2S2	digalactosylated and disialylated biantennary with bisecting GlcNAc
IgG	GP23	FA2G2S2	core fucosylated, digalactosylated and disialylated biantennary
IgG	GP24	FA2BG2S2	core fucosylated, digalactosylated and disialylated biantennary with bisecting GlcNAc

*structure abbreviations – all N-glycans have two core GlcNAcs; F at the start of the abbreviation indicates a core-fucose α1,6-linked to the inner GlcNAc; Mx, number (x) of mannose on core GlcNAcs; Ax, number of antenna (GlcNAc) on trimannosyl core; A2, biantennary with both GlcNAcs as β1,2-linked; A3, triantennary with a GlcNAc linked β1,2 to both mannose and the third GlcNAc linked β1,4 to the α1,3 linked mannose; A4, GlcNAcs linked as A3 with additional GlcNAc β1,6 linked to α1,6 mannose; B, bisecting GlcNAc linked β1,4 to β1,3 mannose; G(x), number (x) of β1,4 linked galactose on antenna; F(x), number (x) of fucose linked α1,3 to antenna GlcNAc; S(x), number (x) of sialic acids linked to galactose

Table 4. Derived glycan traits calculated from initial glycan peaks

Derived plasma glycan traits	Description	Formula
LB	Proportion of mono- and biantennary structures in the total plasma N-glycome	GP1+GP2/2+GP3+GP4+GP5+GP6+GP7+GP8+GP9+GP10+GP11+ GP12+GP13+GP14+GP15+GP16+GP17+GP18+GP20+GP21+GP22+GP23
HB	Proportion of tri- and tetraantennary structures in the total plasma N-glycome	GP24+GP25+GP26+GP27+GP28+GP29+GP30+GP31+GP32+GP33+ GP34+GP35+GP36+GP37+GP38+GP39
G0	Proportion of agalactosylated structures in the total plasma N-glycome	GP1+GP2/2
G1	Proportion of monogalactosylated structures in the total plasma N-glycome	GP3+GP4+GP5+GP6+GP12+GP13
G2	Proportion of digalactosylated structures in the total plasma N-glycome	GP8+GP9+GP10+GP11+GP14+GP15+GP16+GP17+GP18+GP20+ GP21+GP22+GP23
G3	Proportion of trigalactosylated structures in the total plasma N-glycome	GP24+GP25+GP26+GP27+GP28+GP29+GP30+GP31+GP32+GP35
G4	Proportion of tetragalactosylated structures in the total plasma N-glycome	GP33+GP34+GP36+GP37+GP38+GP39
S0	Proportion of asialylated structures in the total plasma N-glycome	GP1+GP2/2+GP3+GP4+GP5+GP6+GP8+GP9+GP10+GP11
S1	Proportion of monosialylated structures in the total plasma N-glycome	GP12+GP13+GP14+GP15+GP16+GP17
S2	Proportion of disialylated structures in the total plasma N-glycome	GP18+GP20+GP21+GP22+GP23+GP24+GP25+GP26
S3	Proportion of trisialylated structures in the total plasma N-glycome	GP27+GP28+GP29+GP30+GP31+GP32+GP33+GP34+GP35
S4	Proportion of tetrasialylated structures in the total plasma N-glycome	GP36+GP37+GP38+GP39
B	Proportion of structures containing bisecting GlcNAc in the total plasma N-glycome	GP2/2+GP3+GP6+GP9+GP11+GP12+GP15+GP17+GP21+GP23
HM	Proportion of high mannose structures in the total plasma N-glycome	GP2/2+GP7+GP19
CF	Proportion of structures containing core fucose in the total plasma N-glycome	GP1+GP2/2+GP4+GP5+GP6+GP10+GP11+GP13+GP16+GP17+GP22 +GP23+GP29+GP31
AF	Proportion of structures containing antennary fucose in the total plasma N-glycome	GP32+GP35+GP39

Table 4 - continued

Derived IgG glycan traits	Description	Formula
G0	Proportion of agalactosylated structures in the total IgG N-glycome	GP1+GP2+GP3+GP4+GP5+GP6
G1	Proportion of monogalactosylated structures in the total IgG N-glycome	GP7+GP8+GP9+GP10+GP11+GP16
G2	Proportion of digalactosylated structures in the total IgG N-glycome	GP12+GP13+GP14+GP15+GP17+GP18+GP19+GP21+GP22+GP23+GP24
S0	Proportion of asialylated structures in the total IgG N-glycome	GP1+GP2+GP3+GP4+GP5+GP6+GP7+GP8+GP9+GP10+GP11+GP12 +GP13+GP14+GP15
S1	Proportion of monosialylated structures in the total IgG N-glycome	GP16+GP17+GP18+GP19
S2	Proportion of disialylated structures in the total IgG N-glycome	GP21+GP22+GP23+GP24
B	Proportion of structures containing bisecting GlcNAc in the total IgG N-glycome	GP3+GP6+GP10+GP11+GP13+GP15+GP19+GP22+GP24
CF	Proportion of structures containing core fucose in the total IgG N-glycome	GP1+GP4+GP6+GP8+GP9+GP10+GP11+GP14+GP15+GP16+GP18+ GP19+GP23+GP24
FBS1/(FS1+FBS1)	Proportion of bisecting GlcNAc in all fucosylated monosialylated structures	GP19 / SUM(GP16 + GP18 + GP19)
FBS1/FS1	Proportion of core fucosylated monosialylated with and without bisecting GlcNAc	GP19 / SUM(GP16 + GP18)
FGS/(F+FG+FGS)	Proportion of sialylated glycans of all fucosylated structures without bisecting GlcNAc	SUM(GP16 + GP18 +GP23) / SUM(GP16 + GP18 + GP23 + GP4 + GP8 + GP9 + GP14)

3.4 Statistical analysis

To remove experimental variation from the measurements, normalization and batch correction was performed on the UHPLC glycan data. To make measurements across samples comparable, normalization by total area was performed. Prior to the batch correction, normalized glycan measurements were log-transformed due to right-skewness of their distributions and the multiplicative nature of batch effects. Batch correction was performed on log-transformed measurements using the ComBat method (R package sva), where the technical source of variation (which sample was analyzed on which plate) was modelled as batch covariate. To correct measurements for experimental noise, estimated batch effects were subtracted from log-transformed measurements.

Data were analyzed and visualized using R programming language (version 4.0.2).

Association analyses between CAD status and baseline glycomic measurements were performed using a regression model. Analyses included glycan measurement as dependent continuous variable, CAD status was included as independent variable, with age and sex included as additional covariates. To gain insight into associations between N-glycome and CAD separately in women and men, sex-stratified analyses were performed. For sex-stratified analyses of association between CAD status and baseline glycomic measurements, two regression models were used. In model 1, glycan measurements were included as dependent continuous variable; CAD status was included as independent variable, with age included as additional covariate. In model 2, glycan measurements were included as dependent continuous variable, and CAD status was included as independent variable, with age, BMI, smoking, and diabetes included as additional covariates. For sex-stratified two-time points analyses of samples through their observation period, two linear mixed-effects models (LMM) were implemented. In first LMM model, glycan measurements were included as dependent continuous variable, time, CAD status, age, and interaction between time and CAD (CAD:time) status were modelled as fixed effects, while individual sample ID was modeled as a random intercept. In second LMM model, glycan measurements were included as dependent continuous variable, time, CAD status, age, BMI, smoking, diabetes, BMI:time, smoking:time, diabetes:time, and CAD:time were modelled as a fixed effects, while individual sample ID was modeled as a random intercept. Prior to analyses, glycan variables were all transformed to standard Normal distribution (mean = 0, sd = 1) by inverse transformation of ranks to Normality (R package "GenABEL", function rntransform). Using rank transformed variables

in analyses makes estimated effects of different glycans in different cohorts comparable as transformed glycan variables have the same standardized variance. False discovery rate was controlled using Benjamini–Hochberg procedure (function p.adjust(method = "BH")).

To examine the relationship between N-glycans and the occurrence of MACE, time-to-event data were compared using cox proportional-hazards model. p-values less than 0.05 were considered significant. Kaplan-Meier curves were utilized for visualization of the survival probabilities.

4. RESULTS

N-glycome composition was analyzed in CAPIRE participants classified by CCTA into CAD- (clean coronary arteries, n = 316) and CAD+ (diffuse coronary atherosclerosis with or without coronary stenosis, n = 156), whose samples were collected at inclusion point and after the 2-year follow up period. Descriptive information on the included participants is provided in Table 5. Briefly, participants in the CAD+ category were more often male, older, and heavier than subjects in the CAD- category; most clinical and metabolic parameters differed between the two groups, as expected. At the two-year follow-up point, a total of 285 samples were collected – CAD+ (101) and CAD− (184).

Table 5. Characteristics of the participants at inclusion point

	All population (n=472)	CAD- (n=316)	CAD+ (n=156)
Age (y), median (IQR)	60.2 (52.6-67)	56.7 (50.9-65.8)	64.7 (58-69.6)
Sex (W), n %	42%	53%	19%
BMI (kg/m^2), median (IQR)	25.9 (23.7-29)	25.4 (23.2-28.2)	27.1 (24.7-29.9)
Diabetes, n (%)	12%	8%	21%
Smoking, n (%)	25%	21%	35%

4.1 Association of N-glycosylation with coronary artery disease

An analysis of differences between CAD+ and CAD− cases was performed using a regression model, with age (and BMI, smoking, and diabetes) included as additional covariates to minimize the impact of these risk factors on the results. While no statistically significant differences were detected in IgG N-glycome (Appendix 2), several statistically significant differences were observed in plasma N-glycome (Table 6).

Firstly, the ability of plasma N-glycans to discriminate individuals with coronary atherosclerosis from those with clear coronary arteries at the inclusion point of the study was investigated. The performance of derived plasma N-glycan traits obtained by averaging specific glycosylation features (refer to Table 3 for detailed descriptions of the derived traits) was evaluated. The analysis revealed that out of the 16 derived plasma glycan traits examined, 10 exhibited significant differences (adjusted p-value < 0.05) between participants with coronary artery disease (CAD+) and those without (CAD-). Notably, glycans with low branching and monogalactosylation along with core fucose displayed a significant negative association with CAD+, while more complex highly branched (tri- and tetraantennary), sialylated glycans with antennary fucose were significantly positively associated with CAD+ participants (Table 6).

Subsequently, a comparison of directly measured glycan traits between the CAD+ and CAD-groups was conducted. Among the 39 directly measured plasma glycan traits (GPs) examined, 20 showed significant differences between the two groups (Table 6). Most pronounced differences (adjusted p-value < 0.001) between the studied groups were observed in glycan peaks GP32, GP35, and GP13. Noteworthy, even after further adjustments for diabetes, smoking, and BMI, the associations remained positively statistically significantly between CAD+ and two plasma N-glycan structures: GP35 (core fucosylated, trigalactosylated and trisialylated structure with core fucose) and GP7 (a high-mannose structure) (Appendix 3 and 4).

Table 6. Statistical analysis of associations between plasma protein N-glycosylation traits and coronary artery disease at the time of inclusion. Glycan data were adjusted for age and sex, whereas the false discovery rate was controlled by the Benjamini-Hochberg method. Only statistically significant differences are shown.

Glycan trait	Effect	SE	p-value	p_{adj}-value
GP4	-0.29	0.1069	5.83E-03	1.29E-02
GP5	-0.31	0.1064	3.13E-03	8.61E-03
GP7	-0.35	0.1057	1.07E-03	5.75E-03
GP9	-0.34	0.1067	1.27E-03	5.75E-03
GP10	-0.32	0.0993	1.12E-03	5.75E-03
GP11	-0.34	0.1065	1.48E-03	5.75E-03
GP13	-0.46	0.1062	1.61E-05	2.94E-04
GP15	-0.29	0.1059	5.48E-03	1.29E-02
GP16	-0.33	0.1030	1.27E-03	5.75E-03
GP17	-0.32	0.1066	2.63E-03	7.62E-03
GP18	-0.33	0.1067	2.02E-03	6.55E-03
GP20	0.39	0.1072	2.47E-04	2.26E-03
GP26	0.27	0.1043	9.17E-03	1.80E-02
GP27	0.32	0.0994	1.36E-03	5.75E-03
GP32	0.52	0.1050	9.98E-07	2.74E-05
GP33	0.37	0.0995	1.84E-04	2.26E-03
GP34	0.23	0.1034	2.50E-02	4.58E-02
GP35	0.51	0.1022	7.55E-07	2.74E-05
GP37	-0.27	0.1042	8.54E-03	1.80E-02
GP39	0.29	0.1050	5.37E-03	1.29E-02
AF	0.37	0.1003	2.31E-04	2.26E-03
B	-0.28	0.1080	8.85E-03	1.80E-02
CF	-0.34	0.1074	1.57E-03	5.75E-03
G1	-0.37	0.1065	6.12E-04	4.21E-03
G3	0.31	0.1074	4.06E-03	1.06E-02
HB	0.30	0.1074	5.88E-03	1.29E-02
LB	-0.26	0.1076	1.48E-02	2.80E-02
S0	-0.32	0.1078	2.59E-03	7.62E-03
S2	0.38	0.1073	3.45E-04	2.71E-03
S3	0.34	0.1074	1.76E-03	6.06E-03

4.1.1 Sex-stratified association of N-glycosylation with coronary artery disease

Published data indicates strong sex-specific differences of protein N-glycome in CVD (40,41), therefore sex-stratified N-glycan analysis was further performed to investigate sex-mediated association with CAD.

4.1.1.1 Sex-stratified association of plasma N-glycosylation with coronary artery disease

At inclusion point, significant plasma N-glycan differences were observed in both women and men, going in the same direction regardless of sex, supporting cumulative statistically significant differences observed in Table 6. All N-glycan abundances for CAD+ and CAD- cases stratified by sex are shown in Tables 7 and 8. In women with angiographically diagnosed CAD, 11 of the 39 directly measured plasma glycan traits (GPs) and two derived glycosylation traits differed significantly between CAD+ and CAD- cases, while in men this was observed for eight out of 39 measured GPs and four derived glycosylation traits. In general, a statistically significant increase in highly branched (tri- and tetraantennary), more complex sialylated glycan species with antennary fucose was observed in CAD+ (Table 7 and 8). Glycans that showed the most significant differences between the studied groups (adjusted p-value < 0.01) are shown on Figure 8.

Table 7. Statistical analysis of sex-stratified associations between 16 derived plasma protein N-glycosylation traits and coronary artery disease at the time of inclusion. Glycan data were adjusted for age, whereas false discovery rates were controlled for by the Benjamini-Hochberg method. Statistically significant differences are in bold.

Glycan trait	Women				Men			
	effect	SE	p-value	p_{adj}-value	effect	SE	p-value	p_{adj}-value
AF	0.73	0.1883	1.17E-04	**3.75E-03**	0.25	0.1253	4.71E-02	1.22E-01
B	-0.33	0.1990	9.33E-02	1.82E-01	-0.23	0.1285	7.13E-02	1.60E-01
CF	-0.29	0.1971	1.31E-01	2.32E-01	-0.34	0.1274	8.00E-03	**3.83E-02**
G0	0.16	0.1839	3.74E-01	4.93E-01	-0.20	0.1276	1.16E-01	2.17E-01
G1	-0.31	0.1989	1.16E-01	2.17E-01	-0.37	0.1257	2.99E-03	**2.22E-02**
G2	-0.27	0.1851	1.38E-01	2.35E-01	0.19	0.1287	1.46E-01	2.42E-01
G3	0.35	0.1952	7.26E-02	1.60E-01	0.27	0.1284	3.64E-02	1.05E-01
G4	0.51	0.1952	8.92E-03	**3.94E-02**	-0.05	0.1294	6.96E-01	7.42E-01
HB	0.39	0.1943	4.12E-02	1.16E-01	0.24	0.1286	6.38E-02	1.49E-01
HM	0.05	0.2018	8.08E-01	8.46E-01	-0.23	0.1274	7.06E-02	1.60E-01
LB	-0.38	0.1946	4.72E-02	1.22E-01	-0.20	0.1288	1.21E-01	2.19E-01
S0	-0.16	0.2003	4.09E-01	5.30E-01	-0.37	0.1272	4.02E-03	**2.42E-02**
S1	-0.46	0.1881	1.50E-02	6.12E-02	-0.09	0.1287	4.75E-01	5.70E-01
S2	0.14	0.2003	4.77E-01	5.70E-01	0.43	0.1266	6.69E-04	**1.05E-02**
S3	0.43	0.1938	2.49E-02	8.82E-02	0.28	0.1283	2.65E-02	8.83E-02
S4	0.47	0.1961	1.56E-02	6.12E-02	-0.05	0.1294	6.88E-01	7.42E-01

Table 8. Statistical analysis of sex-stratified associations between directly measured plasma protein N-glycosylation traits and coronary artery disease at the time of inclusion. Glycan data were adjusted for age, whereas false discovery rates were controlled by the Benjamini-Hochberg method. Statistically significant differences are in bold.

Glycan trait	Women				Men			
	effect	SE	p-value	p_{adj}-value	effect	SE	p-value	p_{adj}-value
GP1	0.14	0.1864	4.49E-01	5.70E-01	-0.17	0.1278	1.83E-01	2.75E-01
GP2	0.11	0.1871	5.65E-01	6.54E-01	-0.18	0.1282	1.66E-01	2.56E-01
GP3	-0.11	0.2019	5.96E-01	6.69E-01	-0.05	0.1290	6.69E-01	7.29E-01
GP4	-0.23	0.1996	2.37E-01	3.43E-01	-0.31	0.1259	1.41E-02	5.97E-02
GP5	-0.21	0.2001	2.95E-01	4.11E-01	-0.36	0.1264	4.19E-03	**2.42E-02**
GP6	-0.03	0.1997	8.76E-01	8.88E-01	-0.25	0.1277	4.77E-02	1.22E-01
GP7	-0.08	0.1998	7.01E-01	7.42E-01	-0.40	0.1248	1.24E-03	**1.52E-02**
GP8	-0.14	0.1990	4.77E-01	5.70E-01	0.02	0.1279	8.79E-01	8.88E-01
GP9	-0.54	0.1945	5.10E-03	**2.67E-02**	-0.27	0.1278	3.58E-02	1.05E-01
GP10	-0.38	0.1698	2.61E-02	8.83E-02	-0.36	0.1217	3.12E-03	**2.22E-02**
GP11	-0.27	0.1930	1.64E-01	2.56E-01	-0.36	0.1264	4.69E-03	**2.58E-02**
GP12	0.09	0.2015	6.50E-01	7.15E-01	-0.08	0.1288	5.35E-01	6.33E-01
GP13	-0.72	0.1917	1.68E-04	**3.75E-03**	-0.33	0.1273	8.94E-03	**3.94E-02**
GP14	0.11	0.2003	5.82E-01	6.67E-01	0.24	0.1252	5.23E-02	1.31E-01
GP15	-0.53	0.1954	6.51E-03	**3.25E-02**	-0.19	0.1284	1.39E-01	2.35E-01
GP16	-0.53	0.1740	2.31E-03	**2.21E-02**	-0.26	0.1263	3.52E-02	1.05E-01
GP17	-0.30	0.1971	1.18E-01	2.17E-01	-0.30	0.1277	1.85E-02	7.03E-02
GP18	-0.59	0.1954	2.61E-03	**2.21E-02**	-0.21	0.1277	9.45E-02	1.82E-01
GP19	0.24	0.1960	2.16E-01	3.21E-01	-0.02	0.1279	8.80E-01	8.88E-01
GP20	0.34	0.1986	8.09E-02	1.69E-01	0.38	0.1271	2.56E-03	**2.21E-02**
GP21	-0.17	0.1983	3.76E-01	4.93E-01	0.15	0.1287	2.32E-01	3.40E-01
GP22	0.12	0.1990	5.56E-01	6.50E-01	0.22	0.1287	8.97E-02	1.82E-01
GP23	-0.40	0.1993	4.20E-02	1.16E-01	0.01	0.1285	9.36E-01	9.36E-01
GP24	-0.27	0.2004	1.68E-01	2.56E-01	-0.09	0.1282	4.59E-01	5.70E-01
GP25	-0.29	0.1999	1.47E-01	2.42E-01	-0.07	0.1274	5.91E-01	6.69E-01
GP26	0.18	0.1970	3.59E-01	4.82E-01	0.29	0.1277	2.07E-02	7.61E-02
GP27	0.64	0.1911	8.44E-04	**1.16E-02**	0.22	0.1250	8.16E-02	1.69E-01
GP28	-0.37	0.2000	6.06E-02	1.45E-01	-0.06	0.1257	6.44E-01	7.15E-01
GP29	-0.29	0.2015	1.49E-01	2.42E-01	-0.18	0.1243	1.53E-01	2.44E-01
GP30	-0.15	0.1990	4.58E-01	5.70E-01	-0.02	0.1271	8.79E-01	8.88E-01
GP31	0.19	0.2018	3.41E-01	4.67E-01	0.21	0.1253	9.33E-02	1.82E-01
GP32	0.55	0.1893	3.56E-03	**2.31E-02**	0.48	0.1253	1.46E-04	**3.75E-03**
GP33	0.71	0.1891	1.70E-04	**3.75E-03**	0.26	0.1253	3.57E-02	1.05E-01
GP34	0.35	0.1984	7.89E-02	1.69E-01	0.19	0.1273	1.33E-01	2.32E-01
GP35	0.83	0.1831	8.22E-06	**9.05E-04**	0.39	0.1255	1.90E-03	**2.08E-02**
GP36	0.57	0.1938	3.22E-03	**2.22E-02**	-0.09	0.1288	4.73E-01	5.70E-01
GP37	-0.22	0.1999	2.60E-01	3.71E-01	-0.27	0.1252	3.23E-02	1.05E-01
GP38	0.37	0.1967	5.50E-02	1.34E-01	-0.12	0.1290	3.44E-01	4.67E-01
GP39	0.68	0.1908	4.13E-04	**7.57E-03**	0.13	0.1266	2.93E-01	4.11E-01
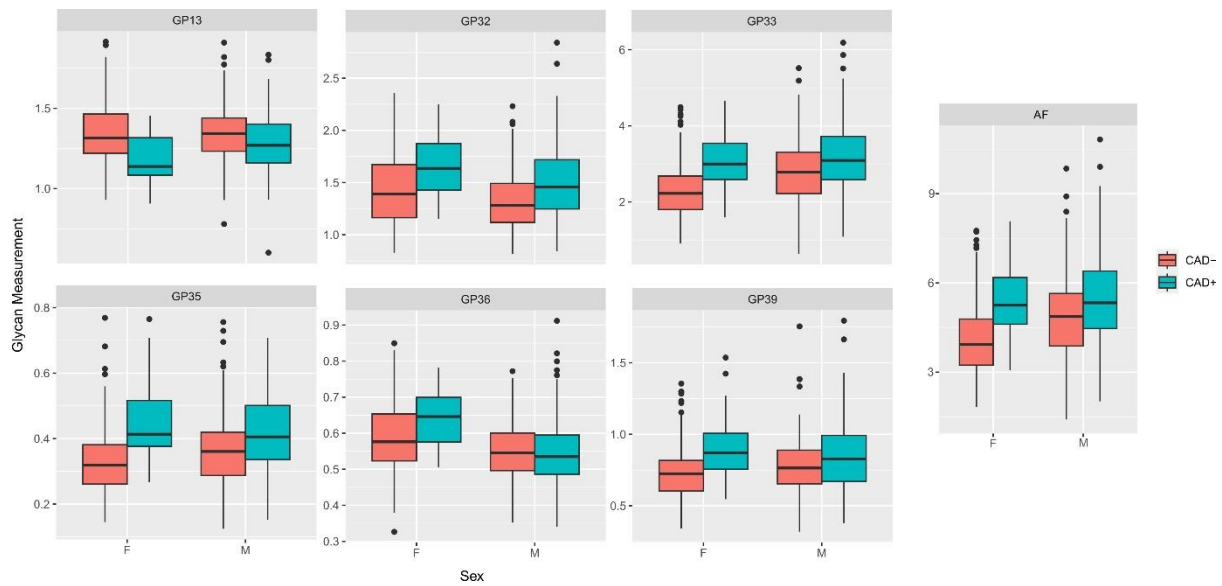
Figure 8. Most prominent differences between CAD+ and CAD- cases in plasma N-glycan traits, stratified by sex. Boxes in the boxplot range from 25th to 75th percentile, with the median represented as a line inside the box. Data outside the whiskers' ends are outliers and are plotted individually.

4.1.1.1.1 Antennary fucosylation and tetragalactosylation are positively associated with coronary artery disease in women

The most prominent difference between the N-glycome of CAD+ and CAD- women was an increase in the derived trait of total antennary fucosylation with CAD+ (Effect = 0.73, SE = 0.1883, p_{adj} = 3.75E-03). This change was driven by an increase in the entirety of highly branched, complex antennary fucosylated structures found in plasma N-glycome (GP27, GP33, GP35 and GP39). The single strongest association was found for GP35 (Effect = 0.83, SE = 0.1831, p_{adj} = 9.05E-04), a triantennary and trisialylated structure with both core and antennary fucose. Furthermore, derived trait increased solely in CAD+ women is tetragalactosylation (Effect = 0.51, SE = 0.1952, p_{adj} = 3.94E-02), together with its corresponding glycan trait GP36 (Effect = 0.57, SE = 0.1938, p_{adj} = 2.22E-02), a tetragalactosylated trisialylated N-glycan structure (Table 7 and 8).

4.1.1.1.2 Core fucosylation, monogalactosylation and asialylation are negatively associated with coronary artery disease in men

Monogalactosylation was significantly lowered in CAD+ men in comparison to CAD- (Effect = -0.37, SE = 0.1257, p_{adj} = 2.22E-02), as well as core fucosylation (Effect = -0.34, SE = 0.1274, p_{adj} = 3.83E-02). This was mainly driven by a decrease in mono- (and digalactosylated) structures with core fucose: GP5, GP10, GP11, GP13. Moreover, asialylation was also lowered (Effect = -0.37, SE = 0.1272, p_{adj} = 2.42E-02) through a decrease of glycan traits GP5, GP10,

and GP11. Conversely, disialylation was increased (Effect = 0.43, SE = 0.1266, p_{adj} = 1.05E-02). This was mainly due to increased glycan traits GP20 and GP26 (Table 7 and 8).

4.1.1.2 Sex-stratified association of IgG N-glycosylation with coronary artery disease

In contrast to plasma N-glycans, significant differences in IgG N-glycans were observed only in women, which were in the opposite direction than in men. All N-glycan abundances for CAD+ and CAD- cases stratified by sex are shown in Tables 9 and 10. In women with angiographically diagnosed CAD, five of the 24 directly measured IgG glycan traits and three out of nine derived glycosylation traits differed significantly between CAD+ and CAD- cases, whereas no differences were found in men. In general, a statistically significant increase in agalactosylated glycan species and a decrease in sialylated glycan species was observed in CAD+ women (Tables 9 and 10, Figure 9).

Table 9. Statistical analysis of sex-stratified associations between directly measured IgG N-glycosylation traits and coronary artery disease at the time of inclusion. Glycan data were adjusted for age, whereas false discovery rates were controlled by the Benjamini-Hochberg method. Statistically significant differences are in bold.

Glycan trait	Women				Men			
	Effect	SE	p-value	p_{adj}-value	Effect	SE	p-value	p_{adj}-value
GP1	0.29	0.1873	**1.16E-01**	3.74E-01	-0.07	0.1267	5.95E-01	9.02E-01
GP2	0.31	0.1966	1.15E-01	3.74E-01	0.01	0.1330	9.40E-01	9.80E-01
GP3	0.38	0.1699	**2.29E-02**	1.20E-01	0.08	0.1273	5.47E-01	9.02E-01
GP4	0.39	0.1670	**1.83E-02**	1.03E-01	0.06	0.1251	6.14E-01	9.02E-01
GP5	-0.10	0.1981	6.05E-01	9.02E-01	-0.05	0.1323	6.89E-01	9.47E-01
GP6	0.52	0.1699	**2.36E-03**	**2.26E-02**	0.17	0.1273	1.80E-01	4.36E-01
GP7	0.10	0.2049	6.24E-01	9.02E-01	-0.04	0.1328	7.47E-01	9.58E-01
GP8	-0.17	0.2045	4.11E-01	7.93E-01	-0.05	0.1292	6.78E-01	9.47E-01
GP9	-0.10	0.2035	6.21E-01	9.02E-01	-0.26	0.1313	**4.48E-02**	2.18E-01
GP10	0.30	0.2030	1.35E-01	3.99E-01	0.11	0.1325	4.00E-01	7.93E-01
GP11	0.30	0.1981	1.29E-01	3.99E-01	0.01	0.1314	9.52E-01	9.80E-01
GP12	0.03	0.1920	8.78E-01	9.58E-01	-0.02	0.1311	8.88E-01	9.58E-01
GP13	-0.15	0.1909	4.20E-01	7.93E-01	-0.23	0.1301	6.99E-02	2.70E-01
GP14	-0.29	0.1590	6.32E-02	2.70E-01	-0.17	0.1220	1.66E-01	4.34E-01
GP15	-0.14	0.1897	4.40E-01	8.06E-01	-0.07	0.1303	5.77E-01	9.02E-01
GP16	-0.51	0.2008	**1.15E-02**	7.84E-02	0.05	0.1330	6.97E-01	9.47E-01
GP17	-0.35	0.1956	6.81E-02	2.70E-01	0.06	0.1330	6.22E-01	9.02E-01
GP18	-0.58	0.1659	**4.71E-04**	**6.40E-03**	-0.04	0.1273	7.30E-01	9.55E-01
GP19	-0.59	0.1982	**2.66E-03**	**2.26E-02**	0.03	0.1325	8.22E-01	9.58E-01
GP20	-0.35	0.1973	7.55E-02	2.70E-01	-0.10	0.1303	4.50E-01	8.06E-01
GP21	-0.50	0.2000	**1.12E-02**	7.84E-02	0.09	0.1326	5.14E-01	8.96E-01
GP22	-0.19	0.2041	3.45E-01	7.32E-01	0.16	0.1324	2.09E-01	4.91E-01
GP23	-0.92	0.1852	**9.41E-07**	**6.40E-05**	-0.03	0.1298	8.40E-01	9.58E-01
GP24	-0.76	0.1964	**1.18E-04**	**2.00E-03**	0.32	0.1309	**1.49E-02**	9.20E-02

Table 10. Statistical analysis of IgG N-glycan derived traits in CAD+ versus CAD- cases at inclusion point. Glycan data were adjusted for age, whereas false discovery rates were controlled for by the Benjamini-Hochberg method. Statistically significant differences are in bold.

Glycan traits	Women				Men			
	Effect	SE	p-value	p_{adj}-value	Effect	SE	p-value	p_{adj}-value
S total	-0.82	0.1705	**1.99E-06**	**6.78E-05**	0.03	0.1296	8.05E-01	9.58E-01
G0 total	0.48	0.1599	**2.51E-03**	**2.26E-02**	0.10	0.1241	4.03E-01	7.93E-01
G1 total	-0.03	0.2040	8.76E-01	9.58E-01	-0.18	0.1293	1.56E-01	4.25E-01
G2 total	-0.28	0.1584	7.29E-02	2.70E-01	-0.17	0.1224	1.74E-01	4.36E-01
F total	-0.02	0.2032	9.38E-01	9.80E-01	0.00	0.1327	9.80E-01	9.80E-01
B total	0.21	0.1915	2.58E-01	5.65E-01	0.19	0.1308	1.48E-01	4.20E-01
FGS/(F+FG+FGS)	-0.71	0.1702	**3.44E-05**	**7.81E-04**	0.01	0.1285	9.66E-01	9.80E-01
FBS1/(FS1+FBS1)	-0.03	0.1840	8.81E-01	9.58E-01	0.02	0.1301	8.86E-01	9.58E-01
FBS1/FS1	-0.03	0.1840	8.81E-01	9.58E-01	0.02	0.1301	8.86E-01	9.58E-01
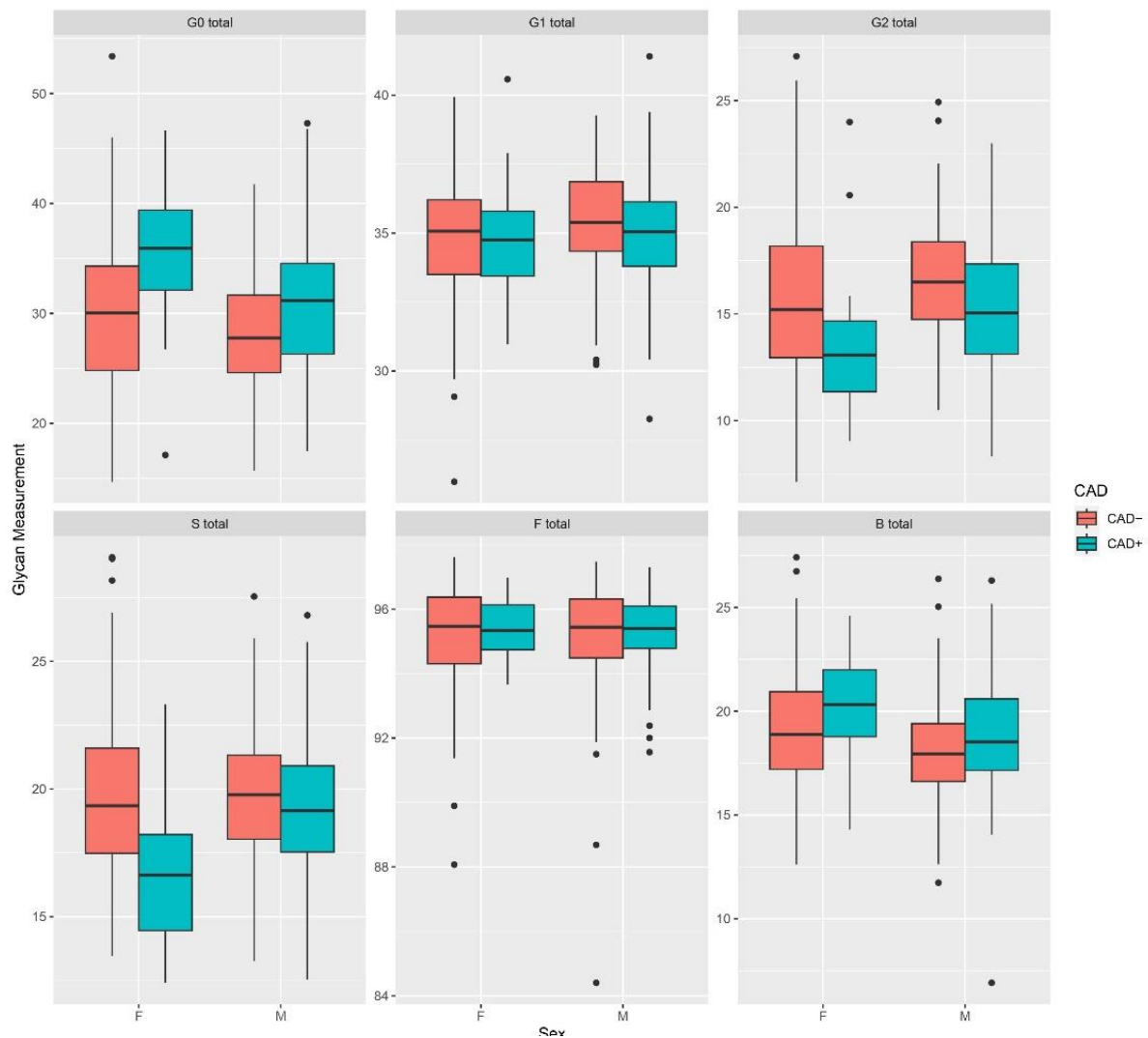
Figure 9. Sex-stratified relative abundance of main IgG glycome derived traits in CAD+ and CAD- cases at inclusion point. G0 - agalactosylation, G1 - monogalactosylation, G2 – digalactosylation, S – sialylation, F – core fucosylation, B – bisecting GlcNAc, F – females, M – males, glycan measurement - expressed as percentage for each derived trait. Boxes represent the 25th and 75th percentiles. Lines inside the box represent the median.

4.1.1.2.1 Sialylation is negatively associated with coronary artery disease in women

The most prominent difference between the IgG N-glycome of CAD+ and CAD- women was a decrease in sialylation (Effect = -0.82, SE = 0.1705, p_{adj} = 6.78E-05) (Table 10, Figure 9). This change was driven by a decrease in the mono- and disialylated core-fucosylated biantennary glycans with or without bisecting GlcNAc (GP18, GP19, GP23, GP24), and increase in asialylated and agalactosylated N-glycan structure with a bisecting GlcNAc and core fucose (GP6). The single strongest association was found for GP23 (Effect = -0.92, SE = 0.1852, p_{adj} = 6.40E-05), a disialylated and digalactosylated biantennary structure with core fucose (Table 9). Interestingly, no differences were observed between CAD+ and CAD− women for total core fucosylation and bisecting GlcNAc, whereas sialylation of all core-fucosylated structures without bisecting GlcNAc was significantly negatively associated with CAD+ (Effect = -0.71, SE = 0.1702, p_{adj} = 7.81E-04). After further adjustment for BMI, diabetes, and smoking, total sialylation remained negatively associated with CAD+ (Effect = -0.63, SE = 0.1781, p_{adj} = 2.65E-02) through a decrease of glycan traits GP23 and GP24 (Appendix 5 and 6). In addition, agalactosylation was significantly increased in CAD+ women in comparison to CAD- (Effect = 0.48, SE = 0.1599, p_{adj} = 2.26E-02) (Table 10, Figure 9). This was mainly driven by an increase in agalactosylated glycan structures (GP1, GP3, GP4), as well as decrease in galactosylated glycan structures with terminal sialic acid (GP16, GP21) (Table 9). After further adjustment for BMI, diabetes, and smoking the association between agactosylation and CAD+ was only nominally significant (Appendix 6).

4.2 Association of N-glycosylation with coronary artery disease during follow-up

It was then investigated whether glycans changed differently in participants with coronary atherosclerosis compared to participants with clean coronaries during the 2-year follow-up period. With respect to change over time, the difference between baseline and follow-up measurements was calculated.

While no statistically significant differences were detected in IgG N-glycome (Appendix 7), several statistically significant differences were observed in plasma N-glycome. After correction for multiple testing, 15 of the 39 directly measured plasma glycan traits showed a statistically significant change (adjusted p-value < 0.05) over time for CAD+ compared with CAD- cases (Table 11). In addition, significant differences in 10 of the 16 derived plasma glycan traits were observed between CAD+ and CAD- cases (Table 11, Figure 10). In particular, low-branched, monogalactosylated glycans with core fucose significantly increased in CAD+ subjects, while triantennary, more complex sialylated glycan species with antennary fucose significantly decreased in CAD+ individuals. Interestingly, these changes are in the opposite direction to those observed at inclusion point.

Table 11. Statistical analysis of associations between directly measured plasma protein N-glycosylation traits and coronary artery disease during the 2-year follow-up period. Glycan data were adjusted for age and sex, whereas the false discovery rate was controlled by the Benjamini-Hochberg method. Only statistically significant differences are shown.

Glycan trait	Effect	SE	p value	p_{adj} value
GP1	0.22	0.0817	8.40E-03	2.72E-02
GP4	0.25	0.0801	2.18E-03	1.35E-02
GP5	0.23	0.0824	6.63E-03	2.54E-02
GP6	0.22	0.0727	2.71E-03	1.35E-02
GP8	0.26	0.0987	1.03E-02	3.13E-02
GP10	0.24	0.0725	1.13E-03	1.25E-02
GP13	0.20	0.0663	2.61E-03	1.35E-02
GP16	0.16	0.0663	1.75E-02	4.19E-02
GP19	-0.21	0.0898	2.08E-02	4.58E-02
GP20	-0.23	0.0891	1.09E-02	3.16E-02
GP27	-0.12	0.0507	1.50E-02	3.75E-02
GP32	-0.25	0.0736	8.16E-04	1.17E-02
GP33	-0.22	0.0568	1.33E-04	7.33E-03
GP35	-0.21	0.0600	4.65E-04	1.17E-02
GP39	-0.19	0.0742	1.21E-02	3.16E-02
AF	-0.19	0.0600	8.49E-04	1.17E-02
CF	0.23	0.0900	1.18E-02	3.16E-02
G0	0.23	0.0800	6.92E-03	2.54E-02
G1	0.28	0.0900	1.62E-03	1.35E-02
G3	-0.23	0.0800	4.75E-03	2.18E-02

Table 11 - continued

HB	-0.23	0.0800	7.39E-03	2.54E-02
LB	0.21	0.0900	2.01E-02	4.58E-02
S0	0.29	0.0900	2.27E-03	1.35E-02
S2	-0.27	0.1000	5.19E-03	2.20E-02
S3	-0.27	0.0900	1.97E-03	1.35E-02
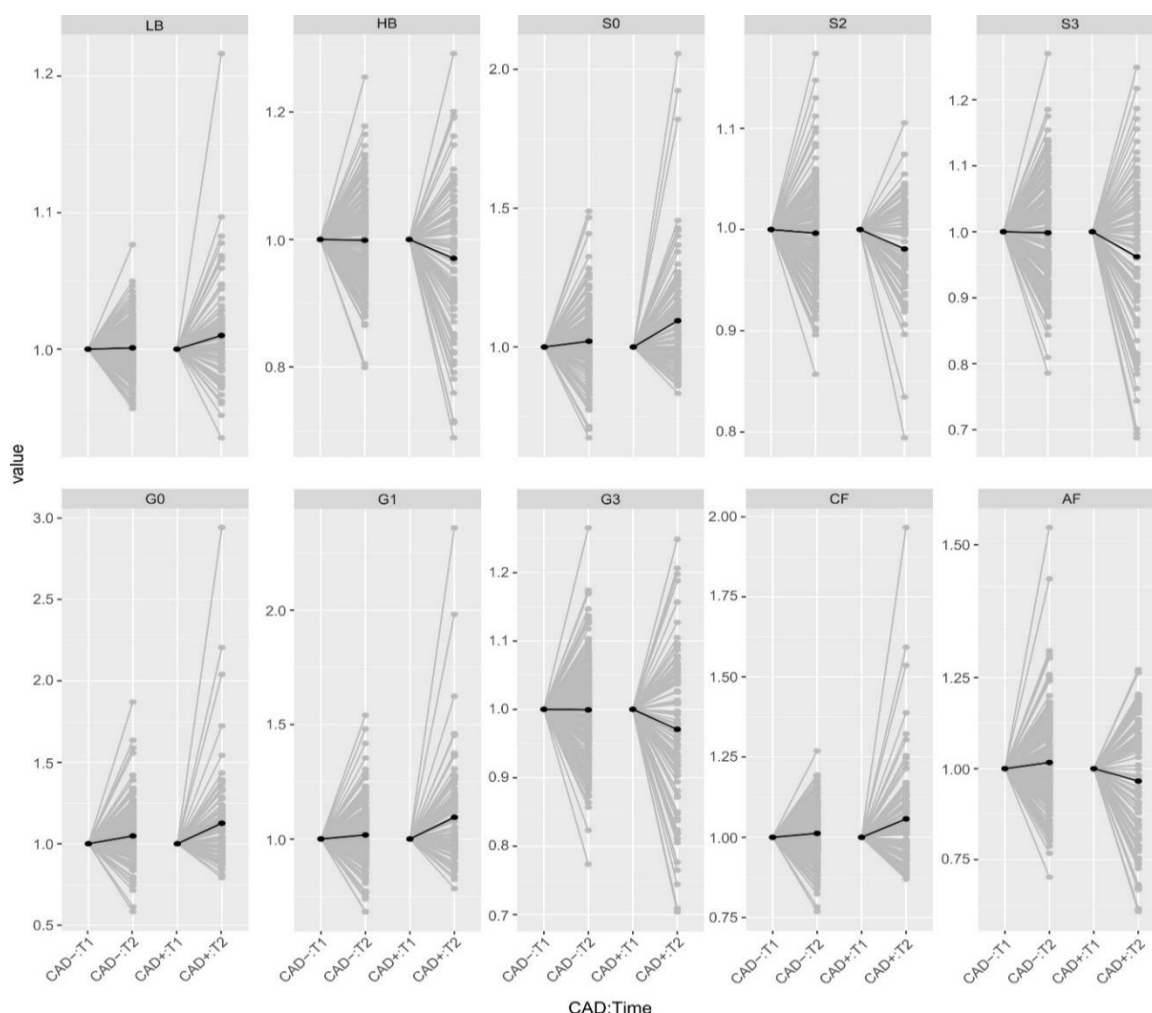
Figure 10. Differences in derived plasma N-glycan traits between CAD+ and CAD- during the two-year follow-up period. LB—low branching, HB—high branching, S0—asialylation, S2—disialylation, S3—trisialylation, G0—agalactosylation, G1—monogalactosylation, G3—trigalactosylation, CF—core fucosylation, AF—antennary fucosylation. Median glycan values for each time point are bolded. Data is normalized to the first point.

It was further found that eight of the 39 directly measured and six of the 16 derived glycan traits significantly changed during follow-up in participants with CAD+ independent of diabetes, BMI, and smoking (Table 12). Branching (Effect = -0.23, SE = 0.0895, p_{adj} = 4.93E-02), antennary fucosylation (Effect = -0.19, SE = 0.0607, p_{adj} = 2.56E-02), trisialylation (Effect = -0.27, SE = 0.0918, p_{adj} = 2.61E-02) and trigalactosylation (Effect = -0.23, SE = 0.0864, p_{adj} = 4.36E-02) significantly decreased in CAD+ cases. This was driven by a decrease in trisialylated trigalactosylated structures (with antennary fucose): GP32, GP33, G935. On the

contrary, monogactosylation (Effect = 0.27, SE = 0.0908, p_{adj} = 2.61E-02) significantly increased in CAD+ cases, through an increase of monogalactosylated glycans with core fucose (GP4, GP5 and GP6).

Table 12. Comparison of plasma N-glycan traits between CAD+ and CAD- cases during the 2-year follow-up period. Glycan data were adjusted for age, sex, diabetes, BMI, and smoking, while false discovery rates were controlled using the Benjamini-Hochberg method. Only significant differences are shown.

Glycan trait	Effect	SE	p value	p_{adj} value
GP1	0.22	0.0817	8.40E-03	2.72E-02
GP4	0.25	0.0801	2.18E-03	1.35E-02
GP5	0.23	0.0824	6.63E-03	2.54E-02
GP6	0.22	0.0727	2.71E-03	1.35E-02
GP8	0.26	0.0987	1.03E-02	3.13E-02
GP10	0.24	0.0725	1.13E-03	1.25E-02
GP13	0.20	0.0663	2.61E-03	1.35E-02
GP16	0.16	0.0663	1.75E-02	4.19E-02
GP19	-0.21	0.0898	2.08E-02	4.58E-02
GP20	-0.23	0.0891	1.09E-02	3.16E-02
GP27	-0.12	0.0507	1.50E-02	3.75E-02
GP32	-0.25	0.0736	8.16E-04	1.17E-02
GP33	-0.22	0.0568	1.33E-04	7.33E-03
GP35	-0.21	0.0600	4.65E-04	1.17E-02
GP39	-0.19	0.0742	1.21E-02	3.16E-02
AF	-0.19	0.0607	2.33E-03	2.56E-02
G1	0.27	0.0908	3.47E-03	2.61E-02
G3	-0.23	0.0864	9.52E-03	4.36E-02
HB	-0.23	0.0895	1.26E-02	4.93E-02
S0	0.27	0.0987	7.34E-03	3.67E-02
S3	-0.27	0.0918	4.27E-03	2.61E-02

4.2.1 Sex-stratified association of N-glycosylation with coronary artery disease during follow-up

Lastly, it was investigated whether glycans were longitudinally stable in CAD+ participants and CAD- participants when stratified by sex. Significant differences during the follow-up period were observed only in plasma N-glycome and specifically in men (Appendix 8 and 9, Table 13 and 14). Herein, plasma N-glycome of CAD+ men had a significantly higher abundance of simpler, asialylated, a- and monogalactosylated glycoforms with core fucose (GP1, GP2, GP4, GP5 and GP6), and, conversely, a lower abundance of highly branched glycan structures with antennary fucose (GP32, GP33 and GP35) in comparison to the inclusion point while N-glycome remained stable in CAD- men and women regardless of CAD diagnosis (Figure 11).

Table 13. Statistical analysis of sex-stratified associations between plasma N-glycosylation traits and coronary heart disease during the 2-year follow-up period. Glycan data were adjusted for age, whereas false discovery rates were controlled by the Benjamini-Hochberg method. Statistically significant differences are shown in bold.

Glycan trait	Women				Men			
	Effect	SE	p value	p_{adj} value	Effect	SE	p value	p_{adj} value
GP1	-0.06	0.1634	6.93E-01	7.48E-01	0.32	0.1122	4.39E-03	**3.22E-02**
GP2	-0.18	0.1392	1.94E-01	4.28E-01	0.33	0.1071	2.80E-03	**2.37E-02**
GP3	-0.12	0.1332	3.78E-01	5.77E-01	0.22	0.0989	2.54E-02	9.99E-02
GP4	-0.18	0.1614	2.60E-01	5.10E-01	0.35	0.1075	1.73E-03	**2.18E-02**
GP5	-0.12	0.1577	4.32E-01	5.87E-01	0.33	0.1159	5.35E-03	**3.46E-02**
GP6	-0.15	0.1628	3.46E-01	5.60E-01	0.32	0.0932	8.12E-04	**2.18E-02**
GP7	-0.24	0.1605	1.39E-01	3.48E-01	0.32	0.1037	2.18E-03	**2.18E-02**
GP8	0.12	0.1865	5.23E-01	6.68E-01	0.32	0.1258	1.23E-02	6.67E-02
GP9	-0.09	0.1832	6.40E-01	7.38E-01	0.26	0.1318	5.24E-02	1.75E-01
GP10	-0.16	0.1352	2.48E-01	5.05E-01	0.31	0.0987	2.05E-03	**2.18E-02**
GP11	-0.21	0.1540	1.83E-01	4.10E-01	0.24	0.0991	1.46E-02	6.98E-02
GP12	-0.20	0.1938	3.03E-01	5.37E-01	0.05	0.1134	6.90E-01	7.48E-01
GP13	-0.13	0.1210	3.02E-01	5.37E-01	0.33	0.0892	2.55E-04	**1.47E-02**
GP14	0.12	0.1883	5.12E-01	6.62E-01	-0.10	0.1235	4.38E-01	5.87E-01
GP15	0.08	0.1815	6.70E-01	7.48E-01	0.24	0.1272	5.93E-02	1.89E-01
GP16	-0.14	0.1130	2.18E-01	4.53E-01	0.20	0.0920	2.97E-02	1.11E-01
GP17	-0.20	0.1076	6.93E-02	2.06E-01	0.20	0.0838	1.72E-02	7.26E-02
GP18	0.04	0.1406	7.55E-01	7.99E-01	-0.02	0.0741	8.35E-01	8.50E-01
GP19	-0.16	0.1693	3.56E-01	5.67E-01	-0.16	0.1263	2.06E-01	4.43E-01
GP20	0.19	0.1715	2.70E-01	5.21E-01	-0.41	0.1220	8.11E-04	**2.18E-02**
GP21	0.22	0.2298	3.41E-01	5.60E-01	-0.11	0.1354	4.36E-01	5.87E-01
GP22	-0.06	0.1307	6.71E-01	7.48E-01	-0.21	0.0721	4.68E-03	**3.22E-02**
GP23	-0.08	0.0899	3.90E-01	5.78E-01	0.09	0.0725	2.15E-01	4.53E-01
GP24	0.08	0.1312	5.47E-01	6.76E-01	0.01	0.0877	9.19E-01	9.19E-01
GP25	0.18	0.2237	4.10E-01	5.87E-01	0.14	0.1279	2.92E-01	5.37E-01
GP26	0.13	0.1222	2.95E-01	5.37E-01	-0.09	0.0954	3.23E-01	5.60E-01
GP27	-0.03	0.1014	7.77E-01	8.06E-01	-0.11	0.0746	1.28E-01	3.27E-01
GP28	0.06	0.1305	6.39E-01	7.38E-01	-0.05	0.0748	5.39E-01	6.74E-01
GP29	0.15	0.1653	3.70E-01	5.77E-01	-0.14	0.0847	1.09E-01	2.85E-01
GP30	0.07	0.1242	5.94E-01	7.11E-01	-0.15	0.0916	9.94E-02	2.73E-01
GP31	-0.04	0.1310	7.51E-01	7.99E-01	-0.15	0.0705	3.13E-02	1.11E-01
GP32	0.07	0.1298	5.88E-01	7.11E-01	-0.39	0.1046	2.67E-04	**1.47E-02**
GP33	-0.05	0.1119	6.44E-01	7.38E-01	-0.25	0.0811	1.95E-03	**2.18E-02**
GP34	0.19	0.1400	1.70E-01	3.97E-01	-0.19	0.1109	8.41E-02	2.43E-01
GP35	-0.08	0.1201	4.94E-01	6.46E-01	-0.23	0.0796	4.19E-03	**3.22E-02**
GP36	0.14	0.1676	4.15E-01	5.87E-01	-0.09	0.1077	3.94E-01	5.78E-01
GP37	0.08	0.1357	5.35E-01	6.74E-01	-0.12	0.0893	1.74E-01	3.99E-01
GP38	0.16	0.1844	3.92E-01	5.78E-01	-0.20	0.1207	1.02E-01	2.74E-01
GP39	0.06	0.1515	6.93E-01	7.48E-01	-0.22	0.0936	1.69E-02	7.26E-02

Table 14. Statistical analysis of sex-stratified associations between 16 derived plasma protein N-glycosylation traits and coronary artery disease during the 2-year follow-up period. Glycan data were adjusted for age, whereas false discovery rates were controlled by the Benjamini-Hochberg method. Statistically significant differences are in bold.

Glycan trait	Women				Men			
	Effect	SE	p value	p_{adj} value	Effect	SE	p value	p_{adj} value
AF	-0.02	0.1127	8.67E-01	8.74E-01	-0.22	0.0803	7.55E-03	**4.61E-02**
B	-0.24	0.1417	9.33E-02	2.63E-01	0.25	0.0998	1.32E-02	6.67E-02
CF	-0.22	0.1551	1.54E-01	3.69E-01	0.34	0.1287	8.46E-03	**4.90E-02**
G0	-0.09	0.1613	5.59E-01	6.83E-01	0.35	0.1154	2.71E-03	**2.37E-02**
G1	-0.16	0.1673	3.45E-01	5.60E-01	0.38	0.1185	1.84E-03	**2.18E-02**
G2	0.05	0.1770	7.64E-01	8.00E-01	-0.24	0.0980	1.53E-02	6.99E-02
G3	0.06	0.1466	6.82E-01	7.48E-01	-0.26	0.1135	2.54E-02	9.99E-02
G4	0.19	0.1817	2.89E-01	5.37E-01	-0.22	0.1154	6.19E-02	1.89E-01
HB	0.11	0.1467	4.36E-01	5.87E-01	-0.25	0.1181	3.85E-02	1.32E-01
HM	-0.24	0.1609	1.42E-01	3.48E-01	0.09	0.1150	4.36E-01	5.87E-01
LB	-0.10	0.1455	4.73E-01	6.26E-01	0.26	0.1180	3.06E-02	1.11E-01
S0	-0.16	0.1824	3.73E-01	5.77E-01	0.40	0.1261	2.00E-03	**2.18E-02**
S1	-0.04	0.1562	8.09E-01	8.31E-01	0.13	0.1139	2.59E-01	5.10E-01
S2	0.19	0.2022	3.39E-01	5.60E-01	-0.42	0.1268	1.03E-03	**2.18E-02**
S3	0.08	0.1520	6.01E-01	7.11E-01	-0.30	0.1197	1.33E-02	6.67E-02
S4	0.18	0.1827	3.32E-01	5.60E-01	-0.22	0.1176	6.16E-02	1.89E-01
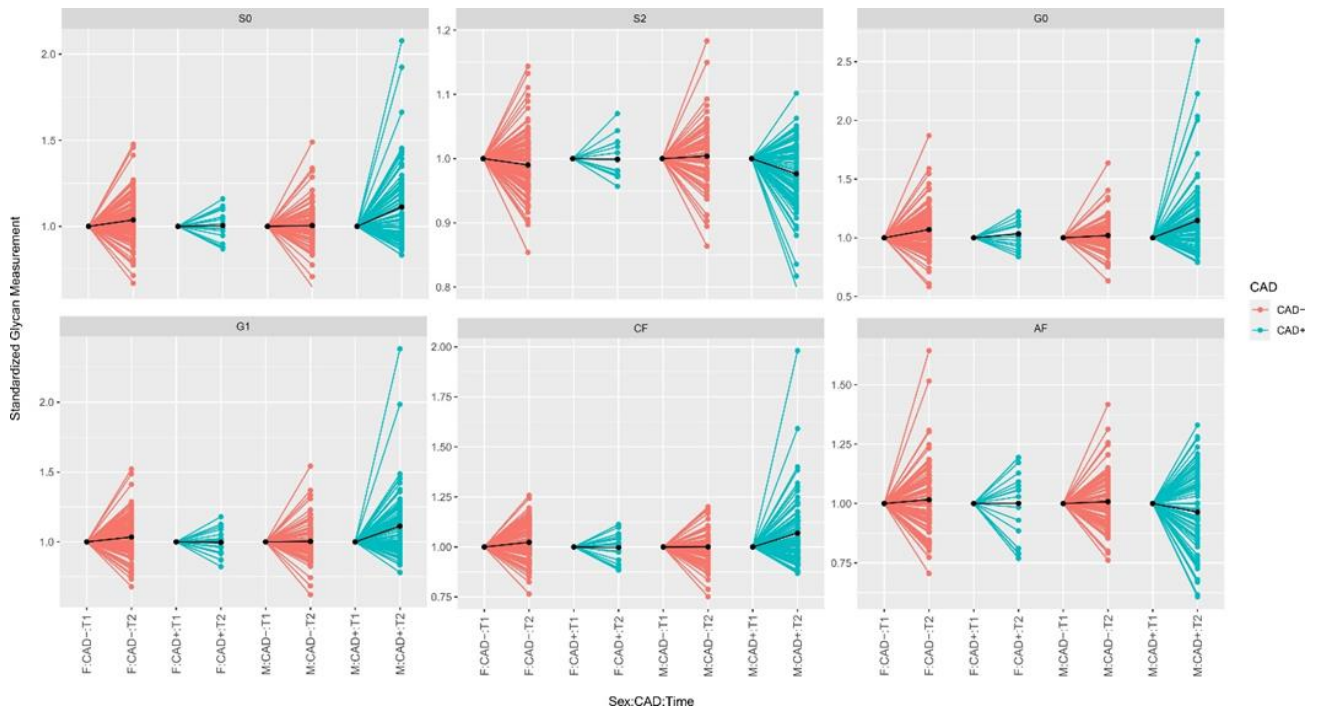
Figure 11. Differences in derived plasma N-glycan traits between CAD+ and CAD- cases during the two-year follow-up period, stratified by sex. S0—asialylation, S2—disialylation, G0—agalactosylation, G1—monogalactosylation, CF—core fucosylation, AF—antennary fucosylation. Median glycan values for each time point are bolded. Data is normalized to the first point

4.3 Association of N-glycosylation with adverse CVD outcomes

During an eight-year follow-up period, 80 MACE occurred, including hospitalizations for cardiovascular disease and cardiovascular deaths. It was investigated whether glycans were able to predict MACE before they occur. IgG N-glycans were not able to predict the occurrence of MACE because no statistically significant associations were observed (Appendix 10). The only exception was a nominally positive association between GP22, digalactosylated, and disialylated biantennary N-glycan with bisecting GlcNAc and the occurrence of MACE (Figure 12). As for plasma N-glycans, subjects with an increased abundance of highly complex branched plasma N-glycans did worse than the rest of the cohort (nominal p-value < 0.05) (Appendix 11). One of the strongest nominal associations was found for GP26, a trigalactosylated and disialylated triantennary N-glycan structure (Figure 12).
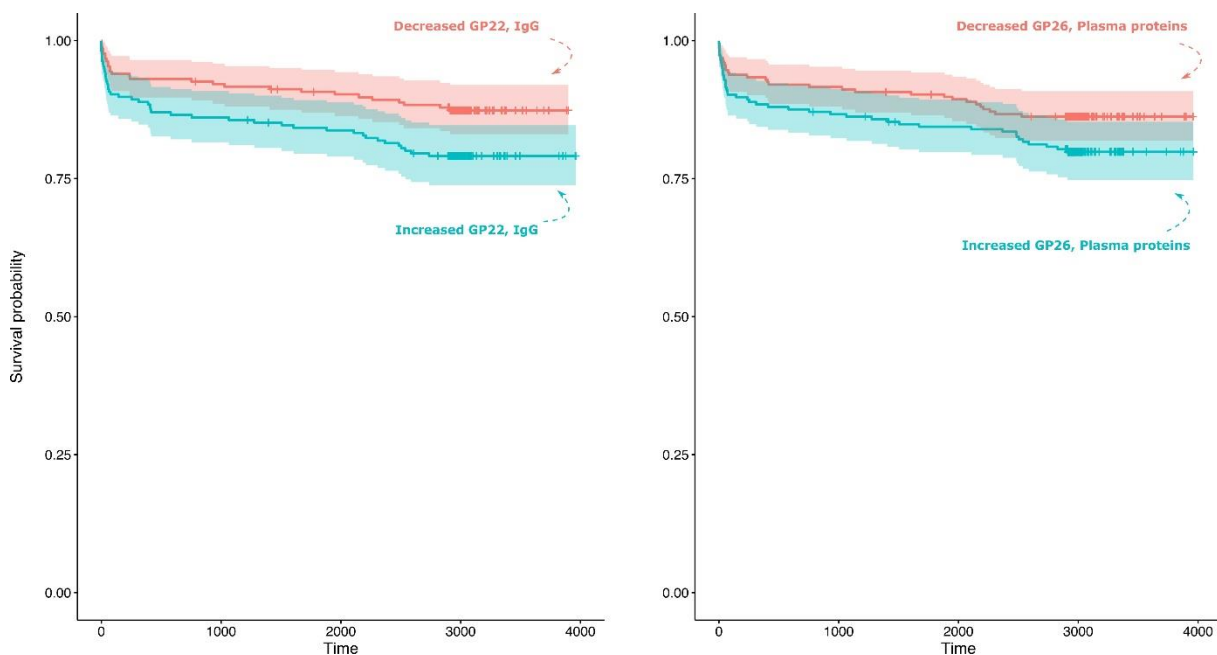
Figure 12. Survival analysis. The Kaplan-Meier curve shows the survival for participants of the study and the ability of N-glycans to differentiate participants who suffered from MACE from those who did not. The Kaplan-Meier survival curve (solid line) describes the probability of survival for the participants. The outer light-colored lines represent the 95% confidence interval. The horizontal axis represents the survival time (in days). Each step means an actual event happens, i.e., adverse CV event.

5. DISCUSSION

The process of glycosylation has a profound impact on the structural properties of plasma proteins, notably IgG, and plays a pivotal role in governing their effector functions, encompassing the regulation of inflammatory responses and the modulation of innate and adaptive immunity (259). A plethora of studies have elucidated substantial alterations in the composition of N-glycans attached to plasma proteins and IgG in various disease states (15,25,116). Consequently, the N-glycome is emerging as a valuable and novel biomarker due to its exquisite sensitivity to (patho)physiological alterations and disease conditions, including CVD (16,26,116). Alterations in protein glycosylation have been implicated in the pathogenesis of CVD through diverse molecular mechanisms, thereby positioning them as significant biomarker candidates for early detection and disease progression (28). These findings, coupled with other noteworthy discoveries within the field, underscore the importance of investigating glycosylation in unraveling the complex relationship between alterations in protein N-glycome and the physiological and pathological processes closely associated with CVD.

CAD stands as one of the most prevalent CVD and represents a significant global healthcare burden (1). Accordingly, within the scope of this thesis, the first comprehensive analysis of the overall composition of plasma protein and IgG N-glycosylation was conducted specifically in CAD. The primary objective was to explore the potential association between coronary atherosclerosis and the N-glycome makeup. To achieve this, separate analyses of the N-glycomic profiles of total plasma proteins and IgG obtained from individuals diagnosed with angiographically confirmed CAD and individuals with healthy coronary arteries was conducted at the time of enrollment, followed by a subsequent assessment two years later. Furthermore, the aim was to assess the potential link between N-glycome patterns and the incidence of adverse CVD events over an eight-year period subsequent to study enrollment.

Significant and substantial alterations were observed in the N-glycosylation profiles of total plasma proteins. Notably, at the enrollment point, individuals diagnosed with CAD exhibited a statistically significant decrease in complex biantennary galactosylated N-glycans with core fucose, while simultaneously displaying an increase in highly branched (tri- and tetra-antennary) sialylated N-glycan structures with terminal fucose. These specific glycan features have been associated with proinflammatory functions attributed to plasma proteins. Particularly noteworthy were the persistently significant positive associations between CAD+ and two specific glycan structures: FA3F1G3S3 (core fucosylated, trigalactosylated and trisialylated structure with antennary fucose) and M6 (high-mannose structure). These

associations remained statistically significant even after accounting for potential confounding factors related to traditional CVD risk factors, such as diabetes, smoking, and BMI.

Given the evidence of sexual dimorphism in CVD (260) and the notable sex differences observed in the association between N-glycans and CVD risk (39–41), a sex-stratified analysis of N-glycome profiles was conducted. The results of the analysis demonstrated that changes in plasma N-glycosylation exhibited consistent trends across both sexes. However, when focusing on the degree of the effect, in men with CAD there was a significant decrease in IgG-specific galactosylated biantennary N-glycan structures with core fucose (FA2[3]G1, FA2G2 and FA2G1S1). Noteworthy, galactosylated plasma N-glycans such as FA2G2S1 and A2G2S2 have previously shown predictive potential for calculating risk of type 2 diabetes and CVD events (41). Conversely, in women with CAD, highly complex N-glycan structures with antennary fucose (A3G3S3, A3F1G3S3, FA3F1G3S3, A4G4S3 and A4F1G4S4), associated with acute phase proteins, displayed a significant increase. Interestingly, glycan structure FA3F1G3S3 is (so far) found only on acute phase protein ceruloplasmin (16). Importantly, published data have suggested a direct relationship between ceruloplasmin levels and cardiovascular events, particularly CAD (211). The identification of an increase in a glycan structure unique to ceruloplasmin further supports its potential biological involvement in CAD development. Moreover, acute phase proteins AGP-1 and A1AT, exhibit significant elevation in plasma levels during inflammation and are extensively decorated with the sLeX epitope, which is recognized as a hallmark of inflammation (36). The synthesis of the sLeX epitope relies heavily on terminal fucosylation and α2,3 sialylation. The observed increase in the abundance of the sLeX epitope could potentially be attributed to the cytokine-mediated upregulation of hepatic enzymes ST3GAL4 and FUT6 (86). Additionally, numerous studies have highlighted a significant association between GlycA, reflecting plasma N-glycan branching (72), and clinical outcomes related to CVD, encompassing atherosclerotic cardiovascular events and mortality, both in the general population and in patients with chronic inflammatory conditions (43,73,75,76,212–214,261–263).

Longitudinal investigation of plasma N-glycan profiles to differentiate individuals with CAD+ from those with CAD- during a two-year follow-up period yielded intriguing and unexpected findings. Specifically, in men, the alterations observed in plasma N-glycans after the follow-up period differed from the patterns observed at enrollment. Contrary to expectations, there was a change in the opposite direction, characterized by a decrease in the branching and abundance of antennary fucose, while biantennary glycan species with core fucose exhibited

an increase. Although previous studies have generally indicated that plasma protein N-glycome remains relatively stable over time (37), it is important to note that specific physiological mechanisms can induce rapid changes, leading to pronounced modifications in plasma protein N-glycosylation. These findings may indicate a possible reversal to a "healthy" glycan profile if the prescribed therapy is followed and/or lifestyle changes are made. It is well-established that classic CVD risk factors, such as smoking, hypertension, diabetes, and high BMI, often result from an unhealthy diet, physical inactivity, and alcohol abuse (2,264), all of which can significantly influence the N-glycosylation profile of plasma proteins (66,67). Consequently, the results of this thesis highlight the potential benefits of identifying therapeutic strategies that directly target glycosylation changes, as they may hold promise for improving cardiovascular health.

In CAD+ women, the initial statistically significant increase in antennary fucosylation observed at enrolment did not maintain significance after the two-year follow-up period. It is worth noting that the women included in the study were at an age where they may be experiencing the transition to menopause (265). In particular, in CAD- cases, hormonal modulation cannot be discounted as a potential factor contributing to the observed non-significant difference between CAD+ and CAD- women following the two-year follow-up period. Previous studies have indeed reported the influence of hormones on abundance of distinct glycan structures (124). Estrogen levels, which are known to decrease during menopause, have been shown to exhibit a negative correlation with the sLeX epitope (266).

Recent studies have revealed that elevated plasma levels of mannose are associated with CAD, independent of traditional CVD risk factors, and have been identified as an independent predictor of adverse CVD events (231). Intriguingly, a significant positive association between a high mannose plasma N-glycan structure (M6) and CAD cases was identified in present study, even after adjusting for conventional CVD risk factors such as age, sex, BMI, diabetes, and smoking. Interestingly, high-mannose plasma N-glycans have been shown to correlate with high cholesterol levels, a major risk factor for the development of atherosclerosis (215). On the other hand, aging is widely recognized as a prominent risk factor for numerous chronic noncommunicable diseases (267), including CAD (2). Extensive research conducted over the past decade has demonstrated that N-glycosylation profiles undergo significant changes with advancing age (15,66,123,268–270). In the context of the aging heart, a connection has been established between the increased presence of mannosylated glycans on cardiomyocytes and the enzyme GMPPB, responsible for synthesizing GDP-mannose (230). Hence, it is plausible

to hypothesize that the augmented flux of free mannose in CAD (231) may contribute to the heightened abundance of high-mannose glycans observed on plasma proteins in this thesis.

Regarding IgG N-glycome, no statistically significant differences between CAD+ and CAD- cases were observed when considering both sexes combined. However, upon conducting sex-stratified analysis of IgG N-glycans, distinct changes between women and men were identified. Notably, significant differences in IgG N-glycome were observed in CAD+ women at enrollment, primarily related to sialylation. Sialylation demonstrated a significant negative association with CAD, independent of traditional CVD risk factors such as age, BMI, diabetes, and smoking. Similarly, previous studies have shown that sialylated IgG glycans without bisecting GlcNAc were inversely associated with the presence of atherosclerotic plaques in the femoral and carotid arteries (39). It has also been suggested that decreased IgG sialylation contributes to the development of vascular cognitive impairment in individuals with atherosclerosis (221), and that it has been associated with increased complement activation, which is associated with atherosclerosis and CVD (222,223). Furthermore, elevated levels of total serum sialic acid (TSA) were previously shown to be positively correlated with CAD, indicating abnormal enzymatic activity (sialidase, sialyltransferase, and trans-sialidase) in CAD and suggesting potential inhibition of these enzymes as a therapeutic approach for CAD (233). These findings imply a potential link between increased enzyme activity, decreased sialylation and CAD.

Alongside sialylation, galactosylation displayed a decreasing trend in CAD+ women. Interestingly, it was previously demonstrated that in women galactosylated IgG glycoform FA2G1 was inversely associated with CVD risk beyond classical risk factors and clinical parameters (40). Moreover, it is known that N-glycosylation is subject to sex-specific hormonal modulation. Estrogen, in particular, has been shown to influence the galactosylation of IgG N-glycans (124). Studies have reported higher levels of IgG galactosylation and sialylation in premenopausal women compared to men, while an increase in agalactosylation has been associated with the transition to menopause (128).

Subsequent N-glycan analysis during the two-year follow-up period did not reveal any statistically significant differences between CAD+ and CAD- women. Similar to the findings for plasma proteins, it is plausible to suggest that hormonal changes during menopause influence the N-glycome of IgG in women, potentially contributing to the lack of statistical significance.

In men, the differences observed were minimal and mainly centered around the presence of bisecting GlcNAc. After the two-year follow-up period, the results indicated a marginal positive association between core fucosylated N-glycan structures with bisecting GlcNAc and CAD. These results are consistent with previous research (39,40). Specifically, study by Birukov et al. demonstrated that a weighted score based on bisected IgG glycoform FA2BG2S1 and FA2G2S2 was associated with higher CVD risk in men (40). Considering the relatively small number of cases in both the CAD+ and CAD- groups following sex stratification, the lack of statistical significance could also be attributed to the limited statistical power of the analysis.

Lastly, the aim of this thesis was to investigate the association between specific N-glycan structures and the occurrence of major adverse cardiovascular events (MACE), comprising hospital admissions for CVD and cardiovascular death. A nominally statistically significant positive association between highly branched plasma N-glycans and MACE was observed, as well as a nominally statistically significant positive association between the presence of IgG disialylated structure with bisecting GlcNAc (A2BG2S2) and MACE. It is worth noting that a previously established association exists between sialylated IgG N-glycan structure with bisecting GlcNAc and elevated CVD risk (199). However, due to the limited number of cases, this association lost statistical significance after adjusting for multiple testing.

The findings of this thesis, along with other research in the field, underscore the significance of protein N-glycosylation in the context of CVD. While the clinical application of glycan-based biomarkers for CVD diagnosis holds promise, it remains in its early stages of development. Glycan analysis of specific proteins, such as IgG, could serve as an initial step towards clinical implementation, as changes in the N-glycome of IgG offer specific insights into the abundance of distinct N-glycan structures and exhibit less overlap with overall inflammation compared to total plasma proteins. Currently, several indexes based on IgG N-glycans derived from plasma/serum (E.g., GlycanAge, GlyCage) have been developed to assess biological age, cardiovascular age, and predict cardiovascular health. Additionally, evidence suggests that IgG N-glycan profiles have the potential to serve as biomarkers for suboptimal health status (23).

In this thesis, the significance of N-glycome profiling of total plasma proteins and IgG in understanding N-glycosylation changes in CAD was demonstrated. The findings align with previous research, emphasizing the interplay between protein N-glycans and the development

of atherosclerotic CVD. This study has revealed that several N-glycan traits are associated with CAD independent of traditional CVD risk factors. This represents a crucial initial step towards further research on the potential use of N-glycans, possibly in combination with other biomarkers, for predicting CAD. However, further investigations focusing on protein-specific analyses and functional studies are necessary to uncover the precise mechanisms underlying these associations. Development of organ-on-a-chip technology for CVD research (271) holds promise for replicating (patho)physiological processes and enabling in-depth exploration of the role of N-glycans in CVD.

The future possibility of replacing invasive diagnostic methods and diagnoses based on nonspecific traditional risk factors with noninvasive techniques (such as coronary CT angiography and *in silico* diagnosis (272)) in conjunction with specific glycan biomarkers could lead to personalized medicine. Investigation performed within this thesis opens avenues for exploring the functional role of N-glycans as a novel biomarker and/or therapeutic target in CAD. Understanding the dynamics and functional implications of N-glycosylation could provide valuable insights for future research and clinical applications.

6. CONCLUSIONS

The analysis of N-glycosylation profiles of plasma proteins has revealed significant alterations in glycan structures associated with CAD – a significant increase in highly branched plasma N-glycan structures and decrease in complex biantennary N-glycans.

Sexual dimorphism was demonstrated in the association between IgG N-glycans and CAD risk, with distinct patterns observed in men and women – the strongest negative association was observed between women with highly sialylated IgG N-glycans and CAD.

Highly branched plasma N-glycans showed potential as independent predictors of adverse outcomes in CAD.

Overall, the findings of this thesis underscore the significance of protein N-glycosylation in CVD and its potential as a diagnostic tool.

7. REFERENCE LIST

1. Lindstrom M, DeCleene N, Dorsey H, Fuster V, Johnson CO, LeGrand KE, Mensah GA, Razo C, Stark B, Varieur Turco J, et al. Global Burden of Cardiovascular Diseases and Risks Collaboration, 1990-2021. *J Am Coll Cardiol* (2022) **80**:2372–2425. doi:10.1016/j.jacc.2022.11.001

2. Hajar R. Risk factors for coronary artery disease: Historical perspectives. *Hear Views* (2017) **18**:109. doi:10.4103/heartviews.heartviews_106_17

3. Greenland P, Knoll MD, Stamler J, Neaton JD, Dyer AR, Garside DB, Wilson PW. Major Risk Factors as Antecedents of Fatal and Nonfatal Coronary Heart Disease Events. *JAMA* (2003) **290**:891–897. doi:10.1001/jama.290.7.891

4. Ridker PM, Buring JE, Rifai N, Cook NR. Development and validation of improved algorithms for the assessment of global cardiovascular risk in women: The Reynolds Risk Score. *JAMA* (2007) **297**:611–619. doi:10.1001/jama.297.6.611

5. Wilson PWF, Pencina M, Jacques P, Selhub J, D'Agostino R, O'Donnell CJ. C-reactive protein and reclassification of cardiovascular risk in the Framingham Heart Study. *Circ Cardiovasc Qual Outcomes* (2008) **1**:92–97. doi:10.1161/CIRCOUTCOMES.108.831198

6. Naghavi M, Falk E, Hecht HS, Jamieson MJ, Kaul S, Berman D, Fayad Z, Budoff MJ, Rumberger J, Naqvi TZ, et al. From Vulnerable Plaque to Vulnerable Patient-Part III: Executive Summary of the Screening for Heart Attack Prevention and Education (SHAPE) Task Force Report. *Am J Cardiol* (2006) **98**:2–15. doi:10.1016/j.amjcard.2006.03.002

7. Deidda M, Noto A, Dessalvi CC, Andreini D, Andreotti F, Ferrannini E, Latini R, Maggioni AP, Magnoni M, Mercuro G. Why Do High-Risk Patients Develop or Not Develop Coronary Artery Disease? Metabolic Insights from the CAPIRE Study. *Metabolites* (2022) **12**:123. doi:10.3390/metabo12020123

8. Ramazi S, Zahiri J. Post-translational modifications in proteins: resources, tools and prediction methods. *Database* (2021) **2021**: doi:10.1093/database/baab012

9. Schjoldager KT, Narimatsu Y, Joshi HJ, Clausen H. Global view of human protein glycosylation pathways and functions. *Nat Rev Mol Cell Biol* (2020) **21**:729–749. doi:10.1038/s41580-020-00294-x

10. Reily C, Stewart TJ, Renfrow MB, Novak J. Glycosylation in health and disease. *Nat Rev Nephrol* (2019) **15**:346–366. doi:10.1038/s41581-019-0129-4

11. Flynn RA, Pedram K, Malaker SA, Batista PJ, Smith BAH, Johnson AG, George BM, Majzoub K, Villalta PW, Carette JE, et al. Small RNAs are modified with N-glycans and displayed on the surface of living cells. *Cell* (2021) **184**:3109-3124.e22. doi:10.1016/j.cell.2021.04.023

12. Gagneux P, Hennet T, Varki A. "Biological Functions of Glycans," in *Essentials of Glycobiology* (Cold Spring Harbor Laboratory Press). doi:10.1101/GLYCOBIOLOGY.4E.7

13. Pinho SS, Alves I, Gaifem J, Rabinovich GA. Immune regulatory networks coordinated by glycans and glycan-binding proteins in autoimmunity and infection. *Cell Mol Immunol* (2023) doi:10.1038/s41423-023-01074-1

14. Haslam SM, Freedberg DI, Mulloy B, Dell A, Stanley P, Prestegard JH. "Structural Analysis of Glycans," in *Essentials of Glycobiology* Available at: http://www.ncbi.nlm.nih.gov/pubmed/12880852

15. Gudelj I, Lauc G, Pezer M. Immunoglobulin G glycosylation in aging and diseases. *Cell Immunol* (2018) **333**:65–79. doi:10.1016/j.cellimm.2018.07.009

16. Clerc F, Reiding KR, Jansen BC, Kammeijer GSM, Bondt A, Wuhrer M. Human plasma protein N-glycosylation. *Glycoconj J* (2016) **33**:309–343. doi:10.1007/s10719-015-9626-2

17. Knopf J, Biermann MH, Muñoz LE, Herrmann M. Antibody glycosylation as a potential biomarker for chronic inflammatory autoimmune diseases. *AIMS Genet* (2016) **03**:280–291. doi:10.3934/genet.2016.4.280

18. Hu M, Lan Y, Lu A, Ma X, Zhang L. Glycan-based biomarkers for diagnosis of cancers and other diseases: Past, present, and future. *Prog Mol Biol Transl Sci* (2019) **162**:1–24. doi:10.1016/bs.pmbts.2018.12.002

19. Rudman N, Gornik O, Lauc G. Altered N-glycosylation profiles as potential biomarkers and drug targets in diabetes. *FEBS Lett* (2019) **593**: doi:10.1002/1873-3468.13495

20. Liu D, Li Q, Zhang X, Wang H, Cao W, Li D, Xing W, Song M, Wang W, Meng Q, et

al. Systematic Review: Immunoglobulin G N-Glycans as Next-Generation Diagnostic Biomarkers for Common Chronic Diseases. *Omi A J Integr Biol* (2019) **23**:607–614. doi:10.1089/omi.2019.0032

21. Connelly MA, Otvos JD, Shalaurova I, Playford MP, Mehta NN. GlycA, a novel biomarker of systemic inflammation and cardiovascular disease risk. *J Transl Med* (2017) **15**: doi:10.1186/s12967-017-1321-6

22. Yu X, Wang Y, Kristic J, Dong J, Chu X, Ge S, Wang H, Fang H, Gao Q, Liu D, et al. Profiling IgG N-glycans as potential biomarker of chronological and biological ages. *Medicine (Baltimore)* (2016) **95**:e4112. doi:10.1097/MD.0000000000004112

23. Meng X, Wang B, Xu X, Song M, Hou H, Wang W, Wang Y. Glycomic biomarkers are instrumental for suboptimal health status management in the context of predictive, preventive, and personalized medicine. *EPMA J* (2022) **13**:195–207. doi:10.1007/s13167-022-00278-1

24. Russell AC, Šimurina M, Garcia MT, Novokmet M, Wang Y, Rudan I, Campbell H, Lauc G, Thomas MG, Wang W. The N-glycosylation of immunoglobulin G as a novel biomarker of Parkinson's disease. *Glycobiology* (2017) **27**:501–510. doi:10.1093/glycob/cwx022

25. Gornik O, Lauc G. Glycosylation of serum proteins in inflammatory diseases. *Dis Markers* (2008) **25**:267–278. doi:10.1155/2008/493289

26. Gudelj I, Lauc G. Protein N-Glycosylation in Cardiovascular Diseases and Related Risk Factors. *Curr Cardiovasc Risk Rep* (2018) **12**: doi:10.1007/s12170-018-0579-4

27. Dashti H, Pabon Porras MA, Mora S. "Glycosylation and Cardiovascular Diseases," in *Advances in Experimental Medicine and Biology* (Springer), 307–319. doi:10.1007/978-3-030-70115-4_15

28. Gudelj I, Lauc G. "Glycans and Cardiovascular Diseases," in *Reference Module in Life Sciences* (Elsevier), 1–11. doi:10.1016/B978-0-12-821618-7.00006-7

29. Scott DW, Patel RP. Endothelial heterogeneity and adhesion molecules N-glycosylation: Implications in leukocyte trafficking in inflammation. *Glycobiology* (2013) **23**:622–633. doi:10.1093/glycob/cwt014

30. Scott DW, Chen J, Chacko BK, Traylor JG, Orr AW, Patel RP. Role of endothelial N-

glycan mannose residues in monocyte recruitment during atherogenesis. *Arterioscler Thromb Vasc Biol* (2012) **32**:e51–e59. doi:10.1161/ATVBAHA.112.253203

31. Huo Y, Xia L. P-selectin Glycoprotein Ligand-1 Plays a Crucial Role in the Selective Recruitment of Leukocytes Into the Atherosclerotic Arterial Wall. *Trends Cardiovasc Med* (2009) **19**:140–145. doi:10.1016/j.tcm.2009.07.006

32. Krishnan S, Huang J, Lee H, Guerrero A, Berglund L, Anuurad E, Lebrilla CB, Zivkovic AM. Combined High-Density Lipoprotein Proteomic and Glycomic Profiles in Patients at Risk for Coronary Artery Disease. *J Proteome Res* (2015) **14**:5109–5118. doi:10.1021/acs.jproteome.5b00730

33. Sukhorukov V, Gudelj I, Pučić-Baković M, Zakiev E, Orekhov A, Kontush A, Lauc G. Glycosylation of human plasma lipoproteins reveals a high level of diversity, which directly impacts their functional properties. *Biochim Biophys Acta - Mol Cell Biol Lipids* (2019) **1864**:643–653. doi:10.1016/j.bbalip.2019.01.005

34. Gabay C, Kushner I. Acute-Phase Proteins and Other Systemic Responses to Inflammation. *N Engl J Med* (1999) **340**:448–454. doi:10.1056/nejm199902113400607

35. Shade K-TC, Anthony RM. Antibody Glycosylation and Inflammation. *Antibodies* (2013) **2**:392–414. doi:10.3390/ANTIB2030392

36. Radovani B, Gudelj I. N-Glycosylation and Inflammation; the Not-So-Sweet Relation. *Front Immunol* (2022) **13**:3235. doi:10.3389/fimmu.2022.893365

37. Gornik O, Wagner J, Pučić M, Knežević A, Redžić I, Lauc G. Stability of N-glycan profiles in human plasma. *Glycobiology* (2009) **19**:1547–1553. doi:10.1093/glycob/cwp134

38. Novokmet M, Lukić E, Vučković F, Durić Ž, Keser T, Rajšl K, Remondini D, Castellani G, Gašparović H, Gornik O, et al. Changes in IgG and total plasma protein glycomes in acute systemic inflammation. *Sci Rep* (2014) **4**:4347. doi:10.1038/srep04347

39. Menni C, Gudelj I, MacDonald-Dunlop E, Mangino M, Zierer J, Bešić E, Joshi PK, Trbojević-Akmačić I, Chowienczyk PJ, Spector TD, et al. Glycosylation Profile of Immunoglobulin G Is Cross-Sectionally Associated with Cardiovascular Disease Risk

Score and Subclinical Atherosclerosis in Two Independent Cohorts. *Circ Res* (2018) **122**:1555–1564. doi:10.1161/CIRCRESAHA.117.312174

40. Birukov A, Plavša B, Eichelmann F, Kuxhaus O, Hoshi RA, Rudman N, Štambuk T, Trbojević-Akmačić I, Schiborn C, Morze J, et al. Immunoglobulin G N-Glycosylation Signatures in Incident Type 2 Diabetes and Cardiovascular Disease. *Diabetes Care* (2022) doi:10.2337/DC22-0833

41. Wittenbecher C, Štambuk T, Kuxhaus O, Rudman N, Vučković F, Štambuk J, Schiborn C, Rahelić D, Dietrich S, Gornik O, et al. Plasma N-glycans as emerging biomarkers of cardiometabolic risk: A prospective investigation in the epic-potsdam cohort study. *Diabetes Care* (2020) **43**:661–668. doi:10.2337/dc19-1507

42. Wu Z, Guo Z, Zheng Y, Wang Y, Zhang H, Pan H, Li Z, Balmer L, Li X, Tao L, et al. IgG N-Glycosylation Cardiovascular Age Tracks Cardiovascular Risk Beyond Calendar Age. *Engineering* (2023) doi:10.1016/j.eng.2022.12.004

43. McGarrah RW, Kelly JP, Craig DM, Haynes C, Jessee RC, Huffman KM, Kraus WE, Shah SH. A novel protein glycan-derived inflammation biomarker independently predicts cardiovascular disease and modifies the association of HDL subclasses with mortality. *Clin Chem* (2017) **63**:288–296. doi:10.1373/clinchem.2016.261636

44. Magnoni M, Andreini D, Gorini M, Moccetti T, Modena MG, Canestrari M, Berti S, Casolo G, Gabrielli D, Marraccini P, et al. Coronary atherosclerosis in outlier subjects at the opposite extremes of traditional risk factors: Rationale and preliminary results of the Coronary Atherosclerosis in outlier subjects: Protective and novel Individual Risk factors Evaluation (CAPIRE) stud. *Am Heart J* (2016) **173**:18–26. doi:10.1016/j.ahj.2015.11.017

45. Plavša B, Szavits-Nossan J, Blivajs A, Rapčan B, Radovani B, Šesto I, Štambuk K, Mustapić V, Đerek L, Rudan D, et al. The N-Glycosylation of Total Plasma Proteins and IgG in Atrial Fibrillation. *Biomolecules* (2023) **13**:605. doi:10.3390/biom13040605

46. Marek KW, Vijay IK, Marth JD. A recessive deletion in the GlcNAc-1-phosphotransferase gene results in peri-implantation embryonic lethality. *Glycobiology* (1999) **9**:1263–1271. doi:10.1093/glycob/9.11.1263

47. Varki A, Kornfeld S. "Historical Background and Overview," in *Essentials of Glycobiology* (Cold Spring Harbor Laboratory Press). doi:10.1101/glycobiology.4e.1

48. Colley KJ, Varki A, Haltiwanger RS, Kinoshita T. "Cellular Organization of Glycosylation," in *Essentials of Glycobiology* (Cold Spring Harbor Laboratory Press). doi:10.1101/GLYCOBIOLOGY.4E.4

49. de Haan N, Pučić-Baković M, Novokmet M, Falck D, Lageveen-Kammeijer G, Razdorov G, Vučković F, Trbojević-Akmačić I, Gornik O, Hanić M, et al. Developments and perspectives in high-throughput protein glycomics: enabling the analysis of thousands of samples. *Glycobiology* (2022) **32**:651–663. doi:10.1093/glycob/cwac026

50. Trbojević-Akmačić I, Lageveen-Kammeijer GSM, Heijs B, Petrović T, Deriš H, Wuhrer M, Lauc G. High-Throughput Glycomic Methods. *Chem Rev* (2022) **122**:15865–15913. doi:10.1021/acs.chemrev.1c01031

51. Keser T, Gornik I, Vučković F, Selak N, Pavić T, Lukić E, Gudelj I, Gašparović H, Biočina B, Tilin T, et al. Increased plasma N-glycome complexity is associated with higher risk of type 2 diabetes. *Diabetologia* (2017) **60**:2352–2360. doi:10.1007/s00125-017-4426-9

52. Kljaković-Gašpić Batinjan M, Petrović T, Vučković F, Hadžibegović I, Radovani B, Jurin I, Đerek L, Huljev E, Markotić A, Lukšić I, et al. Differences in Immunoglobulin G Glycosylation Between Influenza and COVID-19 Patients. *Engineering* (2022) doi:10.1016/j.eng.2022.08.007

53. Bermingham ML, Colombo M, McGurnaghan SJ, Blackbourn LAK, Vučković F, Baković MP, Trbojević-Akmačić I, Lauc G, Agakov F, Agakova AS, et al. N-glycan profile and kidney disease in type 1 diabetes. *Diabetes Care* (2018) **41**:79–87. doi:10.2337/dc17-1042

54. Cvetko A, Kifer D, Gornik O, Klarić L, Visser E, Lauc G, Wilson JF, Štambuk T. Glycosylation alterations in multiple sclerosis show increased proinflammatory potential. *Biomedicines* (2020) **8**:1–14. doi:10.3390/biomedicines8100410

55. Mathew J, Sankar P, Varacallo M. *Physiology, Blood Plasma*. StatPearls Publishing (2023). Available at: http://www.ncbi.nlm.nih.gov/pubmed/17397761

56. Stanley P, Taniguchi N, Aebi M. "N-Glycans," in *Essentials of Glycobiology* (Cold Spring Harbor Laboratory Press). Available at: http://www.ncbi.nlm.nih.gov/pubmed/786163

57. Rebello OD, Nicolardi S, Lageveen-Kammeijer GSM, Nouta J, Gardner RA, Mesker WE, Tollenaar RAEM, Spencer DIR, Wuhrer M, Falck D. A Matrix-Assisted Laser Desorption/Ionization—Mass Spectrometry Assay for the Relative Quantitation of Antennary Fucosylated N-Glycans in Human Plasma. *Front Chem* (2020) **8**: doi:10.3389/fchem.2020.00138

58. Hennig R, Cajic S, Borowiak M, Hoffmann M, Kottler R, Reichl U, Rapp E. Towards personalized diagnostics via longitudinal study of the human plasma N-glycome. *Biochim Biophys Acta - Gen Subj* (2016) **1860**:1728–1738. doi:10.1016/j.bbagen.2016.03.035

59. Knežević A, Polašek O, Gornik O, Rudan I, Campbell H, Hayward C, Wright A, Kolčić I, O'Donoghue N, Bones J, et al. Variability, Heritability and Environmental Determinants of Human Plasma N-Glycome. *J Proteome Res* (2009) **8**:694–701. doi:10.1021/pr800737u

60. Zaytseva OO, Freidin MB, Keser T, Štambuk J, Ugrina I, Šimurina M, Vilaj M, Štambuk T, Trbojević-Akmačić I, Pučić-Baković M, et al. Heritability of Human Plasma N-Glycome. *J Proteome Res* (2020) **19**:85–91. doi:10.1021/acs.jproteome.9b00348

61. Sharapov SZ, Shadrina AS, Tsepilov YA, Elgaeva EE, Tiys ES, Feoktistova SG, Zaytseva OO, Vuckovic F, Cuadrat R, Jäger S, et al. Replication of 15 loci involved in human plasma protein N-glycosylation in 4802 samples from four cohorts. *Glycobiology* (2021) **31**:82–88. doi:10.1093/glycob/cwaa053

62. Sharapov SZ, Tsepilov YA, Klaric L, Mangino M, Thareja G, Shadrina AS, Simurina M, Dagostino C, Dmitrieva J, Vilaj M, et al. Defining the genetic control of human blood plasma N-glycome using genome-wide association study. *Hum Mol Genet* (2019) doi:10.1093/hmg/ddz054

63. Lauc G, Essafi A, Huffman JE, Hayward C, Knežević A, Kattla JJ, Polašek O, Gornik O, Vitart V, Abrahams JL, et al. Genomics meets glycomics-the first gwas study of human N-glycome identifies HNF1A as a master regulator of plasma protein

fucosylation. *PLoS Genet* (2010) **6**:1–14. doi:10.1371/journal.pgen.1001256

64. Huffman JE, Knežević A, Vitart V, Kattla J, Adamczyk B, Novokmet M, Igl W, Pučić M, Zgaga L, Johannson Å, et al. Polymorphisms in B3GAT1, SLC9A9 and MGAT5 are associated with variation within the human plasma N-glycome of 3533 European adults. *Hum Mol Genet* (2011) **20**:5000–5011. doi:10.1093/hmg/ddr414

65. Dotz V, Wuhrer M. N-glycome signatures in human plasma: associations with physiology and major diseases. *FEBS Lett* (2019) **593**:2966–2976. doi:10.1002/1873-3468.13598

66. Knežević A, Gornik O, Polašek O, Pučić M, Redžić I, Novokmet M, Rudd PM, Wright AF, Campbell H, Rudan I, et al. Effects of aging, body mass index, plasma lipid profiles, and smoking on human plasma N-glycans. *Glycobiology* (2010) **20**:959–969. doi:10.1093/glycob/cwq051

67. Deriš H, Tominac P, Vučković F, Astrup A, Blaak EE, Lauc G, Gudelj I. Susceptibility of Human Plasma N-glycome to Low-Calorie and Different Weight-Maintenance Diets. *Int J Mol Sci* (2022) **23**:15772. doi:10.3390/ijms232415772

68. Tudor L, Nedic Erjavec G, Nikolac Perkovic M, Konjevod M, Svob Strac D, Uzun S, Kozumplik O, Jovanovic T, Lauc G, Pivac N. N-glycomic Profile in Combat Related Post-Traumatic Stress Disorder. *Biomolecules* (2019) **9**:834. doi:10.3390/biom9120834

69. Trbojević-Akmačić I, Vučković F, Vilaj M, Skelin A, Karssen LC, Krištić J, Jurić J, Momčilović A, Šimunović J, Mangino M, et al. Plasma N-glycome composition associates with chronic low back pain. *Biochim Biophys Acta - Gen Subj* (2018) **1862**:2124–2133. doi:10.1016/j.bbagen.2018.07.003

70. Gudelj I, Baciarello M, Ugrina I, De Gregori M, Napolioni V, Ingelmo PM, Bugada D, De Gregori S, Derek L, Pučić-Baković M, et al. Changes in total plasma and serum N-glycome composition and patient-controlled analgesia after major abdominal surgery. *Sci Rep* (2016) **6**:31234. doi:10.1038/srep31234

71. Pavić T, Dilber D, Kifer D, Selak N, Keser T, Ljubičić CDS, Vukić Dugac A, Lauc G, Rumora L, Gornik O. N-glycosylation patterns of plasma proteins and immunoglobulin G in chronic obstructive pulmonary disease. *J Transl Med* (2018)

16:1–15. doi:10.1186/s12967-018-1695-0

72. Noel M, Chasman DI, Mora S, Otvos JD, Palmer CD, Parsons PJ, Smoller JW, Cummings RD, Mealer RG. The Inflammation Biomarker GlycA Reflects Plasma N-Glycan Branching. *Clin Chem* (2022) doi:10.1093/clinchem/hvac160

73. Ormseth MJ, Chung CP, Oeser AM, Connelly MA, Sokka T, Raggi P, Solus JF, Otvos JD, Stein CM. Utility of a novel inflammatory marker, GlycA, for assessment of rheumatoid arthritis disease activity and coronary atherosclerosis. *Arthritis Res Ther* (2015) **17**:117. doi:10.1186/s13075-015-0646-x

74. Ritchie SC, Würtz P, Nath AP, Abraham G, Havulinna AS, Fearnley LG, Sarin A-PP, Kangas AJ, Soininen P, Aalto K, et al. The Biomarker GlycA Is Associated with Chronic Inflammation and Predicts Long-Term Risk of Severe Infection. *Cell Syst* (2015) **1**:293–301. doi:10.1016/j.cels.2015.09.007

75. Akinkuolie AO, Buring JE, Ridker PM, Mora S. A novel protein glycan biomarker and future cardiovascular disease events. *J Am Heart Assoc* (2014) **3**:e001221. doi:10.1161/JAHA.114.001221

76. Joshi AA, Lerman JB, Aberra TM, Afshar M, Teague HL, Rodante JA, Krishnamoorthy P, Ng Q, Aridi TZ, Salahuddin T, et al. GlycA Is a Novel Biomarker of Inflammation and Subclinical Cardiovascular Disease in Psoriasis. *Circ Res* (2016) **119**:1242–1253. doi:10.1161/CIRCRESAHA.116.309637

77. Dierckx T, Verstockt B, Vermeire S, van Weyenbergh J. GlycA, a Nuclear Magnetic Resonance Spectroscopy Measure for Protein Glycosylation, is a Viable Biomarker for Disease Activity in IBD. *J Crohn's Colitis* (2019) **13**:389–394. doi:10.1093/ecco-jcc/jjy162

78. Wu D, Struwe WB, Harvey DJ, Ferguson MAJ, Robinson C V. N-glycan microheterogeneity regulates interactions of plasma proteins. *Proc Natl Acad Sci* (2018) **115**:8763–8768. doi:10.1073/pnas.1807439115

79. Molinari M. N-glycan structure dictates extension of protein folding or onset of disposal. *Nat Chem Biol* (2007) **3**:313–320. doi:10.1038/nchembio880

80. Thaysen-Andersen M, Packer NH. Site-specific glycoproteomics confirms that protein structure dictates formation of N-glycan type, core fucosylation and branching.

Glycobiology (2012) **22**:1440–1452. doi:10.1093/glycob/cws110

81. Arnold JN, Saldova R, Abd Hamid UM, Rudd PM. Evaluation of the serum N-linked glycome for the diagnosis of cancer and chronic inflammation. *Proteomics* (2008) **8**:3284–3293. doi:10.1002/pmic.200800163

82. Higai K, Aoki Y, Azuma Y, Matsumoto K. Glycosylation of site-specific glycans of α1-acid glycoprotein and alterations in acute and chronic inflammation. *Biochim Biophys Acta - Gen Subj* (2005) **1725**:128–135. doi:10.1016/j.bbagen.2005.03.012

83. Levander L, Gunnarsson P, Grenegård M, Rydén I, Påhlsson P. Effects of α1-acid glycoprotein fucosylation on its Ca2+ mobilizing capacity in neutrophils. *Scand J Immunol* (2009) **69**:412–420. doi:10.1111/j.1365-3083.2009.02240.x

84. Fournier T, Medjoubi N, Porquet D. Alpha-1-acid glycoprotein. *Biochim Biophys Acta - Protein Struct Mol Enzymol* (2000) **1482**:157–171. doi:10.1016/S0167-4838(00)00153-9

85. Azuma Y, Murata M, Matsumoto K. Alteration of sugar chains on α1-acid glycoprotein secreted following cytokine stimulation of HuH-7 cells in vitro. *Clin Chim Acta* (2000) **294**:93–103. doi:10.1016/S0009-8981(99)00248-X

86. Higai K, Miyazaki N, Azuma Y, Matsumoto K. Interleukin-1β induces sialyl Lewis X on hepatocellular carcinoma HuH-7 cells via enhanced expression of ST3Gal IV and FUT VI gene. *FEBS Lett* (2006) **580**:6069–6075. doi:10.1016/j.febslet.2006.09.073

87. Narisada M, Kawamoto S, Kuwamoto K, Moriwaki K, Nakagawa T, Matsumoto H, Asahi M, Koyama N, Miyoshi E. Identification of an inducible factor secreted by pancreatic cancer cell lines that stimulates the production of fucosylated haptoglobin in hepatoma cells. *Biochem Biophys Res Commun* (2008) **377**:792–796. doi:10.1016/j.bbrc.2008.10.061

88. Wang Y, Kinzie E, Berger FG, Lim SK, Baumann H. Haptoglobin, an inflammation-inducible plasma protein. *Redox Rep* (2001) **6**:379–385. doi:10.1179/135100001101536580

89. Ishibashi Y, Inouye Y, Okano T, Taniguchi A. Regulation of sialyl-Lewis x epitope expression by TNF-α and EGF in an airway carcinoma cell line. *Glycoconj J* (2005) **22**:53–62. doi:10.1007/s10719-005-0292-7

90.	Higai K, Ishihara S, Matsumoto K. NFκB-p65 dependent transcriptional regulation of glycosyltransferases in human colon adenocarcinoma HT-29 by stimulation with tumor necrosis factor α. *Biol Pharm Bull* (2006) **29**:2372–2377. doi:10.1248/bpb.29.2372

91.	Karinch AM, Pan M, Lin C-M, Strange R, Souba WW. Glutamine metabolism in sepsis and infection. *J Nutr* (2001) **131**:2535S-2538S. doi:10.1093/jn/131.9.2535s

92.	Okin D, Medzhitov R. The Effect of Sustained Inflammation on Hepatic Mevalonate Pathway Results in Hyperglycemia. *Cell* (2016) **165**:343–356. doi:10.1016/j.cell.2016.02.023

93.	Chiaradonna F, Ricciardiello F, Palorini R. The Nutrient-Sensing Hexosamine Biosynthetic Pathway as the Hub of Cancer Metabolic Rewiring. *Cells* (2018) **7**:53. doi:10.3390/cells7060053

94.	Ryczko MC, Pawling J, Chen R, Abdel Rahman AM, Yau K, Copeland JK, Zhang C, Surendra A, Guttman DS, Figeys D, et al. Metabolic Reprogramming by Hexosamine Biosynthetic and Golgi N-Glycan Branching Pathways. *Sci Rep* (2016) **6**:23043. doi:10.1038/srep23043

95.	Oswald DM, Jones MB, Cobb BA. Modulation of hepatocyte sialylation drives spontaneous fatty liver disease and inflammation. *Glycobiology* (2020) **30**:346–359. doi:10.1093/glycob/cwz096

96.	Gong M, Garige M, Hirsch K, Lakshman MR. Liver Galβ1,4GlcNAc α2,6-sialyltransferase is down-regulated in human alcoholics: possible cause for the appearance of asialoconjugates. *Metabolism* (2007) **56**:1241–1247. doi:10.1016/j.metabol.2007.04.022

97.	Gonzalez-Quintela A, Alende R, Gude F, Campos J, Rey J, Meijide LM, Fernandez-Merino C, Vidal C. Serum levels of immunoglobulins (IgG, IgA, IgM) in a general adult population and their relationship with alcohol consumption, smoking and common metabolic abnormalities. *Clin Exp Immunol* (2008) **151**:42–50. doi:10.1111/j.1365-2249.2007.03545.x

98.	Reichert JM. Antibody Fc: Linking Adaptive and Innate Immunity. *MAbs* (2014) **6**:619–621. doi:10.4161/mabs.28617

99.   Bournazos S, Ravetch J V. Diversification of IgG effector functions. *Int Immunol* (2017) **29**:303–310. doi:10.1093/intimm/dxx025

100.   Arnold JN, Wormald MR, Sim RB, Rudd PM, Dwek RA. The impact of glycosylation on the biological function and structure of human immunoglobulins. *Annu Rev Immunol* (2007) **25**:21–50. doi:10.1146/annurev.immunol.25.022106.141702

101.   Schwab I, Nimmerjahn F. Intravenous immunoglobulin therapy: How does IgG modulate the immune system? *Nat Rev Immunol* (2013) **13**:176–189. doi:10.1038/nri3401

102.   Trastoy B, Du JJ, Cifuente JO, Rudolph L, García-Alija M, Klontz EH, Deredge D, Sultana N, Huynh CG, Flowers MW, et al. Mechanism of antibody-specific deglycosylation and immune evasion by Streptococcal IgG-specific endoglycosidases. *Nat Commun* (2023) **14**:1705. doi:10.1038/s41467-023-37215-3

103.   Malhotra R, Wormald MR, Rudd PM, Fischer PB, Dwek RA, Sim RB. Glycosylation changes of IgG associated with rheumatooid arthritis can activate complement via the mannose-binding protein. *Nat Med* (1995) **1**:237–243. doi:10.1038/nm0395-237

104.   Wei B, Gao X, Cadang L, Izadi S, Liu P, Zhang HM, Hecht E, Shim J, Magill G, Pabon JR, et al. Fc galactosylation follows consecutive reaction kinetics and enhances immunoglobulin G hexamerization for complement activation. *MAbs* (2021) **13**:1893427. doi:10.1080/19420862.2021.1893427

105.   Goetze AM, Liu YD, Zhang Z, Shah B, Lee E, Bondarenko P V., Flynn GC. High-mannose glycans on the Fc region of therapeutic IgG antibodies increase serum clearance in humans. *Glycobiology* (2011) **21**:949–959. doi:10.1093/glycob/cwr027

106.   Peschke B, Keller CW, Weber P, Quast I, Lünemann JD. Fc-Galactosylation of Human Immunoglobulin Gamma Isotypes Improves C1q Binding and Enhances Complement-Dependent Cytotoxicity. *Front Immunol* (2017) **8**: doi:10.3389/fimmu.2017.00646

107.   Jennewein MF, Goldfarb I, Dolatshahi S, Cosgrove C, Noelette FJ, Krykbaeva M, Das J, Sarkar A, Gorman MJ, Fischinger S, et al. Fc Glycan-Mediated Regulation of Placental Antibody Transfer. *Cell* (2019) **178**:202-215.e14. doi:10.1016/j.cell.2019.05.044

108. Pincetic A, Bournazos S, DiLillo DJ, Maamary J, Wang TT, Dahan R, Fiebiger B-M, Ravetch J V. Type I and type II Fc receptors regulate innate and adaptive immunity. *Nat Immunol* (2014) **15**:707–716. doi:10.1038/ni.2939

109. Dunn-Walters D. Effect of somatic hypermutation on potential N-glycosylation sites in human immunoglobulin heavy chain variable regions. *Mol Immunol* (2000) **37**:107–113. doi:10.1016/S0161-5890(00)00038-9

110. van de Bovenkamp FS, Hafkenscheid L, Rispens T, Rombouts Y. The Emerging Importance of IgG Fab Glycosylation in Immunity. *J Immunol* (2016) **196**:1435–1441. doi:10.4049/jimmunol.1502136

111. Bondt A, Rombouts Y, Selman MHJ, Hensbergen PJ, Reiding KR, Hazes JMW, Dolhain RJEM, Wuhrer M. Immunoglobulin G (IgG) Fab Glycosylation Analysis Using a New Mass Spectrometric High-throughput Profiling Method Reveals Pregnancy-associated Changes. *Mol Cell Proteomics* (2014) **13**:3029–3039. doi:10.1074/mcp.M114.039537

112. Leibiger H, Wüstner D, Stigler RD, Marx U. Variable domain-linked oligosaccharides of a human monoclonal IgG: structure and influence on antigen binding. *Biochem J* (1999) **338**:529–38.

113. Coloma MJ, Trinh RK, Martinez AR, Morrison SL. Position Effects of Variable Region Carbohydrate on the Affinity and In Vivo Behavior of an Anti-(1→6) Dextran Antibody. *J Immunol* (1999) **162**:2162–2170. doi:10.4049/jimmunol.162.4.2162

114. Wright A, Tao MH, Kabat EA, Morrison SL. Antibody variable region glycosylation: position effects on antigen binding and carbohydrate structure. *EMBO J* (1991) **10**:2717–2723. doi:10.1002/j.1460-2075.1991.tb07819.x

115. Pučić M, Knežević A, Vidič J, Adamczyk B, Novokmet M, Polašek O, Gornik O, Šupraha-Goreta S, Wormald MR, Redžic I, et al. High throughput isolation and glycosylation analysis of IgG-variability and heritability of the IgG glycome in three isolated human populations. *Mol Cell Proteomics* (2011) **10**:M111.010090. doi:10.1074/mcp.M111.010090

116. Martinić Kavur M, Lauc G, Pezer M. Systems Glycobiology: Immunoglobulin G Glycans as Biomarkers and Functional Effectors in Aging and Diseases. *Compr*

Glycosci (2021)439–478. doi:10.1016/B978-0-12-819475-1.00086-9

117. Štambuk J, Vučković F, Habazin S, Hanić M, Novokmet M, Nikolaus S, Tran F, Schreiber S, Franke A, Rosenstiel P, et al. Distinct Longitudinal Changes in Immunoglobulin G N-Glycosylation Associate with Therapy Response in Chronic Inflammatory Diseases. *Int J Mol Sci* (2022) **23**:8473. doi:10.3390/ijms23158473

118. Ferrucci L, Fabbri E. Inflammageing: chronic inflammation in ageing, cardiovascular disease, and frailty. *Nat Rev Cardiol* (2018) **15**:505–522. doi:10.1038/s41569-018-0064-2

119. Klarić L, Tsepilov YA, Stanton CM, Mangino M, Sikka TT, Esko T, Pakhomov E, Salo P, Deelen J, McGurnaghan SJ, et al. Glycosylation of immunoglobulin G is regulated by a large network of genes pleiotropic with inflammatory diseases. *Sci Adv* (2020) **6**:24. doi:10.1126/sciadv.aax0301

120. Lauc G, Huffman JE, Pučić M, Zgaga L, Adamczyk B, Mužinić A, Novokmet M, Polašek O, Gornik O, Krištić J, et al. Loci Associated with N-Glycosylation of Human Immunoglobulin G Show Pleiotropy with Autoimmune Diseases and Haematological Cancers. *PLoS Genet* (2013) **9**:e1003225. doi:10.1371/journal.pgen.1003225

121. Wahl A, van den Akker E, Klaric L, Štambuk J, Benedetti E, Plomp R, Razdorov G, Trbojević-Akmačić I, Deelen J, van Heemst D, et al. Genome-Wide Association Study on Immunoglobulin G Glycosylation Patterns. *Front Immunol* (2018) **9**: doi:10.3389/fimmu.2018.00277

122. Štambuk J, Nakić N, Vučković F, Pučić-Baković M, Razdorov G, Trbojević-Akmačić I, Novokmet M, Keser T, Vilaj M, Štambuk T, et al. Global variability of the human IgG glycome. *Aging (Albany NY)* (2020) **12**:15222–15259. doi:10.18632/aging.103884

123. Krištić J, Vučković F, Menni C, Klarić L, Keser T, Beceheli I, Pučić-Baković M, Novokmet M, Mangino M, Thaqi K, et al. Glycans are a novel biomarker of chronological and biological ages. *Journals Gerontol - Ser A Biol Sci Med Sci* (2014) **69**:779–789. doi:10.1093/gerona/glt190

124. Ercan A, Kohrt WM, Cui J, Deane KD, Pezer M, Yu EW, Hausmann JS, Campbell H, Kaiser UB, Rudd PM, et al. Estrogens regulate glycosylation of IgG in women and men. *JCI Insight* (2017) **2**: doi:10.1172/jci.insight.89703

125. Peng J, Vongpatanasin W, Sacharidou A, Kifer D, Yuhanna IS, Banerjee S, Tanigaki K, Polasek O, Chu H, Sundgren NC, et al. Supplementation With the Sialic Acid Precursor N-Acetyl-D-Mannosamine Breaks the Link Between Obesity and Hypertension. *Circulation* (2019) **140**:2005–2018. doi:10.1161/CIRCULATIONAHA.119.043490

126. Tijardović M, Marijančević D, Bok D, Kifer D, Lauc G, Gornik O, Keser T. Intense Physical Exercise Induces an Anti-inflammatory Change in IgG N-Glycosylation Profile. *Front Physiol* (2019) **10**: doi:10.3389/fphys.2019.01522

127. Sarin H V., Gudelj I, Honkanen J, Ihalainen JK, Vuorela A, Lee JH, Jin Z, Terwilliger JD, Isola V, Ahtiainen JP, et al. Molecular Pathways Mediating Immunosuppression in Response to Prolonged Intensive Physical Training, Low-Energy Availability, and Intensive Weight Loss. *Front Immunol* (2019) **10**: doi:10.3389/fimmu.2019.00907

128. Deriš H, Kifer D, Cindrić A, Petrović T, Cvetko A, Trbojević-Akmačić I, Kolčić I, Polašek O, Newson L, Spector T, et al. Immunoglobulin G glycome composition in transition from premenopause to postmenopause. *iScience* (2022) **25**:103897. doi:10.1016/j.isci.2022.103897

129. Greto VL, Cvetko A, Štambuk T, Dempster NJ, Kifer D, Deriš H, Cindrić A, Vučković F, Falchi M, Gillies RS, et al. Extensive weight loss reduces glycan age by altering IgG N-glycosylation. *Int J Obes* (2021) **45**:1521–1531. doi:10.1038/s41366-021-00816-3

130. Deriš H, Tominac P, Vučković F, Briški N, Astrup A, Blaak EE, Lauc G, Gudelj I. Effects of low-calorie and different weight-maintenance diets on IgG glycome composition. *Front Immunol* (2022) **13**: doi:10.3389/fimmu.2022.995186

131. Vidarsson G, Dekkers G, Rispens T. IgG subclasses and allotypes: From structure to effector functions. *Front Immunol* (2014) **5**:520. doi:10.3389/fimmu.2014.00520

132. Dekkers G, Treffers L, Plomp R, Bentlage AEH, Boer M de, Koeleman CAM, Lissenberg-Thunnissen SN, Visser R, Brouwer M, Mok JY, et al. Decoding the human immunoglobulin G-glycan repertoire reveals a spectrum of Fc-receptor- and complement-mediated-effector activities. *Front Immunol* (2017) **8**:877. doi:10.3389/fimmu.2017.00877

133. Temming AR, de Taeye SW, de Graaf EL, de Neef LA, Dekkers G, Bruggeman CW, Koers J, Ligthart P, Nagelkerke SQ, Zimring JC, et al. Functional Attributes of Antibodies, Effector Cells, and Target Cells Affecting NK Cell–Mediated Antibody-Dependent Cellular Cytotoxicity. *J Immunol* (2019) **203**:3126–3135. doi:10.4049/jimmunol.1900985

134. Wada R, Matsui M, Kawasaki N. Influence of N-glycosylation on effector functions and thermal stability of glycoengineered IgG1 monoclonal antibody with homogeneous glycoforms. *MAbs* (2019) **11**:350–372. doi:10.1080/19420862.2018.1551044

135. Baković MP, Selman MHJ, Hoffmann M, Rudan I, Campbell H, Deelder AM, Lauc G, Wuhrer M. High-Throughput IgG Fc N-Glycosylation Profiling by Mass Spectrometry of Glycopeptides. *J Proteome Res* (2013) **12**:821–831. doi:10.1021/pr300887z

136. Huffman JE, Pučić-Baković M, Klarić L, Hennig R, Selman MHJ, Vučković F, Novokmet M, Krištić J, Borowiak M, Muth T, et al. Comparative Performance of Four Methods for High-throughput Glycosylation Analysis of Immunoglobulin G in Genetic and Epidemiological Research. *Mol Cell Proteomics* (2014) **13**:1598–1610. doi:10.1074/mcp.M113.037465

137. Arnold JN, Dwek RA, Rudd PM, Sim RB. Mannan binding lectin and its interaction with immunoglobulins in health and in disease. *Immunol Lett* (2006) **106**:103–110. doi:10.1016/j.imlet.2006.05.007

138. Karsten CM, Pandey MK, Figge J, Kilchenstein R, Taylor PR, Rosas M, McDonald JU, Orr SJ, Berger M, Petzold D, et al. Anti-inflammatory activity of IgG1 mediated by Fc galactosylation and association of FcγRIIB and dectin-1. *Nat Med* (2012) **18**:1401–1406. doi:10.1038/nm.2862

139. Subedi GP, Barb AW. The immunoglobulin G1 N-glycan composition affects binding to each low affinity Fc γ receptor. *MAbs* (2016) **8**:1512–1524. doi:10.1080/19420862.2016.1218586

140. Keusch J, Lydyard PM, Berger EG, Delves PJ. B lymphocyte galactosyltransferase protein levels in normal individuals and in patients with rheumatoid arthritis. *Glycoconj J* (1998) **15**:1093–1097. doi:10.1023/A:1006957711557

141. Hess C, Winkler A, Lorenz AK, Holecska V, Blanchard V, Eiglmeier S, Schoen AL, Bitterling J, Stoehr AD, Petzold D, et al. T cell-independent B cell activation induces immunosuppressive sialylated IgG antibodies. *J Clin Invest* (2013) **123**:3788–3796. doi:10.1172/JCI65938

142. Bartsch YC, Eschweiler S, Leliavski A, Lunding HB, Wagt S, Petry J, Lilienthal GM, Rahmöller J, de Haan N, Hölscher A, et al. IgG Fc sialylation is regulated during the germinal center reaction following immunization with different adjuvants. *J Allergy Clin Immunol* (2020) **146**:652–666. doi:10.1016/j.jaci.2020.04.059

143. Cao Y, Song Z, Guo Z, Zhao X, Gong Y, Zhao K, Qu C, Huang Y, Li Y, Gao Y, et al. Cytokines in the Immune Microenvironment Change the Glycosylation of IgG by Regulating Intracellular Glycosyltransferases. *Front Immunol* (2022) **12**: doi:10.3389/fimmu.2021.724379

144. Schindler C, Levy DE, Decker T. JAK-STAT signaling: From interferons to cytokines. *J Biol Chem* (2007) **282**:20059–20063. doi:10.1074/jbc.R700016200

145. Bas M, Terrier A, Jacque E, Dehenne A, Pochet-Béghin V, Beghin C, Dezetter A-S, Dupont G, Engrand A, Beaufils B, et al. Fc Sialylation Prolongs Serum Half-Life of Therapeutic Antibodies. *J Immunol* (2019) **202**:1582–1594. doi:10.4049/jimmunol.1800896

146. Kaneko Y, Nimmerjahn F, Ravetch J V. Anti-inflammatory activity of immunoglobulin G resulting from Fc sialylation. *Science (80-)* (2006) **313**:670–673. doi:10.1126/science.1129594

147. Raju TS. Terminal sugars of Fc glycans influence antibody effector functions of IgGs. *Curr Opin Immunol* (2008) **20**:471–478. doi:10.1016/j.coi.2008.06.007

148. Quast I, Keller CW, Maurer MA, Giddens JP, Tackenberg B, Wang LX, Münz C, Nimmerjahn F, Dalakas MC, Lünemann JD. Sialylation of IgG Fc domain impairs complement-dependent cytotoxicity. *J Clin Invest* (2015) **125**:4160–4170. doi:10.1172/JCI82695

149. Pfeifle R, Rothe T, Ipseiz N, Scherer HU, Culemann S, Harre U, Ackermann JA, Seefried M, Kleyer A, Uderhardt S, et al. Regulation of autoantibody activity by the IL-23-T H 17 axis determines the onset of autoimmune disease. *Nat Immunol* (2017)

18:104–113. doi:10.1038/ni.3579

150.   Kurata I, Matsumoto I, Ohyama A, Osada A, Ebe H, Kawaguchi H, Kaneko S, Kondo
        Y, Tsuboi H, Tomioka A, et al. Potential involvement of OX40 in the regulation of
        autoantibody sialylation in arthritis. *Ann Rheum Dis* (2019) **78**:1488–1496.
        doi:10.1136/annrheumdis-2019-215195

151.   Lanoue A, Batista FD, Stewart M, Neuberger MS. Interaction of CD22 with α2,6-
        linked sialoglycoconjugates: Innate recognition of self to dampen B cell
        autoreactivity? *Eur J Immunol* (2002) **32**:348–355. doi:10.1002/1521-
        4141(200202)32:2<348::AID-IMMU348>3.0.CO;2-5

152.   Engdahl C, Bondt A, Harre U, Raufer J, Pfeifle R, Camponeschi A, Wuhrer M,
        Seeling M, Mårtensson IL, Nimmerjahn F, et al. Estrogen induces St6gal1 expression
        and increases IgG sialylation in mice and patients with rheumatoid arthritis: A
        potential explanation for the increased risk of rheumatoid arthritis in postmenopausal
        women. *Arthritis Res Ther* (2018) **20**:84. doi:10.1186/s13075-018-1586-z

153.   Jones MB, Oswald DM, Joshi S, Whiteheart SW, Orlando R, Cobb BA. B-cell-
        independent sialylation of IgG. *Proc Natl Acad Sci U S A* (2016) **113**:7207–7212.
        doi:10.1073/pnas.1523968113

154.   Irons EE, Punch PR, Lau JTY. Blood-Borne ST6GAL1 Regulates Immunoglobulin
        Production in B Cells. *Front Immunol* (2020) **11**:617. doi:10.3389/fimmu.2020.00617

155.   Manhardt CT, Punch PR, Dougher CWL, Lau JTY. Extrinsic sialylation is
        dynamically regulated by systemic triggers in vivo. *J Biol Chem* (2017) **292**:13514–
        13520. doi:10.1074/jbc.C117.795138

156.   Oswald DM, Lehoux SD, Zhou JY, Glendenning LM, Cummings RD, Cobb BA.
        ST6Gal1 in plasma is dispensable for IgG sialylation. *Glycobiology* (2022)
        doi:10.1093/glycob/cwac039

157.   Glendenning LM, Zhou JY, Reynero KM, Cobb BA. Divergent Golgi trafficking
        limits B cell-mediated IgG sialylation. *J Leukoc Biol* (2022) **112**:1555–1566.
        doi:10.1002/JLB.3MA0522-731R

158.   Shields RL, Lai J, Keck R, O'Connell LY, Hong K, Gloria Meng Y, Weikert SHA,
        Presta LG. Lack of fucose on human IgG1 N-linked oligosaccharide improves binding

to human FcγRIII and antibody-dependent cellular toxicity. *J Biol Chem* (2002) **277**:26733–26740. doi:10.1074/jbc.M202069200

159. Shinkawa T, Nakamura K, Yamane N, Shoji-Hosaka E, Kanda Y, Sakurada M, Uchida K, Anazawa H, Satoh M, Yamasaki M, et al. The absence of fucose but not the presence of galactose or bisecting N-acetylglucosamine of human IgG1 complex-type oligosaccharides shows the critical role of enhancing antibody-dependent cellular cytotoxicity. *J Biol Chem* (2003) **278**:3466–3473. doi:10.1074/jbc.M210665200

160. Patel KR, Roberts JT, Subedi GP, Barb AW. Restricted processing of CD16a/Fc receptor IIIa N-glycans from primary human NK cells impacts structure and function. *J Biol Chem* (2018) **293**:3477–3489. doi:10.1074/jbc.ra117.001207

161. Subedi GP, Barb AW. CD16a with oligomannose-type N-glycans is the only "low-affinity" Fc γ receptor that binds the IgG crystallizable fragment with high affinity in vitro. *J Biol Chem* (2019) **293**:16842–16850. doi:10.1074/jbc.RA118.004998

162. Van Coillie J, Schulz MA, Bentlage AEH, de Haan N, Ye Z, Geerdes DM, van Esch WJE, Hafkenscheid L, Miller RL, Narimatsu Y, et al. Role of N-Glycosylation in FcγRIIIa interaction with IgG. *Front Immunol* (2022) **13**: doi:10.3389/fimmu.2022.987151

163. Patel KR, Rodriguez Benavente MC, Walter Lorenz W, Mace EM, Barb AW. Fc γ receptor IIIa/CD16a processing correlates with the expression of glycan-related genes in human natural killer cells. *J Biol Chem* (2021) **296**:100183. doi:10.1074/jbc.RA120.015516

164. Oosterhoff JJ, Larsen MD, van der Schoot CE, Vidarsson G. Afucosylated IgG responses in humans – structural clues to the regulation of humoral immunity. *Trends Immunol* (2022) **43**:800–814. doi:10.1016/j.it.2022.08.001

165. Martin TC, Šimurina M, Zabczynska M, Kavur M, Rydlewska M, Pezer M, Kozłowska K, Burri A, Vilaj M, Turek-Jabrocka R, et al. Decreased Immunoglobulin G Core Fucosylation, A Player in Antibody-dependent Cell-mediated Cytotoxicity, is Associated with Autoimmune Thyroid Diseases. *Mol Cell Proteomics* (2020) **19**:774–792. doi:10.1074/mcp.RA119.001860

166. Kuehn HS, Nunes-Santos CJ, Rosenzweig SD. Germline IKZF1 mutations and their

impact on immunity: IKAROS-associated diseases and pathophysiology. *Expert Rev Clin Immunol* (2021) **17**:407–416. doi:10.1080/1744666X.2021.1901582

167. Endreffy I, Bjørklund G, Szerafin L, Chirumbolo S, Urbina MA, Endreffy E. Plasma alpha-L-fucosidase activity in chronic inflammation and autoimmune disorders in a pediatric cohort of hospitalized patients. *Immunol Res* (2017) **65**:1025–1030. doi:10.1007/s12026-017-8943-x

168. Plomp R, Ruhaak LR, Uh HW, Reiding KR, Selman M, Houwing-Duistermaat JJ, Slagboom PE, Beekman M, Wuhrer M. Subclass-specific IgG glycosylation is associated with markers of inflammation and metabolic health. *Sci Rep* (2017) **7**:12325. doi:10.1038/s41598-017-12495-0

169. Huang G, Li Z, Li Y, Liu G, Sun S, Gu J, Kameyama A, Li W, Dong W. Loss of core fucosylation in both ST6GAL1 and its substrate enhances glycoprotein sialylation in mice. *Biochem J* (2020) **477**:1179–1201. doi:10.1042/BCJ20190789

170. Ferrara C, Brünker P, Suter T, Moser S, Püntener U, Umaña P. Modulation of therapeutic antibody effector functions by glycosylation engineering: Influence of golgi enzyme localization domain and co-expression of heterologous β1, 4-N-acetylglucosaminyltransferase III and Golgi α-mannosidase II. *Biotechnol Bioeng* (2006) **93**:851–861. doi:10.1002/bit.20777

171. Klasić M, Markulin D, Vojta A, Samaržija I, Biruš I, Dobrinić P, Ventham NT, Trbojević-Akmačić I, Šimurina M, Štambuk J, et al. Promoter methylation of the MGAT3 and BACH2 genes correlates with the composition of the immunoglobulin G glycome in inflammatory bowel disease. *Clin Epigenetics* (2018) **10**:75. doi:10.1186/s13148-018-0507-y

172. Ho CH, Chen SH, Tsai HW, Wu IC, Chang TT. Fully galactosyl-fucosyl-bisected IgG 1 reduces anti-HBV efficacy and liver histological improvement. *Antiviral Res* (2019) **163**:1–10. doi:10.1016/j.antiviral.2018.12.021

173. Roth GA, Mensah GA, Johnson CO, Addolorato G, Ammirati E, Baddour LM, Barengo NC, Beaton A, Benjamin EJ, Benziger CP, et al. Global Burden of Cardiovascular Diseases and Risk Factors, 1990–2019: Update From the GBD 2019 Study. *J Am Coll Cardiol* (2020) **76**:2982–3021. doi:10.1016/J.JACC.2020.11.010

174. Visseren FLJ, Mach F, Smulders YM, Carballo D, Koskinas KC, Bäck M, Benetos A, Biffi A, Boavida J-M, Capodanno D, et al. 2021 ESC Guidelines on cardiovascular disease prevention in clinical practice. *Eur J Prev Cardiol* (2022) **29**:5–115. doi:10.1093/eurjpc/zwab154

175. Timmis A, Vardas P, Townsend N, Torbica A, Katus H, De Smedt D, Gale CP, Maggioni AP, Petersen SE, Huculeci R, et al. European Society of Cardiology: cardiovascular disease statistics 2021. *Eur Heart J* (2022) **43**:716–799. doi:10.1093/eurheartj/ehab892

176. Hackam DG, Anand SS. Emerging Risk Factors for Atherosclerotic Vascular Disease. *JAMA* (2003) **290**:932. doi:10.1001/jama.290.7.932

177. Noels H, Weber C, Koenen RR. Chemokines as Therapeutic Targets in Cardiovascular Disease. *Arterioscler Thromb Vasc Biol* (2019) **39**:583–592. doi:10.1161/ATVBAHA.118.312037

178. Mindur JE, Swirski FK. Growth Factors as Immunotherapeutic Targets in Cardiovascular Disease. *Arterioscler Thromb Vasc Biol* (2019) **39**:1275–1287. doi:10.1161/ATVBAHA.119.311994

179. Wu X, Li Y, Zhang S, Zhou X. Ferroptosis as a novel therapeutic target for cardiovascular disease. *Theranostics* (2021) **11**:3052–3059. doi:10.7150/thno.54113

180. Thomas MR, Lip GYH. Novel Risk Markers and Risk Assessments for Cardiovascular Disease. *Circ Res* (2017) **120**:133–149. doi:10.1161/CIRCRESAHA.116.309955

181. Laggerbauer B, Engelhardt S. MicroRNAs as therapeutic targets in cardiovascular disease. *J Clin Invest* (2022) **132**: doi:10.1172/JCI159179

182. Wu Y, Zhan S, Xu Y, Gao X. RNA modifications in cardiovascular diseases, the potential therapeutic targets. *Life Sci* (2021) **278**:119565. doi:10.1016/j.lfs.2021.119565

183. Liu Y-P, Zhang T-N, Wen R, Liu C-F, Yang N. Role of Posttranslational Modifications of Proteins in Cardiovascular Disease. *Oxid Med Cell Longev* (2022) **2022**:1–16. doi:10.1155/2022/3137329

184. Wu Z, Jankowski V, Jankowski J. Irreversible post-translational modifications – Emerging cardiovascular risk factors. *Mol Aspects Med* (2022) **86**:101010.

doi:10.1016/j.mam.2021.101010

185. Libby P. The changing landscape of atherosclerosis. *Nature* (2021) **592**:524–533. doi:10.1038/s41586-021-03392-8

186. Sorriento D, Iaccarino G. Inflammation and cardiovascular diseases: The most recent findings. *Int J Mol Sci* (2019) **20**: doi:10.3390/ijms20163879

187. Pu Q, Yu C. Glycosyltransferases, glycosylation and atherosclerosis. *Glycoconj J* (2014) **31**:605–611. doi:10.1007/s10719-014-9560-8

188. Huopaniemi L, Kolmer M, Niittymäki J, Pelto-Huikko M, Renkonen R. Inflammation-induced transcriptional regulation of Golgi transporters required for the synthesis of sulfo sLex glycan epitopes. *Glycobiology* (2004) **14**:1285–1294. doi:10.1093/glycob/cwh131

189. Scott DW, Dunn TS, Ballestas ME, Litovsky SH, Patel RP. Identification of a high-mannose ICAM-1 glycoform: Effects of ICAM-1 hypoglycosylation on monocyte adhesion and outside in signaling. *Am J Physiol - Cell Physiol* (2013) **305**:C228–C237. doi:10.1152/ajpcell.00116.2013

190. Regal-McDonald K, Xu B, Barnes JW, Patel RP. High-mannose intercellular adhesion molecule-1 enhances CD16+ monocyte adhesion to the endothelium. *Am J Physiol - Hear Circ Physiol* (2019) **317**:H1028–H1038. doi:10.1152/AJPHEART.00306.2019

191. Regal-McDonald K, Somarathna M, Lee T, Litovsky SH, Barnes J, Peretik JM, Traylor JG, Orr AW, Patel RP. Assessment of ICAM-1 N-glycoforms in mouse and human models of endothelial dysfunction. *PLoS One* (2020) **15**:e0230358. doi:10.1371/journal.pone.0230358

192. Zhang J, Liu Y, Deng X, Chen L, Yang X, Yu C. ST6GAL1 negatively regulates monocyte transendothelial migration and atherosclerosis development. *Biochem Biophys Res Commun* (2018) **500**:249–255. doi:10.1016/j.bbrc.2018.04.053

193. Woodard-Grice A V., McBrayer AC, Wakefield JK, Zhuo Y, Bellis SL. Proteolytic shedding of ST6Gal-I by BACE1 regulates the glycosylation and function of α4β1 integrins. *J Biol Chem* (2008) **283**:26364–26373. doi:10.1074/jbc.M800836200

194. Linton MF, Yancey PG, Davies SS, Jerome WG, Linton EF, Song WL, Doran AC, Vickers KC. *The Role of Lipids and Lipoproteins in Atherosclerosis*. MDText.com,

Inc. (2000). Available at: http://www.ncbi.nlm.nih.gov/pubmed/25520374

195. Huang J, Lee H, Zivkovic AM, Smilowitz JT, Rivera N, German JB, Lebrilla CB. Glycomic Analysis of High Density Lipoprotein Shows a Highly Sialylated Particle. *J Proteome Res* (2014) **13**:681–691. doi:10.1021/pr4012393

196. Melajärvi N, Gylling H, Miettinen TA. Sialic acids and the metabolism of low density lipoprotein. *J Lipid Res* (1996) **37**:1625–31. Available at: http://www.ncbi.nlm.nih.gov/pubmed/8864946

197. Lindbohm N, Gylling H, Rajaratnam RA, Miettinen TA. Sialic acid content of low-density lipoprotein in women with coronary artery disease. *J Lab Clin Med* (2000) **136**:110–115. doi:10.1067/mlc.2000.108148

198. Nioi P, Sigurdsson A, Thorleifsson G, Helgason H, Agustsdottir AB, Norddahl GL, Helgadottir A, Magnusdottir A, Jonasdottir A, Gretarsdottir S, et al. Variant ASGR1 Associated with a Reduced Risk of Coronary Artery Disease. *N Engl J Med* (2016) **374**:2131–2141. doi:10.1056/nejmoa1508419

199. Pullen B, Vidanapathirana A, Sandeman L, Everest-Dass A, Kolarich D, Tan J, Psaltis P, Nicholls S, Packer N, Bursill C. Deletion of the Asialyloglycoprotein Receptor-1 (ASGR-1) Causes Athero-protective Effects in vitro and in vivo and Changes the Plaque Glycome. *Hear Lung Circ* (2023) **32**:S410. doi:10.1016/j.hlc.2023.06.571

200. Kataoka H, Kume N, Miyamoto S, Minami M, Murase T, Sawamura T, Masaki T, Hashimoto N, Kita T. Biosynthesis and post-translational processing of lectin-like oxidized low density lipoprotein receptor-1 (LOX-1). N-linked glycosylation affects cell-surface expression and ligand binding. *J Biol Chem* (2000) **275**:6573–9. doi:10.1074/jbc.275.9.6573

201. Qian Y, Zhang X, Zhou L, Yun X, Xie J, Xu J, Ruan Y, Ren S. Site-specific N-glycosylation identification of recombinant human lectin-like oxidized low density lipoprotein receptor-1 (LOX-1). *Glycoconj J* (2012) **29**:399–409. doi:10.1007/s10719-012-9408-z

202. Betteridge KB, Arkill KP, Neal CR, Harper SJ, Foster RR, Satchell SC, Bates DO, Salmon AHJ. Sialic acids regulate microvessel permeability, revealed by novel in vivo studies of endothelial glycocalyx structure and function. *J Physiol* (2017) **595**:5015–

5035. doi:10.1113/JP274167

203. Tertov VV, Kaplun VV, Sobenin IA, Boytsova EY, Bovin NV, Orekhov AN. Human plasma trans-sialidase causes atherogenic modification of low density lipoprotein. *Atherosclerosis* (2001) **159**:103–115. doi:10.1016/S0021-9150(01)00498-1

204. Glanz VY, Myasoedova VA, Grechko A V., Orekhov AN. Trans-sialidase Associated with Atherosclerosis: Defining the Identity of a Key Enzyme Involved in the Pathology. *Curr Drug Targets* (2019) **20**:938–941. doi:10.2174/1389450120666190308111619

205. Sarphie TG. Interactions of IgG and β-VLDL with aortic valve endothelium from hypercholesterolemic rabbits. *Atherosclerosis* (1987) **68**:199–212. doi:10.1016/0021-9150(87)90199-7

206. Subramanian SP, Gundry RL. The known unknowns of apolipoprotein glycosylation in health and disease. *iScience* (2022) **25**:105031. doi:10.1016/j.isci.2022.105031

207. Soehnlein O, Libby P. Targeting inflammation in atherosclerosis — from experimental insights to the clinic. *Nat Rev Drug Discov* (2021) **20**:589–610. doi:10.1038/s41573-021-00198-1

208. Stakhneva EM, Kashtanova EV, Polonskaya YV, Striukova EV, Shramko VS, Sadovski EV, Kurguzov AV, Murashov IS, Chernyavskii AM, Ragino YI. The Search for Associations of Serum Proteins with the Presence of Unstable Atherosclerotic Plaque in Coronary Atherosclerosis. *Int J Mol Sci* (2022) **23**:12795. doi:10.3390/ijms232112795

209. Wågsäter D, Johansson D, Fontaine V, Vorkapic E, Bäcklund A, Razuvaev A, Mäyränpää MI, Hjerpe C, Caidahl K, Hamsten A, et al. Serine protease inhibitor A3 in atherosclerosis and aneurysm disease. *Int J Mol Med* (2012) **30**:288–294. doi:10.3892/ijmm.2012.994

210. Ward LJ, Olausson P, Li W, Yuan X-M. Proteomics and multivariate modelling reveal sex-specific alterations in distinct regions of human carotid atheroma. *Biol Sex Differ* (2018) **9**:54. doi:10.1186/s13293-018-0217-3

211. Arenas De Larriva AP, Limia-Pérez L, Alcalá-Díaz JF, Alonso A, López-Miranda J, Delgado-Lista J. Ceruloplasmin and coronary heart disease-a systematic review.

Nutrients (2020) **12**:1–15. doi:10.3390/nu12103219

212. Duprez DA, Otvos J, Sanchez OA, Mackey RH, Tracy R, Jacobs DR. Comparison of the predictive value of GlycA and other biomarkers of inflammation for total death, incident cardiovascular events, noncardiovascular and noncancer inflammatory-related events, and total cancer events. *Clin Chem* (2016) **62**:1020–1031. doi:10.1373/clinchem.2016.255828

213. Fashanu OE, Oyenuga AO, Zhao D, Tibuakuu M, Mora S, Otvos JD, Stein JH, Michos ED. GlycA, a Novel Inflammatory Marker, and its Association with Peripheral Arterial Disease and Carotid Plaque: The Multi-Ethnic Study of Atherosclerosis. *Angiology* (2019) **70**:737. doi:10.1177/0003319719845185

214. Tibuakuu M, Fashanu OE, Zhao D, Otvos JD, Brown TT, Haberlen SA, Guallar E, Budoff MJ, Palella FJ, Martinson JJ, et al. GlycA, a novel inflammatory marker, is associated with subclinical coronary disease. *AIDS* (2019) **33**:547–557. doi:10.1097/QAD.0000000000002079

215. Bai L, Li Q, Li L, Lin Y, Zhao S, Wang W, Wang R, Li Y, Yuan J, Wang C, et al. Plasma High-Mannose and Complex/Hybrid N-Glycans Are Associated with Hypercholesterolemia in Humans and Rabbits. *PLoS One* (2016) **11**:e0146982. doi:10.1371/journal.pone.0146982

216. Ley K. Role of the adaptive immune system in atherosclerosis. *Biochem Soc Trans* (2020) **48**:2273–2281. doi:10.1042/BST20200602

217. Roy P, Orecchioni M, Ley K. How the immune system shapes atherosclerosis: roles of innate and adaptive immunity. *Nat Rev Immunol* (2022) **22**:251–265. doi:10.1038/s41577-021-00584-1

218. Kimura T, Tse K, Sette A, Ley K. Vaccination to modulate atherosclerosis. *Autoimmunity* (2015) **48**:152–160. doi:10.3109/08916934.2014.1003641

219. Tay C, Liu Y-H, Kanellakis P, Kallies A, Li Y, Cao A, Hosseini H, Tipping P, Toh B-H, Bobik A, et al. Follicular B Cells Promote Atherosclerosis via T Cell–Mediated Differentiation Into Plasma Cells and Secreting Pathogenic Immunoglobulin G. *Arterioscler Thromb Vasc Biol* (2018) **38**: doi:10.1161/ATVBAHA.117.310678

220. Björkbacka H, Alm R, Persson M, Hedblad B, Nilsson J, Fredrikson GN. Low Levels

of Apolipoprotein B-100 Autoantibodies Are Associated With Increased Risk of Coronary Events. *Arterioscler Thromb Vasc Biol* (2016) **36**:765–771. doi:10.1161/ATVBAHA.115.306938

221. Wang M, Chen X, Tang Z, Zhang W, Hou H, Sun X, Shi Y, Lu X, Li P, Ji L, et al. Association Between Immunoglobulin G N-glycosylation and Vascular Cognitive Impairment in a Sample With Atherosclerosis: A Case-Control Study. *Front Aging Neurosci* (2022) **14**: doi:10.3389/fnagi.2022.823468

222. Patzelt J, Verschoor A, Langer HF. Platelets and the complement cascade in atherosclerosis. *Front Physiol* (2015) **6**: doi:10.3389/fphys.2015.00049

223. Carter AM. Complement Activation: An Emerging Player in the Pathogenesis of Cardiovascular Disease. *Scientifica (Cairo)* (2012) **2012**:1–14. doi:10.6064/2012/402783

224. Gao Q, Dolikun M, Štambuk J, Wang H, Zhao F, Yiliham N, Wang Y, Trbojević-Akmačić I, Zhang J, Fang H, et al. Immunoglobulin G N-Glycans as Potential Postgenomic Biomarkers for Hypertension in the Kazakh Population. *Omi A J Integr Biol* (2017) **21**:380–389. doi:10.1089/omi.2017.0044

225. Wang Y, Klarić L, Yu X, Thaqi K, Dong J, Novokmet M, Wilson J, Polasek O, Liu Y, Krištić J, et al. The Association Between Glycosylation of Immunoglobulin G and Hypertension. *Medicine (Baltimore)* (2016) **95**:e3379. doi:10.1097/MD.0000000000003379

226. Fuchs FD, Whelton PK. High Blood Pressure and Cardiovascular Disease. *Hypertension* (2020) **75**:285–292. doi:10.1161/HYPERTENSIONAHA.119.14240

227. Lemmers RFH, Vilaj M, Urda D, Agakov F, Šimurina M, Klaric L, Rudan I, Campbell H, Hayward C, Wilson JF, et al. IgG glycan patterns are associated with type 2 diabetes in independent European populations. *Biochim Biophys Acta - Gen Subj* (2017) **1861**:2240–2249. doi:10.1016/j.bbagen.2017.06.020

228. Rao GH. Cardiometabolic Diseases: A Global Perspective. *J Cardiol Cardiovasc Ther* (2018) **12**: doi:10.19080/JOCCT.2018.12.555834

229. Meng X, Cao W, Liu D, Elijah IM, Xing W, Hou H, Xu X, Song M, Wang Y. Bidirectional Causality Between Immunoglobulin G N-Glycosylation and Metabolic

Traits: A Mendelian Randomization Study. *Engineering* (2022) doi:10.1016/j.eng.2022.11.004

230. Franzka P, Krüger L, Schurig MK, Olecka M, Hoffmann S, Blanchard V, Hübner CA. Altered Glycosylation in the Aging Heart. *Front Mol Biosci* (2021) **8**:1–16. doi:10.3389/fmolb.2021.673044

231. Ferrannini E, Marx N, Andreini D, Campi B, Saba A, Gorini M, Ferrannini G, Milzi A, Magnoni M, Maseri A, et al. Mannose as a biomarker of coronary artery disease: Angiographic evidence and clinical significance. *Int J Cardiol* (2022) **346**:86–92. doi:10.1016/j.ijcard.2021.11.038

232. Zhang L, Wei T-T, Li Y, Li J, Fan Y, Huang F-Q, Cai Y-Y, Ma G, Liu J-F, Chen Q-Q, et al. Functional Metabolomics Characterizes a Key Role for N-Acetylneuraminic Acid in Coronary Artery Diseases. *Circulation* (2018) **137**:1374–1390. doi:10.1161/CIRCULATIONAHA.117.031139

233. Zhang C, Chen J, Liu Y, Xu D. Sialic acid metabolism as a potential therapeutic target of atherosclerosis. *Lipids Health Dis* (2019) **18**:173. doi:10.1186/s12944-019-1113-5

234. Suzuki H, Chikada M, Yokoyama MK, Kurokawa MS, Ando T, Furukawa H, Arito M, Miyairi T, Kato T. Aberrant Glycosylation of Lumican in Aortic Valve Stenosis Revealed by Proteomic Analysis. *Int Heart J* (2016) **57**:104–111. doi:10.1536/ihj.15-252

235. Angel PM, Drake RR, Park Y, Clift CL, West C, Berkhiser S, Hardiman G, Mehta AS, Bichell DP, Su YR. Spatial N-glycomics of the human aortic valve in development and pediatric endstage congenital aortic valve stenosis. *J Mol Cell Cardiol* (2021) **154**:6–20. doi:10.1016/j.yjmcc.2021.01.001

236. Wang X, Inoue S, Gu J, Miyoshi E, Noda K, Li W, Mizuno-Horikawa Y, Nakano M, Asahi M, Takahashi M, et al. Dysregulation of TGF-β1 receptor activation leads to abnormal lung development and emphysema-like phenotype in core fucose-deficient mice. *Proc Natl Acad Sci* (2005) **102**:15791–15796. doi:10.1073/pnas.0507375102

237. Wang X, Gu J, Ihara H, Miyoshi E, Honke K, Taniguchi N. Core Fucosylation Regulates Epidermal Growth Factor Receptor-mediated Intracellular Signaling. *J Biol Chem* (2006) **281**:2572–2577. doi:10.1074/jbc.M510893200

238. Makki N, Thiel K, Miller F. The Epidermal Growth Factor Receptor and Its Ligands in Cardiovascular Disease. *Int J Mol Sci* (2013) **14**:20597–20613. doi:10.3390/ijms141020597

239. Rosenkranz S. TGF-β1 and angiotensin networking in cardiac remodeling. *Cardiovasc Res* (2004) **63**:423–432. doi:10.1016/j.cardiores.2004.04.030

240. Nagai-Okatani C, Minamino N. Aberrant Glycosylation in the Left Ventricle and Plasma of Rats with Cardiac Hypertrophy and Heart Failure. *PLoS One* (2016) **11**:e0150210. doi:10.1371/journal.pone.0150210

241. Montpetit ML, Stocker PJ, Schwetz TA, Harper JM, Norring SA, Schaffer L, North SJ, Jang-Lee J, Gilmartin T, Head SR, et al. Regulated and aberrant glycosylation modulate cardiac electrical signaling. *Proc Natl Acad Sci* (2009) **106**:16517–16522. doi:10.1073/pnas.0905414106

242. Itakura Y, Hasegawa Y, Kikkawa Y, Murakami Y, Sugiura K, Nagai-Okatani C, Sasaki N, Umemura M, Takahashi Y, Kimura T, et al. Spatiotemporal changes of tissue glycans depending on localization in cardiac aging. *Regen Ther* (2023) **22**:68–78. doi:10.1016/j.reth.2022.12.009

243. Kettunen J, Ritchie SC, Anufrieva O, Lyytikäinen L-P, Hernesniemi J, Karhunen PJ, Kuukasjärvi P, Laurikka J, Kähönen M, Lehtimäki T, et al. Biomarker Glycoprotein Acetyls Is Associated With the Risk of a Wide Spectrum of Incident Diseases and Stratifies Mortality Risk in Angiography Patients. *Circ Genomic Precis Med* (2018) **11**: doi:10.1161/CIRCGEN.118.002234

244. Jang S, Ogunmoroti O, Ndumele CE, Zhao D, Rao VN, Fashanu OE, Tibuakuu M, Otvos JD, Benson E-M, Ouyang P, et al. Association of the Novel Inflammatory Marker GlycA and Incident Heart Failure and Its Subtypes of Preserved and Reduced Ejection Fraction. *Circ Hear Fail* (2020) **13**: doi:10.1161/CIRCHEARTFAILURE.120.007067

245. Harada PH, Benseñor IM, Bittencourt MS, Nasir K, Blaha MJ, Jones SR, Toth PP, Lotufo PA. Composite acute phase glycoproteins with coronary artery calcification depends on metabolic syndrome presence – The Brazilian Longitudinal Study of Adult Health (ELSA-Brasil). *J Cardiol* (2019) **73**:408–415. doi:10.1016/j.jjcc.2018.09.006

246. Lawler PR, Mora S. Glycosylation Signatures of Inflammation Identify Cardiovascular Risk. *Circ Res* (2016) **119**:1154–1156. doi:10.1161/CIRCRESAHA.116.310005

247. Purmalek MM, Carlucci PM, Dey AK, Sampson M, Temesgen-Oyelakin Y, Sakhardande S, Lerman JB, Fike A, Davis M, Chung JH, et al. Association of lipoprotein subfractions and glycoprotein acetylation with coronary plaque burden in SLE. *Lupus Sci Med* (2019) **6**:e000332. doi:10.1136/lupus-2019-000332

248. Lim SY, Hendra C, Yeo XH, Tan XY, Ng BH, Laserna AKC, Tan SH, Chan MY, Khan SH, Chen S-M, et al. N-glycan profiles of acute myocardial infarction patients reveal potential biomarkers for diagnosis, severity assessment and treatment monitoring. *Glycobiology* (2022) **32**:469–482. doi:10.1093/glycob/cwab129

249. Fortin E, Ferrannini G, Campi B, Mellbin L, Norhammar A, Näsman P, Saba A, Ferrannini E, Rydén L. Plasma mannose as a novel marker of myocardial infarction across different glycaemic states: a case control study. *Cardiovasc Diabetol* (2022) **21**:195. doi:10.1186/s12933-022-01630-5

250. Cheeseman J, Kuhnle G, Stafford G, Gardner RA, Spencer DI, Osborn HM. Sialic acid as a potential biomarker for cardiovascular disease, diabetes and cancer. *Biomark Med* (2021) **15**:911–928. doi:10.2217/bmm-2020-0776

251. Gayral S, Garnotel R, Castaing-Berthou A, Blaise S, Fougerat A, Berge E, Montheil A, Malet N, Wymann MP, Maurice P, et al. Elastin-derived peptides potentiate atherosclerosis through the immune Neu1–PI3Kγ pathway. *Cardiovasc Res* (2014) **102**:118–127. doi:10.1093/cvr/cvt336

252. Sieve I, Ricke-Hoch M, Kasten M, Battmer K, Stapel B, Falk CS, Leisegang MS, Haverich A, Scherr M, Hilfiker-Kleiner D. A positive feedback loop between IL-1β, LPS and NEU1 may promote atherosclerosis by enhancing a pro-inflammatory state in monocytes and macrophages. *Vascul Pharmacol* (2018) **103**–**105**:16–28. doi:10.1016/j.vph.2018.01.005

253. White EJ, Gyulay G, Lhoták Š, Szewczyk MM, Chong T, Fuller MT, Dadoo O, Fox-Robichaud AE, Austin RC, Trigatti BL, et al. Sialidase down-regulation reduces non-HDL cholesterol, inhibits leukocyte transmigration, and attenuates atherosclerosis in ApoE knockout mice. *J Biol Chem* (2018) **293**:14689–14706. doi:10.1074/jbc.RA118.004589

254. Demina EP, Smutova V, Pan X, Fougerat A, Guo T, Zou C, Chakraberty R, Snarr BD, Shiao TC, Roy R, et al. Neuraminidases 1 and 3 Trigger Atherosclerosis by Desialylating Low-Density Lipoproteins and Increasing Their Uptake by Macrophages. *J Am Heart Assoc* (2021) **10**: doi:10.1161/JAHA.120.018756

255. Heimerl M, Sieve I, Ricke-Hoch M, Erschow S, Battmer K, Scherr M, Hilfiker-Kleiner D. Neuraminidase-1 promotes heart failure after ischemia/reperfusion injury by affecting cardiomyocytes and invading monocytes/macrophages. *Basic Res Cardiol* (2020) **115**:62. doi:10.1007/s00395-020-00821-z

256. Guo Z, Tuo H, Tang N, Liu F-Y, Ma S-Q, An P, Yang D, Wang M-Y, Fan D, Yang Z, et al. Neuraminidase 1 deficiency attenuates cardiac dysfunction, oxidative stress, fibrosis, inflammatory via AMPK-SIRT3 pathway in diabetic cardiomyopathy mice. *Int J Biol Sci* (2022) **18**:826–840. doi:10.7150/ijbs.65938

257. Chen Q-Q, Ma G, Liu J-F, Cai Y-Y, Zhang J-Y, Wei T-T, Pan A, Jiang S, Xiao Y, Xiao P, et al. Neuraminidase 1 is a driver of experimental cardiac hypertrophy. *Eur Heart J* (2021) **42**:3770–3782. doi:10.1093/eurheartj/ehab347

258. Austen WG, Edwards JE, Frye RL, Gensini GG, Gott VL, Griffith LS, McGoon DC, Murphy ML, Roe BB. A reporting system on patients evaluated for coronary artery disease. Report of the Ad Hoc Committee for Grading of Coronary Artery Disease, Council on Cardiovascular Surgery, American Heart Association. *Circulation* (1975) **51**:5–40. doi:10.1161/01.cir.51.4.5

259. Marth JD, Grewal PK. Mammalian glycosylation in immunity. *Nat Rev Immunol* (2008) **8**:874–887. doi:10.1038/nri2417

260. Colafella KMM, Denton KM. Sex-specific differences in hypertension and associated cardiovascular disease. *Nat Rev Nephrol* (2018) **14**:185–201. doi:10.1038/nrneph.2017.189

261. Gruppen EG, Connelly MA, Vart P, Otvos JD, Bakker SJL, Dullaart RPF. GlycA, a novel proinflammatory glycoprotein biomarker, and high-sensitivity C-reactive protein are inversely associated with sodium intake after controlling for adiposity: The Prevention of Renal and Vascular End-Stage Disease study. *Am J Clin Nutr* (2016) **104**:415–422. doi:10.3945/ajcn.116.133744

262. Ballout RA, Remaley AT. GlycA: a new biomarker for systemic inflammation and cardiovascular disease (CVD) risk assessment. *J Lab Precis Med* (2020) **5**:17–17. doi:10.21037/jlpm.2020.03.03

263. Mehta NN, Dey AK, Maddineni R, Kraus WE, Huffman KM. GlycA measured by NMR spectroscopy is associated with disease activity and cardiovascular disease risk in chronic inflammatory diseases. *Am J Prev Cardiol* (2020) **4**:100120. doi:10.1016/j.ajpc.2020.100120

264. Brown JC, Gerhardt TE, Kwon E. Risk Factors For Coronary Artery Disease. *Risk Factors Coron Artery Dis* (2022)1–219. doi:10.3109/9781420014570

265. McKinlay SM, Brambilla DJ, Posner JG. The normal menopause transition. *Maturitas* (1992) **14**:103–115. doi:10.1016/0378-5122(92)90003-M

266. Brinkman-Van Der Linden ECM, Havenaar EC, Van Ommen ECR, Van Kamp GJ, Gooren LJG, Van Dijk W. Oral estrogen treatment induces a decrease in expression of sialyl Lewis x on α1-acid glycoprotein in females and male-to-female transsexuals. *Glycobiology* (1996) **6**:407–412. doi:10.1093/glycob/6.4.407

267. Niccoli T, Partridge L. Ageing as a Risk Factor for Disease. *Curr Biol* (2012) **22**:R741–R752. doi:10.1016/j.cub.2012.07.024

268. Ruhaak LR, Uh HW, Beekman M, Hokke CH, Westendorp RGJ, Houwing-Duistermaat J, Wuhrer M, Deelder AM, Slagboom PE. Plasma protein N-glycan profiles are associated with calendar age, familial longevity and health. *J Proteome Res* (2011) **10**:1667–1674. doi:10.1021/pr1009959

269. Ding N, Sun HN, Sun W, Qu Y, Liu X, Yao Y, Liang X, Chen CC, Li Y. Human serum N-glycan profiles are age and sex dependent. *Age Ageing* (2011) **40**:568–575. doi:10.1093/ageing/afr084

270. Vanhooren V, Desmyter L, Liu XE, Cardelli M, Franceschi C, Federico A, Libert C, Laroy W, Dewaele S, Contreras R, et al. N-glycomic changes in serum proteins during human aging. *Rejuvenation Res* (2007) **10**:521–531. doi:10.1089/rej.2007.0556

271. Liu Y, Lin L, Qiao L. Recent developments in organ-on-a-chip technology for cardiovascular disease research. *Anal Bioanal Chem* (2023) doi:10.1007/s00216-023-04596-9

272. Buckler AJ, Marlevi D, Skenteris NT, Lengquist M, Kronqvist M, Matic L, Hedin U. In silico model of atherosclerosis with individual patient calibration to enable precision medicine for cardiovascular disease. *Comput Biol Med* (2023) **152**:106364. doi:10.1016/j.compbiomed.2022.106364

8. APPENDICES

Appendix 1. List of abbreviations

Abbreviation	Meaning
2-AB	2-aminobenzanide
2-PB	2-picoline borane
A1AT	α1-antitrypsin
AACT	α1-antichymotrypsin
ADCC	Antibody dependent cellular cytotoxicity
ADCP	Antibody dependent cellular phagocytosis
AF	Atrial fibrillation
AGP-1	α1-acid glycoprotein
AMI	Acute myocardial infarction
ApoB	Apolipoprotein B
AS	Aortic valve stenosis
ASGR-1	Asialoglycoprotein receptor-1
Asn (N)	Asparagine
B4GALT1	β-1,4-galactosyltransferase 1
BACE1	Beta-Site APP-Cleaving Enzyme 1
BMI	Body mass index
CAD	Coronary artery disease
CAD-	Subjects with clean coronary arteries
CAD+	Subjects with angiographically diagnosed coronary artery disease
CD	Crohn's disease
CDC	Complement dependent cytotoxicity
CH_3CH_2OH	Ethanol
CH_3CN	Acetonitrile
CH_3COOH	Acetic acid
CRP	C-reactive protein
cTnI	Cardiac troponin 1
CVD	Cardiovascular disease
DMSO	Dimethyl sulfoxide
EFGR	Epidermal growth factor receptor
ER	Endoplasmatic reticulum
EU	Emission unit
Fab	Antigen binding fragment
Fc	Crystallizable fragment
Fuc, F	Fucose
FUCA-1	α-L-fucosidase
FUT6	Fucosyltransferase 6
GA	Golgi Apparatus
Gal, G	Galactose
GalNAc	N-acetylgalactosamine
GlcNAc	N-acetylglucosamine
Glc	Glucose
GMPPB	GDP-mannose pyrophosphorylase B
GP	Glycan peak
GWAS	Genome wide association studies

HBP	Hexamine biosynthesis pathway
HCl	Hydrochloride acid
HCOOH	Formic acid
HDL	High density lipoprotein
HFD	High fat diet
HILIC-UHPLC-FLR	Ultra-high performance liquid chromatography based on hydrophilic interactions with fluorescence detection
HM-ICAM-1	High-mannose ICAM-1
HNF1α	Hepatocyte nuclear factor 1α
HPT	Haptoglobin
ICAM-1	Intercellular cell adhesion molecule 1
IFN-γ	Interferon γ
IgG	Immunoglobulin G
IL-17	Interleukin 17
IL-1β	Interleukin 1β
IL-21	Interleukin 21
IL-22	Interleukin 22
IL-23	Interleukin 23
IL-27	Interleukin 27
IL-6	Interleukin 6
KCl	Potassium chloride
KH_2PO_4	Potassium dihydrogen phosphate
LDL	Low density lipoprotein
Man, M	Mannose
ManNAc	N-acetyl-D-mannosamine
MBL	Mannose binding lectin
MGAT3	N-Acetylglucosaminyltransferase 3
NaCl	Sodium chloride
Na_2HPO_4	Disodium hydrogen phosphate
NaOH	Sodium hydroxide
NCD	Non-communicable disease
NEU-1	Neuraminidase 1
Neu5Ac, S	N-acetylneuraminic acid
NH_4HCO_3	Ammonium bicarbonate
NH_4OH	Ammonia, solution
NK cells	Natural killer cells
NMR	Nuclear magnetic resonance
N-prGO	Nitrogen-doped reduced graphene oxide
ox-LDL receptor 1	Lectin-like oxidized low density lipoprotein receptor 1
PBS	Phosphate buffered saline
PNGase F	N-glycosidase F
PTM	Posttranslational modification
QC	Quality control
RA	Rheumatoid arthritis
SDS	Sodium diphosphate sulphate
SHS	Suboptimal health status
sLeA	Sialyl Lewis A
sLeX	Sialyl Lewis X

SNP	Single nucleotide polymorphism
SPE	Solid phase extraction
ST3GAL4	β-galactoside α-2,3-sialyltransferase 4
ST6GAL1	β-galactoside α-2,6-sialyltransferase 1
Tfh	T follicular helper cell
TGF-β1	Transforming growth factor β1
Th1	T helper cell 1
Th17	T helper cell 17
TNFα	Tumor necrosis factor
TPOAb	Thyroid peroxidase antibody
Tris	Tris(hydroxymethyl)aminomethane
TSA	Total sialic acid
UPLC	Ultra-high performance liquid chromatography
VCAM-1	Vascular cell adhesion molecule 1
VLDL	Very low-density lipoprotein

Appendix 2. Statistical analysis of associations between IgG N-glycosylation traits and coronary artery disease at the time of inclusion. Glycan data were adjusted for age and sex whereas the false discovery rate was controlled by the Benjamini-Hochberg method. Statistically significant differences are in bold.

Glycan trait	Effect	SE	p-value	p_{adj}-value
GP1	0.00	0.1035	9.92E-01	9.92E-01
GP2	0.06	0.1094	5.67E-01	7.09E-01
GP3	0.11	0.1010	2.69E-01	5.04E-01
GP4	0.12	0.0988	2.27E-01	4.55E-01
GP5	-0.10	0.1073	3.29E-01	5.48E-01
GP6	0.21	0.1011	**3.99E-02**	4.25E-01
GP7	0.01	0.1099	9.47E-01	9.88E-01
GP8	-0.11	0.1082	3.05E-01	5.37E-01
GP9	-0.19	0.1080	8.04E-02	4.25E-01
GP10	0.14	0.1095	1.88E-01	4.33E-01
GP11	0.08	0.1082	4.78E-01	7.09E-01
GP12	0.03	0.1065	7.83E-01	9.40E-01
GP13	-0.17	0.1062	1.03E-01	4.25E-01
GP14	-0.14	0.0955	1.39E-01	4.25E-01
GP15	-0.06	0.1061	5.66E-01	7.09E-01
GP16	-0.09	0.1089	4.16E-01	6.56E-01
GP17	-0.02	0.1096	8.56E-01	9.51E-01
GP18	-0.15	0.1003	1.35E-01	4.25E-01
GP19	-0.14	0.1091	2.08E-01	4.45E-01
GP20	-0.14	0.1073	1.82E-01	4.33E-01
GP21	-0.07	0.1089	5.12E-01	7.09E-01
GP22	0.06	0.1096	5.60E-01	7.09E-01
GP23	-0.25	0.1064	**1.98E-02**	4.25E-01
GP24	-0.01	0.1092	9.55E-01	9.88E-01
G0 total	0.15	0.0974	1.16E-01	4.25E-01
G1 total	-0.14	0.1085	1.81E-01	4.33E-01
G2 total	-0.14	0.0955	1.41E-01	4.25E-01
S total	-0.18	0.1040	8.91E-02	4.25E-01
F total	-0.02	0.1093	8.25E-01	9.51E-01
B total	0.15	0.1057	1.42E-01	4.25E-01

Appendix 3. Statistical analysis of associations between directly measured plasma protein N-glycosylation traits and coronary artery disease at the time of inclusion. Glycan data were adjusted for age, sex, BMI, smoking and diabetes whereas the false discovery rate was controlled by the Benjamini-Hochberg method. Statistically significant differences are in bold.

Glycan trait	Effect	SE	p-value	p_{adj}-value*
GP1	-0.05	0.1074	6.63E-01	7.62E-01
GP2	-0.13	0.1099	2.52E-01	3.75E-01
GP3	0.01	0.1117	9.52E-01	9.56E-01
GP4	-0.13	0.1067	2.37E-01	3.75E-01
GP5	-0.14	0.1051	1.87E-01	3.18E-01
GP6	-0.19	0.1125	8.89E-02	2.13E-01
GP7	-0.35	0.1096	1.48E-03	**4.06E-02**
GP8	-0.01	0.1119	9.56E-01	9.56E-01
GP9	-0.27	0.1095	1.51E-02	1.10E-01
GP10	-0.13	0.0970	1.91E-01	3.18E-01
GP11	-0.30	0.1094	6.67E-03	8.25E-02
GP12	-0.06	0.1118	5.79E-01	7.08E-01
GP13	-0.22	0.1012	2.92E-02	1.23E-01
GP14	0.11	0.1084	3.26E-01	4.72E-01
GP15	-0.29	0.1092	7.50E-03	8.25E-02
GP16	-0.16	0.1026	1.12E-01	2.27E-01
GP17	-0.28	0.1101	9.53E-03	8.74E-02
GP18	-0.19	0.1018	6.26E-02	1.81E-01
GP19	-0.08	0.1088	4.62E-01	6.06E-01
GP20	0.24	0.1080	2.63E-02	1.20E-01
GP21	0.02	0.1116	8.27E-01	8.86E-01
GP22	0.22	0.1084	3.75E-02	1.38E-01
GP23	-0.03	0.1120	8.12E-01	8.86E-01
GP24	-0.12	0.1086	2.51E-01	3.75E-01
GP25	-0.09	0.1079	3.76E-01	5.17E-01
GP26	0.14	0.1040	1.71E-01	3.07E-01
GP27	0.19	0.0989	5.81E-02	1.81E-01
GP28	-0.08	0.1078	4.54E-01	6.06E-01
GP29	-0.10	0.1070	3.64E-01	5.14E-01
GP30	-0.07	0.1087	5.43E-01	6.78E-01
GP31	0.17	0.1059	1.02E-01	2.24E-01
GP32	0.29	0.0990	3.01E-03	5.51E-02
GP33	0.24	0.0992	1.65E-02	1.10E-01
GP34	0.18	0.1051	8.30E-02	2.12E-01
GP35	0.36	0.1027	4.54E-04	**2.50E-02**
GP36	0.03	0.1076	8.00E-01	8.86E-01
GP37	-0.21	0.1073	5.41E-02	1.81E-01
GP38	-0.05	0.1111	6.65E-01	7.62E-01
GP39	0.16	0.1057	1.23E-01	2.33E-01

Appendix 4. Statistical analysis of associations between derived plasma protein N-glycosylation traits and coronary artery disease at the time of inclusion. Glycan data were adjusted for age, sex, BMI, smoking and diabetes whereas the false discovery rate was controlled by the Benjamini-Hochberg method. Statistically significant differences are in bold

Glycan	effect	SE	pval	p.adj
AF	0.23	0.0999	**2.06E-02**	1.10E-01
B	-0.24	0.1115	**3.37E-02**	1.33E-01
CF	-0.18	0.1078	8.49E-02	2.12E-01
G0	-0.08	0.1075	4.74E-01	6.06E-01
G1	-0.19	0.1058	7.64E-02	2.10E-01
G2	0.06	0.1107	5.98E-01	7.15E-01
G3	0.18	0.1093	9.62E-02	2.20E-01
G4	0.02	0.1106	8.38E-01	8.86E-01
HB	0.17	0.1093	1.20E-01	2.33E-01
HM	-0.25	0.1104	**2.21E-02**	1.10E-01
LB	-0.13	0.1091	2.48E-01	3.75E-01
S0	-0.17	0.1084	1.07E-01	2.27E-01
S1	-0.15	0.1109	1.73E-01	3.07E-01
S2	0.25	0.1090	**1.93E-02**	1.10E-01
S3	0.20	0.1091	6.13E-02	1.81E-01
S4	0.02	0.1111	8.75E-01	9.08E-01

Appendix 5. Statistical analysis of sex-stratified associations between directly measured IgG N-glycosylation traits and coronary artery disease at the time of inclusion. Glycan data were adjusted for age, BMI, smoking and diabetes whereas the false discovery rate was controlled by the Benjamini-Hochberg method. Statistically significant differences are in bold.

Glycan trait	Women				Men			
	Effect	SE	p-value	p_{adj}-value	Effect	SE	p-value	p_{adj}-value
GP1	0.33	0.2029	9.41E-02	4.92E-01	-0.09	0.1318	4.86E-01	8.83E-01
GP2	0.22	0.2124	2.91E-01	8.09E-01	-0.08	0.1378	5.76E-01	9.11E-01
GP3	0.38	0.1811	**3.56E-02**	2.30E-01	-0.03	0.1307	8.26E-01	9.52E-01
GP4	0.37	0.1784	**3.72E-02**	2.30E-01	-0.05	0.1273	6.62E-01	9.38E-01
GP5	-0.19	0.2131	3.66E-01	8.16E-01	-0.09	0.1381	5.16E-01	8.83E-01
GP6	0.26	0.1776	1.33E-01	4.92E-01	-0.03	0.1250	7.98E-01	9.49E-01
GP7	0.05	0.2205	8.05E-01	9.49E-01	-0.05	0.1388	7.34E-01	9.49E-01
GP8	-0.12	0.2218	5.76E-01	9.11E-01	0.06	0.1323	6.51E-01	9.38E-01
GP9	0.03	0.2178	8.71E-01	9.87E-01	-0.19	0.1341	1.45E-01	4.92E-01
GP10	-0.02	0.2106	9.28E-01	9.91E-01	0.01	0.1325	9.13E-01	9.91E-01
GP11	0.02	0.2079	9.41E-01	9.91E-01	-0.11	0.1341	4.10E-01	8.21E-08
GP12	0.05	0.2056	8.09E-01	9.49E-01	0.01	0.1366	9.17E-01	9.91E-01
GP13	-0.19	0.2052	3.36E-01	8.16E-01	-0.17	0.1328	1.95E-01	6.03E-01
GP14	-0.26	0.1717	1.27E-01	4.92E-01	-0.05	0.1239	6.90E-01	9.38E-01
GP15	-0.26	0.2019	1.91E-01	6.03E-01	-0.04	0.1322	7.34E-01	9.49E-01
GP16	-0.37	0.2162	8.09E-02	4.59E-01	0.11	0.1376	4.36E-01	8.47E-01
GP17	-0.25	0.2078	2.21E-01	6.54E-01	0.12	0.1386	3.72E-01	8.16E-01
GP18	-0.46	0.1769	**8.45E-03**	9.57E-02	0.09	0.1295	4.94E-01	8.83E-01
GP19	-0.49	0.2112	**1.79E-02**	1.53E-01	0.12	0.1372	3.66E-01	8.16E-01
GP20	-0.33	0.2100	1.09E-01	4.92E-01	0.06	0.1317	6.48E-01	9.38E-01
GP21	-0.49	0.2151	**2.17E-02**	1.64E-01	0.11	0.1379	4.01E-01	8.21E-01
GP22	-0.14	0.2152	5.19E-01	8.83E-01	0.22	0.1377	1.13E-01	4.92E-01
GP23	-0.58	0.1892	**2.08E-03**	**2.91E-02**	0.13	0.1270	3.06E-01	8.09E-01
GP24	-0.64	0.2074	**1.79E-03**	**2.91E-02**	0.41	0.1353	**2.14E-03**	**2.91E-02**

Appendix 6. Statistical analysis of sex-stratified associations between derived IgG N-glycosylation traits and coronary artery disease at the time of inclusion. Glycan data were adjusted for age, BMI, smoking and diabetes whereas the false discovery rate was controlled by the Benjamini-Hochberg method. Statistically significant differences are in bold.

| Glycan traits	Women				Men			
	Effect	SE	p-value	p_{adj}-value	Effect	SE	p-value	p_{adj}-value
S total	-0.63	0.1781	**3.89E-04**	**2.65E-02**	0.19	0.1306	1.40E-01	4.92E-01
G0 total	0.40	0.1708	**1.80E-02**	1.53E-01	-0.05	0.1249	6.81E-01	9.38E-01
G1 total	-0.12	0.2207	5.65E-01	9.11E-01	-0.11	0.1335	3.90E-01	8.21E-01
G2 total	-0.26	0.1707	1.18E-01	4.92E-01	-0.05	0.1241	6.77E-01	9.38E-01
F total	-0.01	0.2183	9.75E-01	9.91E-01	0.01	0.1386	9.54E-01	9.91E-01
B total	-0.06	0.1993	7.75E-01	9.49E-01	0.06	0.1310	6.39E-01	9.38E-01
FGS/(F+FG+FGS)	-0.56	0.1800	**1.66E-03**	**2.91E-02**	0.13	0.1312	3.09E-01	8.09E-01
FBS1/(FS1+FBS1)	-0.06	0.1988	7.73E-01	9.49E-01	0.00	0.1360	9.91E-01	9.91E-01
FBS1/FS1	-0.06	0.1988	7.73E-01	9.49E-01	0.00	0.1360	9.91E-01	9.91E-01

Appendix 7. Statistical analysis of associations between derived IgG N-glycosylation traits and coronary artery disease during the 2-year follow-up period. Glycan data were adjusted for age and sex whereas the false discovery rate was controlled by the Benjamini-Hochberg method. Statistically significant differences are in bold.

Glycan trait	Effect	SE	p-value	p_{adj}-value
GP1	0.02	0.0597	7.74E-01	8.60E-01
GP2	-0.10	0.0523	6.52E-02	4.89E-01
GP3	-0.01	0.0724	8.99E-01	8.99E-01
GP4	-0.05	0.0484	2.76E-01	7.94E-01
GP5	-0.14	0.0969	1.45E-01	7.26E-01
GP6	0.03	0.0409	4.56E-01	7.94E-01
GP7	-0.05	0.0492	3.18E-01	7.94E-01
GP8	-0.03	0.0559	5.78E-01	7.94E-01
GP9	-0.11	0.0500	**2.39E-02**	3.59E-01
GP10	0.11	0.0474	**1.83E-02**	3.59E-01
GP11	0.02	0.0416	6.55E-01	7.94E-01
GP12	-0.02	0.0494	6.62E-01	7.94E-01
GP13	0.07	0.0559	2.33E-01	7.94E-01
GP14	0.04	0.0489	4.67E-01	7.94E-01
GP15	0.09	0.0538	1.01E-01	6.04E-01
GP16	-0.01	0.0425	8.13E-01	8.71E-01
GP17	-0.07	0.0723	3.20E-01	7.94E-01
GP18	0.03	0.0497	5.73E-01	7.94E-01
GP19	0.02	0.0500	7.07E-01	8.16E-01
GP20	-0.09	0.1096	4.12E-01	7.94E-01
GP21	0.02	0.1181	8.75E-01	8.99E-01
GP22	0.06	0.0683	4.16E-01	7.94E-01
GP23	0.02	0.0534	6.57E-01	7.94E-01
GP24	0.04	0.0612	5.59E-01	7.94E-01
G0 total	-0.04	0.0494	3.94E-01	7.94E-01
G1 total	-0.03	0.0637	5.89E-01	7.94E-01
G2 total	0.04	0.0492	3.98E-01	7.94E-01
S total	0.03	0.0486	5.37E-01	7.94E-01
F total	0.06	0.0566	2.74E-01	7.94E-01
B total	0.10	0.0487	**4.67E-02**	4.67E-01

Appendix 8. Statistical analysis of sex-stratified associations between derived IgG N-glycosylation traits and coronary artery disease during the 2-year follow-up period. Glycan data were adjusted for age and sex whereas the false discovery rate was controlled by the Benjamini-Hochberg method. Statistically significant differences are in bold.

Glycan peak	Women				Men			
	Effect	SE	p-value	p_{adj}-value	Effect	SE	p-value	p_{adj}-value
GP1	0.15	0.1120	1.89E-01	6.76E-01	0.00	0.0879	9.60E-01	9.98E-01
GP2	-0.08	0.0867	3.59E-01	8.41E-01	-0.02	0.0790	7.72E-01	9.41E-01
GP3	0.12	0.1492	4.26E-01	8.93E-01	-0.03	0.0956	7.29E-01	9.41E-01
GP4	0.03	0.1017	7.50E-01	9.41E-01	-0.03	0.0638	5.92E-01	9.41E-01
GP5	-0.21	0.1989	2.89E-01	8.41E-01	-0.20	0.1271	1.13E-01	6.36E-01
GP6	0.05	0.0839	5.12E-01	8.93E-01	0.09	0.0530	8.65E-02	6.26E-01
GP7	-0.06	0.0830	4.63E-01	8.93E-01	-0.02	0.0755	7.66E-01	9.41E-01
GP8	-0.19	0.0902	**3.43E-02**	5.83E-01	-0.03	0.0835	7.26E-01	9.41E-01
GP9	-0.08	0.1020	4.57E-01	8.93E-01	-0.11	0.0704	1.32E-01	6.36E-01
GP10	-0.05	0.1027	6.49E-01	9.41E-01	0.16	0.0608	**9.71E-03**	2.45E-01
GP11	-0.05	0.0940	5.77E-01	9.41E-01	0.05	0.0540	3.47E-01	8.41E-01
GP12	-0.01	0.1024	9.55E-01	9.98E-01	-0.03	0.0631	6.86E-01	9.41E-01
GP13	-0.12	0.1171	3.21E-01	8.41E-01	0.12	0.0744	9.63E-02	6.26E-01
GP14	-0.03	0.0976	7.56E-01	9.41E-01	-0.01	0.0641	8.77E-01	9.62E-01
GP15	-0.12	0.1168	3.19E-01	8.41E-01	0.11	0.0655	8.87E-02	6.26E-01
GP16	0.12	0.0815	1.50E-01	6.36E-01	-0.06	0.0604	2.85E-01	8.41E-01
GP17	-0.14	0.1477	3.53E-01	8.41E-01	-0.11	0.0940	2.36E-01	7.69E-01
GP18	0.00	0.1100	9.88E-01	9.98E-01	-0.05	0.0630	4.16E-01	8.93E-01
GP19	-0.08	0.1117	4.92E-01	8.93E-01	0.09	0.0629	1.45E-01	6.36E-01
GP20	-0.37	0.2219	1.01E-01	6.26E-01	-0.08	0.1410	5.95E-01	9.41E-01
GP21	-0.05	0.2564	8.36E-01	9.62E-01	-0.03	0.1448	8.52E-01	9.62E-01
GP22	-0.32	0.1237	**1.08E-02**	2.45E-01	0.18	0.0938	6.27E-02	6.09E-01
GP23	0.17	0.1251	1.84E-01	6.76E-01	-0.08	0.0666	2.37E-01	7.69E-01
GP24	-0.03	0.1269	7.89E-01	9.42E-01	0.06	0.0794	4.23E-01	8.93E-01
S total	0.00	0.1025	9.98E-01	9.98E-01	-0.02	0.0623	7.49E-01	9.41E-01
G0 total	0.05	0.1027	6.09E-01	9.41E-01	-0.01	0.0648	8.26E-01	9.62E-01
G1 total	-0.16	0.1154	1.73E-01	6.76E-01	-0.01	0.0896	9.17E-01	9.89E-01
G2 total	-0.03	0.1011	7.75E-01	9.41E-01	0.00	0.0621	9.79E-01	9.98E-01
F total	0.10	0.1061	3.40E-01	8.41E-01	0.03	0.0811	6.74E-01	9.41E-01
B total	0.02	0.1092	8.73E-01	9.62E-01	0.16	0.0621	8.96E-03	2.45E-01
FGS/(F+FG+FGS)	0.05	0.1084	6.75E-01	9.41E-01	-0.03	0.0601	6.61E-01	9.41E-01
FBS1/(FS1+FBS1)	-0.08	0.1061	4.80E-01	8.93E-01	0.11	0.0566	6.24E-02	6.09E-01
FBS1/FS1	-0.08	0.1061	4.80E-01	8.93E-01	0.11	0.0566	6.24E-02	6.09E-01

Appendix 9. Differences in sex-stratified IgG glycome composition during the follow-up period in CAD- and CAD+ cases. G0 - agalactosylation, G1 - monogalactosylation, G2 – digalactosylation, S – sialylation, F – core fucosylation, B – bisecting Glc-NAc, F – females, M – males, T - timepoint. Data is normalized to the first point.
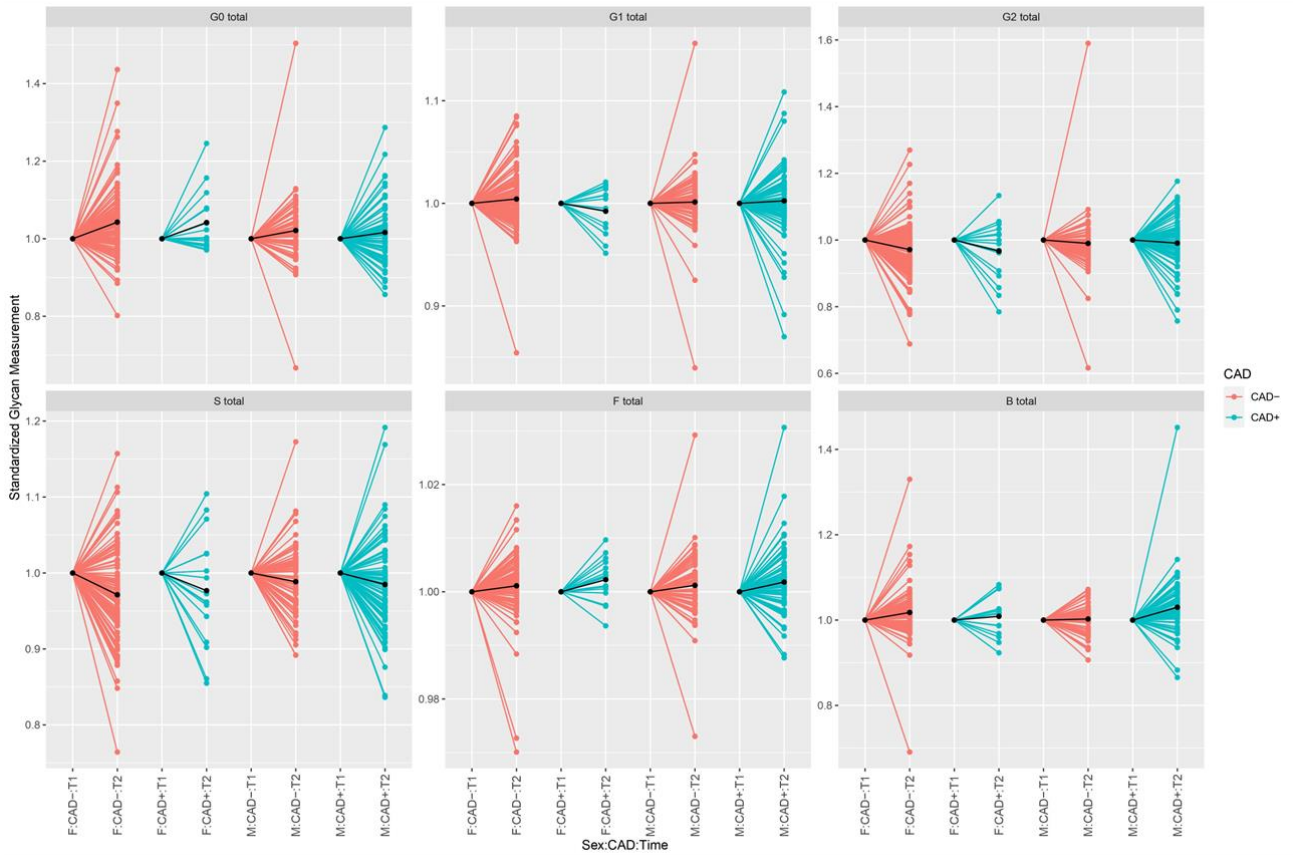
Appendix 10. Statistical analysis of relationship between IgG N-glycosylation traits and adverse CVD outcomes during the 8-year follow-up period. False discovery rates were controlled by the Benjamini-Hochberg method. Statistically significant differences are in bold

Glycan trait	Effect	SE	p-value	p_{adj}-value
GP1	-1.43	3.2757	6.58E-01	9.89E-01
GP2	-0.15	0.2431	5.14E-01	9.89E-01
GP3	-2.04	6.4466	7.52E-01	9.89E-01
GP4	0.00	0.0246	9.43E-01	9.89E-01
GP5	0.22	3.0307	9.43E-01	9.89E-01
GP6	0.03	0.0726	7.02E-01	9.89E-01
GP7	-0.10	0.4241	8.14E-01	9.89E-01
GP8	-0.05	0.0719	4.86E-01	9.89E-01
GP9	0.00	0.0843	9.78E-01	9.89E-01
GP10	0.04	0.0992	6.77E-01	9.89E-01
GP11	0.64	0.7418	3.93E-01	9.89E-01
GP12	0.05	0.2079	8.25E-01	9.89E-01
GP13	0.17	2.2522	9.41E-01	9.89E-01
GP14	0.00	0.0473	9.67E-01	9.89E-01
GP15	0.29	0.3534	4.09E-01	9.89E-01
GP16	-0.18	0.2442	4.62E-01	9.89E-01
GP17	0.17	0.4936	7.35E-01	9.89E-01
GP18	-0.02	0.0689	7.48E-01	9.89E-01
GP19	0.31	0.2583	2.36E-01	9.89E-01
GP20	-1.08	1.7692	5.34E-01	9.89E-01
GP21	1.18	0.9105	2.02E-01	9.89E-01
GP22	5.83	**2.2355**	**1.64E-02**	9.89E-01
GP23	-0.03	0.2383	8.84E-01	9.89E-01
GP24	0.35	0.2556	1.78E-01	9.89E-01
B total	0.04	0.0425	3.21E-01	9.89E-01
F total	0.00	0.0743	9.89E-01	9.89E-01
G0 total	0.00	0.0206	9.88E-01	9.89E-01
G1 total	-0.02	0.0564	7.50E-01	9.89E-01
G2 total	0.00	0.0414	9.18E-01	9.89E-01
S total	0.01	0.0443	8.65E-01	9.89E-01

Appendix 11. Statistical analysis of relationship between plasma N-glycosylation traits and adverse CVD outcomes during the 8-year follow-up period. False discovery rates were controlled by the Benjamini-Hochberg method. Statistically significant differences are in bold

Glycan trait	Effect	SE	p-value	p_{adj}-value
GP1	-0.28	0.1226	**2.32E-02**	9.85E-02
GP2	-0.14	0.1127	2.22E-01	4.20E-01
GP3	0.08	0.1073	4.41E-01	6.38E-01
GP4	-0.33	0.1160	**4.50E-03**	6.67E-02
GP5	-0.22	0.1154	**5.22E-02**	1.69E-01
GP6	-0.20	0.1070	6.42E-02	1.86E-01
GP7	-0.11	0.1115	3.11E-01	4.76E-01
GP8	0.08	0.1219	5.17E-01	7.11E-01
GP9	-0.03	0.1120	8.17E-01	9.06E-01
GP10	-0.26	0.1214	**2.97E-02**	1.09E-01
GP11	-0.07	0.1105	5.14E-01	7.11E-01
GP12	0.05	0.1090	6.65E-01	8.49E-01
GP13	-0.31	0.1196	**1.03E-02**	7.65E-02
GP14	0.16	0.1181	1.76E-01	3.90E-01
GP15	0.11	0.1119	3.46E-01	5.15E-01
GP16	-0.14	0.1184	2.37E-01	4.20E-01
GP17	-0.03	0.1098	7.70E-01	9.01E-01
GP18	-0.02	0.1198	8.89E-01	9.06E-01
GP19	0.15	0.1152	2.06E-01	4.19E-01
GP20	0.20	0.1114	6.76E-02	1.86E-01
GP21	0.13	0.1165	2.83E-01	4.47E-01
GP22	0.16	0.1158	1.64E-01	3.90E-01
GP23	0.12	0.1129	2.84E-01	4.47E-01
GP24	0.07	0.1178	5.40E-01	7.24E-01
GP25	0.14	0.1178	2.50E-01	4.30E-01
GP26	0.34	0.1205	**4.40E-03**	6.67E-02
GP27	0.14	0.1208	2.29E-01	4.20E-01
GP28	0.16	0.1175	1.77E-01	3.90E-01
GP29	-0.02	0.1193	8.85E-01	9.06E-01
GP30	0.16	0.1200	1.93E-01	4.08E-01
GP31	0.26	0.1241	**3.73E-02**	1.28E-01
GP32	0.32	0.1198	**6.84E-03**	6.84E-02
GP33	0.18	0.1207	1.28E-01	3.35E-01
GP34	0.13	0.1231	2.74E-01	4.47E-01
GP35	0.22	0.1177	5.75E-02	1.76E-01
GP36	0.05	0.1220	6.69E-01	8.49E-01
GP37	-0.02	0.1222	8.52E-01	9.06E-01
GP38	0.04	0.1199	7.59E-01	9.01E-01
GP39	0.03	0.1140	8.08E-01	9.06E-01
AF	0.17	0.1196	1.60E-01	3.90E-01
B	-0.04	0.1068	6.79E-01	8.49E-01

Appendix 11 - continued

CF	-0.27	0.1130	**1.75E-02**	8.76E-02
G0	-0.26	0.1210	**2.91E-02**	1.09E-01
G1	-0.32	0.1150	**4.85E-03**	6.67E-02
G2	0.14	0.1123	2.18E-01	4.20E-01
G3	0.29	0.1167	**1.16E-02**	7.65E-02
G4	0.02	0.1172	8.63E-01	9.06E-01
HB	0.27	0.1173	**2.33E-02**	9.85E-02
HM	0.02	0.1091	8.76E-01	9.06E-01
LB	-0.28	0.1192	**1.70E-02**	8.76E-02
S0	-0.32	0.1134	**4.71E-03**	6.67E-02
S1	-0.04	0.1203	7.15E-01	8.74E-01
S2	0.30	0.1115	**7.46E-03**	6.84E-02
S3	0.29	0.1170	**1.25E-02**	7.65E-02
S4	0.01	0.1159	9.16E-01	9.16E-01

9. CURRICULUM VITAE

Barbara Radovani was born on July 6, 1995, in Rijeka, Croatia. She graduated from high school in 2014, and in the same year, she enrolled in the "Biotechnology and Drug Research" undergraduate program at the Department of Biotechnology, University of Rijeka, where she ranked among the top 10 percent of students on the acceptance list.

Throughout her undergraduate studies, Barbara demonstrated remarkable academic performance, receiving a scholarship for excellence, and being honored with the Rector's Award for excellence. As part of her graduate program, "Drug Research and Development," she seized the opportunity to participate in the student exchange Erasmus+ program at the Universitat Autònoma de Barcelona. This experience allowed her to engage with diverse perspectives and expand her knowledge.

In 2019, Barbara obtained her graduate degree, and she furthered her professional development through a six-month internship at Metgen Oy in Finland. This internship provided her with hands-on experience working with various high-throughput instruments and methods, enhancing her practical skills in the field. Shortly after her return, she joined Genos Glycoscience Research Laboratory as a doctoral researcher, simultaneously enrolling in the postgraduate doctoral program "Biology" at the Faculty of Science. Since 2022, Barbara has been working as a PhD research assistant at the Department of Biotechnology, University of Rijeka. During her academic and professional career, she has actively participated in numerous national and international conferences, meetings, and workshops and is co-author of seven publications.